Cape Peninsula
University of Technology

PLASTIC WASTE GASIFICATION USING A SMALL SCALE IR REACTOR: EXPERIMENTAL AND MODELLING ANALYSIS

by

SARAH MARIELLE GUYEMAT MBOUROU

Thesis submitted in fulfilment of the requirements for the degree

Master of Technology: Electrical Engineering

in the Faculty of Electrical Engineering

at the Cape Peninsula University of Technology

Supervisor: Dr ML Adonis

Bellville Campus
May 2016

i

DECLARATION

I, Sarah Marielle Guyemat Mbourou, declare that the contents of this dissertation/thesis represent my own unaided work, and that the thesis has not previously been submitted for academic examination towards any qualification. Furthermore, it represents my own opinions and not necessarily those of the Cape Peninsula University of Technology.

_____   _____

Signed   **Date**

ABSTRACT

The generation of municipal solid waste has increased significantly due to the exponential population growth and it has become a global issue. Gasification technology, an alternative method for waste treatment is a thermochemical process where carbon-based material are exposed to an environment deprived in oxygen, was used for this project.

The aim of this thesis is to study the gasification of plastic waste which is a potential alternative energy source using infrared heaters. To achieve this goal, fundamental studies have been numerically and experimentally conducted for an infrared gasifier and subsequently establishing the temperature profile for gasification using a small scale reactor.

A detailed study on low density polyethylene was conducted using Infrared Spectrometry and thermal decomposition techniques such as Thermogravimetry and Differential Scanning Calorimetry were performed to establish the temperature at which plastic pellets sample used for this research gasify. The gasification behaviour of pelletized low density polyethylene (plastic pellets) was tested and three case studies were done to evaluate the most suitable temperature profile for the reactor to gasify the low density polyethylene at high temperature for less amount of time. Subsequently, the reactor model was simulated and results validate the use of reactor at an optimum temperature of 800 °C for a gasification process with less residue content.

The reactor designed for this research is fully functional and validates the temperature behaviour predicted during simulation. The experimental results show infrared heaters are suitable for gas production using this gasification process.

ACKNOWLEDGEMENTS

First of all, I would like to acknowledge God Almighty my Father for His Word and Wisdom infused in me which gave me the strength and ability to complete this thesis.

- My sincere gratitude towards Dr Marco Adonis from the Cape Peninsula University of Technology for his supervision, advice, understanding, support and encouragement to move forward with the completion of this thesis. I am really grateful for the privilege of conducting this research under his supervision.

- I thank Genevieve Gordon from the Department of Chemical Engineering at the Cape Peninsula University of Technology for her immensurable work and effort put in this project, for her guidance in the expected outcome with experiments. Additional thanks to Mogamad Shareef Karem from the Department of Mechanical Engineering. I am deeply grateful for the collaboration with the University of Stellenbosch for FTIR Spectrometry experiments done under the supervision of Dr Hans Andre Eyeghe-Bickong, and for thermal decomposition analysis conducted at the University of Western Cape under the supervision of Dr Wafeeq Davids.

- I am forever grateful to my spouse Dr Hans Andre Eyeghe-Bickong and my children Asmara Shanice, Andree Marcie and Christie for their love, encouragement, support and standing by me to always go beyond what was expected. You are the main reason for me to thrive always. I love you all and thank you for being part of me.

- I am thankful towards my colleagues and friends at the Centre for Distributed Power and Electronics Systems at the Cape Peninsula University of Technology for their support advice during this research. May you all receive my heartfelt gratitude.

Lastly, I am indebted to the staff and students at CPUT for their assistance and support.

DEDICATION

For Asmara Shanice, Andree Marcie and Christie.

TABLE OF CONTENTS

LIST OF FIGURES

LIST OF TABLES

NOMENCLATURE

A	Surface area, m^2
Cp	Specific heat, $J/kg*K$
F	View factor
k	Thermal conductivity, $W/m*K$
M	Average moisture content
qir,FIRh	FIR transfer rate from FIR heater, W
qir,FIR,wire	FIR transfer rate to wire, W
G FIR	Heat generation, W/m3 W/m^3
r	Resistivity, Ω.m
T	Temperature, ^{0} C or K
v	Air velocity, m/s

Greeks

α	Thermal diffusivity, m^2/s
ρ	Density, kg/m^3
σ	Stephan–Boltzmann constant, W/m^2*K^4
ε	Emissivity

Subscripts

FIR	Far-infrared
IR	Infrared
r	Radiation
s	Surface or surrounding
ceram	Ceramic
i	Surface i
ir	Irradiation
j	Surface j
h	Heater

LIST OF ABBREVIATIONS

PE	Polyethylene
PP	Polypropylene
PS	Polystyrene
PET	Polyethylene terephthalate
HDPE	High density polyethylene
LDPE	Low density polyethylene
HC	Hydrocarbon
CO	Carbon monoxide
CO_2	Carbon dioxide
CH_4	Methane
H_2	Hydrogen
C	Carbon
DaQ	Data acquisition device
MSW	Municipal Solid Waste
N_2O	Nitrous Oxide
UNEP	United Nations Environmental Program
PVC	Polyvinyl chloride
HCL	Hydrogen chloride

CHAPTER 1 : INTRODUCTION

Worldwide energy consumption is rapidly increasing in modern times, especially due to exponential population growth. Since fossil fuel-based resources are finite and rapidly consumed, finding replacement options for power generation is crucial. Due to increasing demand driven by both developed and developing countries, fossil fuels reserves are expected to diminish in the future. Several billion barrels of petroleum are consumed per year in the world, out of which 630 thousand barrels per day were consumed in South Africa in 2013 (Portal, 2015).

The global production of plastic is also increasing and for most countries the growing consumption of plastics results in an increase of waste generated by householders and industries and this is becoming a challenge to different waste disposal methods.

An amount of 1.628 million tons of plastics consumption in South Africa in 2012 contributed approximately 1.6 % to South Africa's gross domestic product and 14.2 % to the manufacturing sector (SA, 2015). A majority of these plastics were then discarded and ended up in landfills as non-biodegradable waste. Some plastics are recycled in South Africa with a recovery of 32.9 % of all plastics packaging materials (SA, 2015) and as plastics cannot be used in the same application after they are recycled (due to contaminations and other issues), the markets and consumer applications for recycled plastics are limited (Anaraki, 2012; Yanga et al., 2012). Due to the high energy density of plastics, plastics have the potential of being a viable energy source (He et al., 2009).

The plastic industry is ranked as one of the few-billion dollar industries (PlasticsEurop, 2012; SA, 2014; Steyn, 2015). Energy consumption worldwide is rapidly increasing and especially due to plastics used in everyday life and with the increase of waste every year linked to growing population, discarded plastic products and packaging constitute a growing portion of the Municipal Solid Waste (MSW) stream. Plastics contained in the MSW are mainly thermoplastics: Polyethylene (PE), Polypropylene (PP), Polystyrene (PS), and Polyvinyl Chloride (PVC) (Xiao et al., 2007; Toledo et al., 2011) and occupy two thirds of plastic sales worldwide. There are different alternative methods for the treatment of MSW and plastic waste. The most common are landfilling, incineration, mechanical recycling and chemical recycling (Toledo et al., 2011).

In addition, landfilling is the preferred method of waste disposal in most African countries and being the main method of waste disposal it presents serious negative impacts on the

1

environment (Management, 2005). In South Africa, there are 817 legal landfill sites including 97 in the Western Cape and up to 15,000 unrecorded communal sites (Africa, 2010). As a result, there is an increase in environmental pollution levels and the environment pollution is expected to increase significantly for the upcoming century unless government environmental policies changes and pollution abatement technologies are applied regarding wastes. Given the challenges of limited landfill space and the environmental impacts of landfilling, alternative methods for the treatment of plastic waste is of the paramount importance for the environment and economy. Instead of paying to dispose these wastes, municipalities may generate income from waste products as waste contains valuable unused energy (Panda et al., 2010; Council, n.d.). Furthermore, alternative methods for waste plastic utilization will result in the reduction of landfill space requirement. Also, there will be an associated greenhouse gas emissions.

With regards to electricity, there is still a growing need for electrification in sparsely populated areas and with the capacity of the existing distribution infrastructures these significantly slow down the electrification programme in South Africa (Magubane, 2011). The South African Department of Energy states in its annual report that the growing demand for electricity has put an additional pressure on South Africa's ailing distribution. The electricity distribution industry is facing serious backlog with regards to infrastructure and refurbishment (Magubane, 2011). Although the Including Block tariff implemented on 24 February 2010 seemed to protect the poor against electricity price increase, it has unfortunately been a drawback for the average households (Salga et al., 2011). For instance, during winter the consumption of electricity usually increases; therefore, the more one uses electricity, the more one pays whatever his domestic/residential household is (as a customer).

1.1 Plastics

The term plastic comes from Greek word which means "to form". Plastics are typically classified according to their composition and/or performance. The identification of plastic materials is based on their polymer to meet different requirements. Plastics can be formed during their fabrication into simple to extremely complex shapes due to the additives, filling and reinforcements made in the base polymer. Plastics are classified into two major groups: thermoplastics and thermosets.

1.1.1 Thermoplastics

The most encountered ones are Polyethylene (PE), Polystyrene (PS), Polypropylene (PP) and Polyvinyl Chloride (PVC). Thermoplastics are plastics that during processing soften when heat is applied or harden during cooling. They can turn into new plastic products that are capable of being repeatedly softened by reheating (UNEP, 2009).

1.1.2 Thermosets

Thermosets are plastics which exhibit an increase in their flow-ability on application of heat. At higher temperature, they solidify and stay at this state. Moreover, they become infusible and insoluble. They cannot be re softened with heat.

With regards to plastic consumption, the South African largest market consumer of plastics is packaging as indicated in Figure 1.1 with 54.5 % in the market sector, about 820 000 tonnes (SA, 2014).
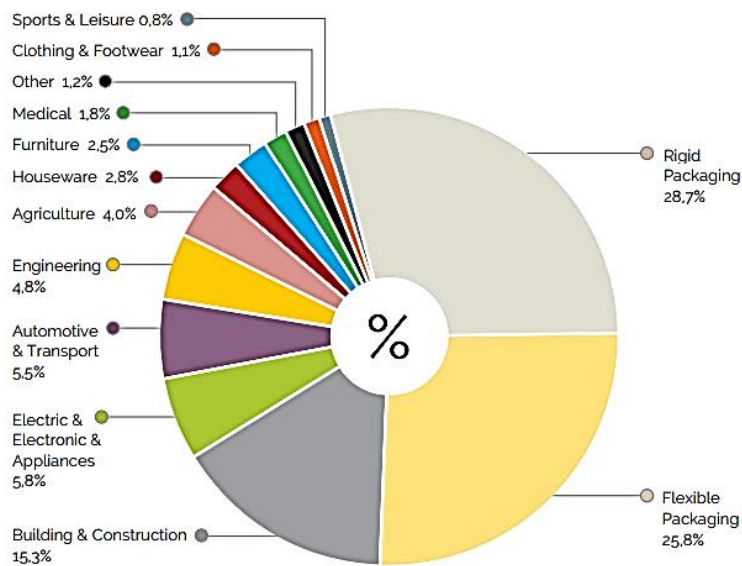
Figure 1.1: Plastic consumption in South Africa (SA, 2014)

1.2 Current techniques

Although landfilling has been proven advantageous in comparison to simple disposal of waste in discharges where waste is not categorised according to their classes and toxicity, it has many disadvantages such as the space/area occupation as waste takes more and more land space (Shi et al., 2011). It also has a bad odour and leads to greenhouse gas emissions. Consequently, this method of waste disposal raises pollution and health concerns (Varadi et al., 2007) as well as concerns with the appearance of the landfill site (Sharp & Jr, 1992). Current techniques of waste management are indicated in Table 1.1 and the number of legal landfill sites in South Africa by province in Table 1.2 respectively.

Table 1.1: Current techniques used for waste management

Techniques	Advantages	Disadvantages
Waste Incineration		
	Volume and weight reduced	Formation and reformation of toxic dioxins and furans
	Immediate waste reduction	
	Destruction in seconds	
	Incineration can be done at generation site	
Waste Landfill		
	cheapest method of disposal	Tend to be located in close proximity to poor communities and informal settlements
		Formation of greenhouse gas
Waste Recycling (Conventional)		
	Reuse of some plastic materials	A labour intensive process
		Polymer may lose its quality

Table 1.2: Legal landfill sites by province in 2010 (Africa, 2010)

Provinces	Legal landfill sites
Western Cape	97
Eastern Cape	120
Northern Cape	103
Free State	67

KwaZulu-Natal	119
North West	35
Gauteng	160
Mpumalanga	72
Limpopo	44
South Africa	817

1.3   The importance of gasification for handling plastic waste

Plastic waste is considered as one of the most promising resources for fuel production due to its high heat of combustion and including the increasing availability in local communities. Plastics, contrary to paper and wood, do not absorb much moisture and the water content of plastic waste is significantly lower than the water content of biomass (UNEP, 2009).

The conversion processes of plastic waste into fuel are subject to the type of plastics to be targeted and the properties of other waste that possibly will be used in the process. In addition, for an effective conversion of plastic into energy resource some appropriate technology configurations are required that not only vary based on how they are selected according to local, environmental, social, economic and technical characteristics but also on how the feedstock is processed. Each type of plastic waste conversion method has it is own suitable feedstock. The composition of various plastics that are used as feedstock may increase the possibility of that specific plastic composition to contain undesirable substances such as nitrogen, halogens, sulphur or other hazardous substances which pose risk to humans and to the environment (UNEP, 2009). The use of gasification technology was proven to be efficient for non-recyclable plastic except PVC (Anonymous, 2006) and may reduce the amount of waste disposed to landfill (Cheng & Hu, 2010) (with emission of gases in the atmosphere). Consequently, due to its high calorific values, the use of plastic materials in the gasification process may help in the generation of electricity for an appropriate electricity distribution in households. Table 1.3 shows an example of heating values of different types of waste and solid fuel (UNEP, 2009).

Table 1.3: Heating values of several fuel and waste types (UNEP, 2009)

Fuel of waste	Typical heating value (kcal/kg)
Refuse derived fuel	4000 - 5000
Refuse derived paper and plastic fuel	6000 - 8000
Coal	6000 – 8000

Heavy oil	9500
Wood/paper	4300
Plastics (polyethylene)	11000
Typical municipal waste	1000 - 1500

1.4 Problem statement

Mechanical recycling presents an important resource in the reuse of plastic products whereas chemical recycling refers to the conversion of plastic materials into liquids or gases. These primary products serve as feedstock in the production of new-petrochemicals and plastics. However, some limitations exist with regards to mechanical recycling. It only uses single polymer plastics, therefore limiting the use of complex and contaminated plastics as opposed to chemical recycling which offers a wide range of possibilities as it involves several processes. Conventional solutions of plastic waste disposal such as landfill and incineration have serious negative impacts on the environment and on health due to greenhouse emissions.

Among alternative methods for plastic waste treatment to landfilling, pyrolysis and gasification present interesting alternatives with possibility of electricity generation from waste (Stephen, 2009). This will be useful as the demand in electricity has increased significantly throughout South Africa with of an electrification rate of 75 % and still 12.3 million of population are without electricity (IEA, 2011) as indicated in Table 1.4. Therefore, the purpose of this project is the use of plastics to supply alternative energy to ailing electricity network by presenting a mathematical model to improve the conversion of plastic waste into syngas, simulate and test infrared heaters that will help in improving the efficiency of a packed bed reactor using indirect infrared heating capable of handling plastic wastes. As a result, the present research attempts to find an alternative way to support the energy production in South Africa and help reducing plastic waste and its negative impact to the environment.

Table 1.4: Electricity access in Africa 2009 (IEA, 2011)

	Electrification rate (%)	Population without electricity (millions)
Angola	26.2	13.7

Benin	24.8	6.7
Botswana	45.4	1.1
Burkina Faso	14.6	12.6
Cameroon	48.7	10
Congo	37.1	2.3
Cote d'Ivoire	47.3	11.1
DR Congo	11.1	58.7
Eritrea	32	3.4
Ethiopia	17	68.7
Gabon	36.7	0.9
Ghana	60.5	9.4
Kenya	16.1	33.4
Lesotho	16	1.7
Madagascar	19	15.9
Malawi	9	12.7
Mauritius	99.4	0
Mozambique	11.7	20.2
Namibia	34	1.4
Nigeria	50.6	76.4
Senegal	42	7.3
South Africa	75	12.3
Sudan	35.9	27.1
Tanzania	13.9	37.7
Togo	20	5.3
Uganda	9	28.1
Zambia	18.8	10.5
Zimbabwe	41.5	7.3
Other Africa	17	89.1
Sub-Saharan Africa	30.5	585.2
Algeria	99.3	0.2
Egypt	99.6	0.3
Libya	99.8	0
Morocco	97	1
Tunisia	99.5	0.1
North Africa	99	1.6
Africa	41.8	586.8

1.5 Research aims and objectives

The aims of the present research are to model and simulate infrared heaters for plastic waste gasification. The study includes the following:

- Heater optimization to get the best peak wavelength in specific temperature that will match the spectral absorption rate of the plastic waste.
- Mathematical analysis using software such as COMSOL Multiphysics, Matlab and LabVIEW for the modelling, simulation and data acquisition of the infrared reactor.

The objectives of this research are:

- To develop a lab scale IR reactor
- To characterize plastic wastes
- To study the gasifier numerically through modelling/simulation
- To study the influence of infrared radiation on plastics through gasification experiments

Subsequently, this research project focuses on the use of waste plastic pellets as a raw material to the gasification process.

1.6 Scope of works

The methodology for this research involves infrared investigation by modelling and simulating the heater. The study considered the following:

- Modelling, simulation and experimental testing of an infrared gasifier. Modelling and simulation are dealt here with regard to the mathematical equations representing the energy balance in an infrared reactor. The modelling techniques consist of defining parameters, the geometry, materials used, and physics of the model. COMSOL Mutiphysics, MATLAB SIMULINK and LabVIEW softwares were used as computational tools to complete the simulations observing the temperature distribution inside a gasifier.
- Spectral property of heater and low density polyethylene and wavelength measurement of waste plastics using infrared spectroscopy , Fourier transform infrared spectroscopy (FTIR)
- Experimental analysis of the influence of the heater temperature, the incidence radiation and the number of heaters used: four heaters, three heaters and two heaters
- Model validation by comparing experimental data and numerical simulation

- Temperature measurement and data acquisition to determine the most suitable temperature for the gasification of plastics

1.7 Significance of research project

The importance of focusing on modelling an infrared heater is to improve the conversion of plastic waste into syngas and heating value of the gas produced for electricity generation. For this reason it will improve the efficiency of gasification of plastic waste as well as reducing plastic waste and its negative impact to the environment. As a result, the present research attempts to find an alternative way to support the energy production in South Africa.

1.8 Thesis outline

This thesis consists of eight chapters and appendices that are organised as follow:

- **Chapter 1**

  This chapter presents the introduction as well as background to this given project. It also presents an awareness of the problem investigated, the objective of the study, the problem statement, the significance of the research project as well as the research design and methodology that were applied in this work.

- **Chapter 2**

  In this chapter the literature established a collection of theoretical information about thermal processes applied to municipal solid waste, especially the gasification process, the synthetic gas (syngas) and applications based on infrared radiation

- **Chapter 3**

  This chapter gives a brief theory of infrared radiation, as well as different modes of heat transfer such as conduction, convection and radiation with the black body concept and energy balance. The study also looks at the classification of industrial infrared heaters.

- **Chapter 4**

  Chapter 4 discusses the design of a small laboratory scale gasification plant as well as the numerical model development of the gasifier such the energy balance and plastic pellet properties (polyethylene) used for gasification.

- **Chapter 5**

  This chapter deals with the system simulation based on the software COMSOL Multiphysics, the model development and implementation.

- **Chapter 6**

Chapter 6 is devoted to experimental equipment and procedures used for this study.

- **Chapter 7**

  This chapter contains result of experiments conducted during the time of this study and a discussion of results.

- **Chapter 8**

  A conclusion is presented in this chapter with regards to the results of the work for this thesis. Based on the results of work undertaken for this thesis, a conclusion is presented in this chapter. Also, flowing from the work undertaken, some concluding remarks are made regarding with possible future avenues of research.

CHAPTER 2 : LITERATURE REVIEW

2.1   Introduction

This chapter gives an introductory review of gasification processes as well as infrared applications on heating and drying.

Plastics are synthetic organic materials produced by polymerisation and typically classified according to their composition and/or performance. They are of high molecular mass and may contain other substances beside polymers to improve the performance and/or reduce costs. These polymers can be moulded or extruded into desired shapes. There are mainly two major groups of plastics: thermosets and thermoplastics. Being ranked as one of the most lucrative industries, plastics are used in everyday life and with the increase of waste every year linked to growing population, discarded plastic products and packaging constitute a growing portion of the Municipal Solid Waste (MSW) stream. Plastics contained in the MSW are mostly thermoplastics: Polyethylene (PE), Polypropylene (PP), Polystyrene (PS), and Polyvinyl Chloride (PVC) (Xiao et al., 2007; Toledo et al., 2011) with two thirds of plastic sales worldwide. There are different alternative methods for the treatment of MSW and plastic waste. The most common are landfilling, incineration, mechanical recycling and chemical recycling and energy recovery (Toledo et al., 2011). Feedstock recycling converts plastic material into useful basic chemicals.

However, the recycling of plastic waste is a rather limited process due to its contamination with other class of residues such as food waste (Wu & Williams, 2010). As a consequence, the main destinations of disposal of plastic waste are still incineration and principally landfilling in South Africa as in indicated in Table 2.1.

Table 2.1: Key waste estimated for South Africa in 2011 (DEA, 2012)

Type of Waste	Amount in tonnes
Waste landfilled	98 million
General waste	59 million
Unclassified waste	48 million
Hazardous waste	1 million
Total waste generated	108 million

Municipal waste includes household and industrial waste. Industrial waste constitutes about 21% of the municipal waste in South Africa. The Department of Science and Technology (2012) report states that South African municipalities still rely on landfilling process as the primary solution for the management of waste as indicated in Table 2.2. This shows that the technology option still remains under-utilized within municipalities compared.

Table 2.2: Percentage municipal waste contribution by province in South Africa, 2011 (DEA, 2012)

Province	Kg/capita/annum	Waste generated as % of total waste
Western Cape	675	20
Eastern Cape	113	4
Northern Cape	547	3
Free State	199	3
KwaZulu Natal	158	9
North West	68	1
Gauteng	761	45
Mpumalanga	518	10
Limpopo	103	3

2.2   Thermal processes applied to Municipal Solid Waste

Thermal processes for energy recovery applied to Municipal Solid Waste (MSW) are an essential component of a Waste Management System. Different alternative methods of waste-to-energy technologies with respect to MSW are shown in Figure 2.1.
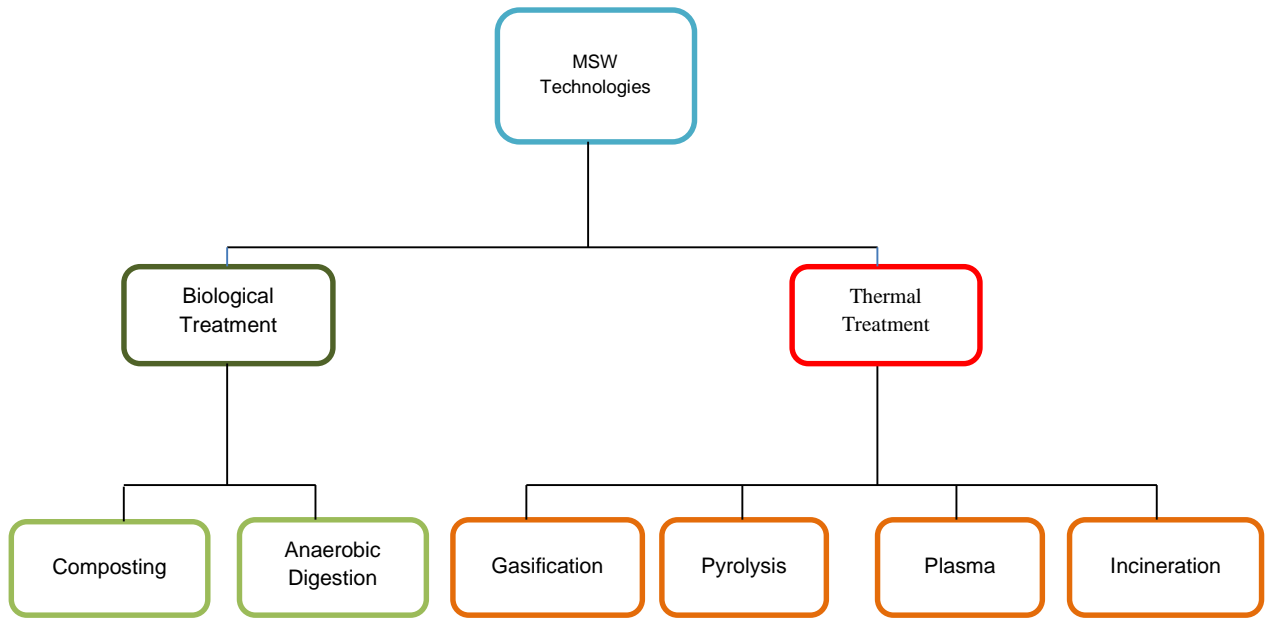
Figure 2.1: Municipal Solid Waste Technologies

2.2.1 Incineration

Combustion or incineration as referred to waste combustion is the thermal conversion or total oxidation with air as the oxidising medium, to produce carbon dioxide and water if pure hydrocarbons are used as fuel. This chemical reaction is complete and the incineration temperature is dependent on the fuel and oxidizing medium. The combustion applied in waste incineration is about 1200 °C and the flue gas temperature is about 160 °C (Nordgreen, 2011). Combustion can be applied to small scales (domestic applications: provides heat for cooking, space heating) as well as to large scale operations (industrial scale applications with electricity generation) (Meng, 2012). The main advantages of incineration are reduction of waste in terms of mass and volume, reduction of gas emission from anaerobic decomposition and a significant conversion of land with regards to landfilling (Ryu, 2010). Although incineration has great advantages it doesn't remove completely all waste accumulated, in addition, toxic pollutants are produced in residues such as fly ash, dioxin, etc. While the waste burned by incineration to produce energy, fossil carbon contained in the waste is released in the atmosphere as CO_2 together with a lesser quantity of other greenhouse gases such as nitrous oxide (N_2O) and CH_4 (Ryu, 2010).

2.2.2 Pyrolysis

The pyrolysis process consists of the degradation of waste in an environment deprived of oxygen or air (Shi et al., 2011; Bridgwater et al., 2002). It requires an external heat source as the waste must be dried before the pyrolysis reactions occur and the reaction temperatures are within the range 250 - 700 °C. The main products of pyrolysis are solid/ash coke residue, condensable oils, waxes and tars and gases such as carbon monoxide, hydrogen, hydrocarbons, water vapour and nitrogen (Stephen, 2009). The drawback of the pyrolysis process is its high tar content that limits its application, and the fly ash collected is disposed as hazardous waste, therefore needs further treatment or may be recycled in construction materials (Arena & Mastellone, 2006).

Bajus (2011) studied the recovery of two types of waste by co-pyrolysis. The thermal cracking was performed under atmospheric pressure at 450 °C and 500 °C with a mixture of 8.5 g of plastics and 8.5 g of woody material. The polymers used in the feedstock are virgin plastic in the form of pellets with the exception of PET in bottles and PVC in powder. The temperature in the injection chamber was 240 °C and the time analysis was about 80 minutes. It was observed that when the reaction temperature increases the liquid and solid yields seem to decrease too. The obtained results showed an improvement on the overall efficiency of the slow pyrolysis of woody material by adding plastics in the mixture. This improvement might be the cause of higher heat and mass transfer rates and for this reason this will result in higher production of alkanes and alkenes as gas formation increases with the temperature and reaction time.

Wu & Williams (2010) investigated the production of hydrogen from polypropylene, polystyrene, high density polyethylene and their mixture and real world plastic waste with a two-stage pyrolysis-gasification reactor. The experiments were conducted with and without a Ni-Mg-Al catalyst at temperatures of 800 °C and 850 °C to investigate the influence of plastic type on the product distribution as well the production of hydrogen with regards to the process conditions. Their results showed that at a gasification temperature of 800 °C for the non-catalytic experiment, lower gas yield obtained at 11.2 wt% in relation to the mass of plastic where compared with the polypropylene it yields 59.6 wt%, for the HDPE 53.5 wt% and for the waste plastic 45.5 wt% respectively. Whereas the gas yield in terms of the weight of polypropylene increased significantly from 68.1 wt% to 252.3 wt% by using a Ni-Mg-Al-CaO catalyst at the same gasification temperature (Wu & Williams, 2010). Moreover, it was observed that major oil is produced for the non-catalytic reaction. Although the presence of Ni-Mg-Al catalyst had

significantly enhanced the steam gasification-pyrolysis of plastics for the production of hydrogen, it however presents the lowest production of hydrogen at gasification temperature of 800 °C. In addition, a great improvement in terms of gas yield and hydrogen production was noticed with regards to steam pyrolysis-gasification of PP, PS and HDPE by using the Ni-Mg-Al catalyst.

2.2.3 Gasification

Gasification is a thermochemical process where carbon-based materials such as paper, plastic, and petroleum based waste or biomass as shown in Figure 2.2 are exposed to an environment deprived in oxygen. Therefore, the combustion does not occur as opposed to combustion which uses excess air. It is the conversion of solid or liquid fuels into combustible gas. The main part of the gasification process is the gasifier, a vessel in which the thermochemical process takes place with a combination of heat and pressure and the amount of air is generally between 20 % and 40 % (Brems et al., 2013). The reaction takes place at high temperature generally higher than 800 °C. The material or feedstock is converted into a synthesis gas also called syngas, which is a high energy carrier (Bridgwater et al., 2002). The resulting syngas is then cleaned to remove any impurity and once cleaned it can therefore be suitable for several uses (Varadi et al., 2007; Stiegel & Rusell, 2001; Okajima et al., n.d.):

- Electricity generation
- Manufacture of chemical, hydrogen or transportation of fuel
- Basic chemical feedstock in petrochemical industries
- Syngas treatment to produce steam for use in fuel cell

The thermal efficiency of a gasification process can be more than 75 % and the carbonaceous material feedstock used in gasification may contain gaseous, liquid and solid products such as wood, paper, coal, coke, plastics and biomass.

The process produces carbon monoxide (CO), carbon dioxide (CO_2), hydrogen, methane (CH_4) (Lorcet, 2009), nitrogen and other gases depending on the plastic composition and the gasifying agent such as air, pure oxygen and steam.
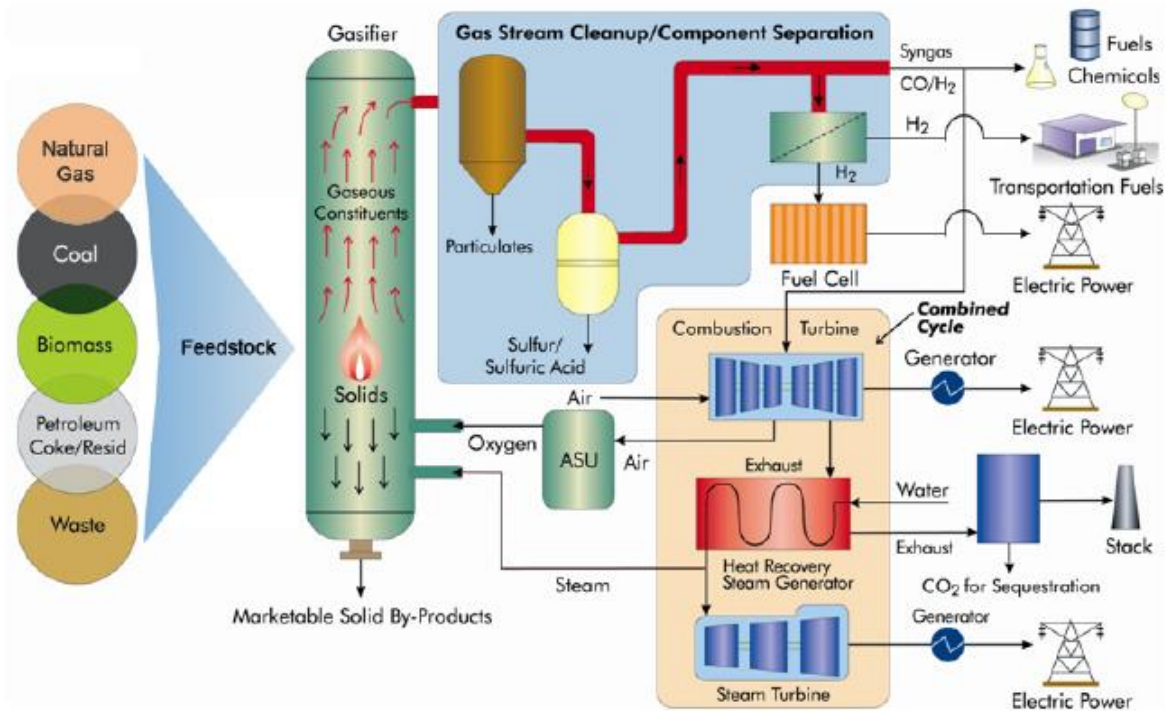
Figure 2.2: Overview of Gasification-based systems options (Olliver, 2012)

Plastic materials are ideal for the gasification process due to their high calorific values. The gasification technology was proven to be efficient for non-recyclable plastic except PVC (Anonymous, 2006). For this reason, the gasification of plastic waste may not only reduce the amount of waste disposed to landfill (with emission of gases in the atmosphere), it will consequently help in the generation of electricity for an appropriate electricity distribution in households.

The gasification process in Figure 2.3 may be represented schematically by:

$$Carbonaceous\ fuel + heat \rightarrow solid + gas$$
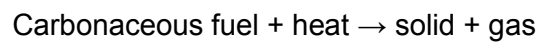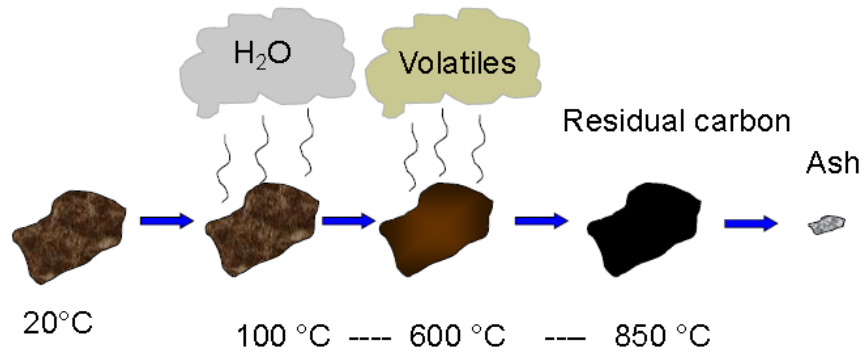
Figure 2.3: Gasification process (Kurkela, 2010)

The main reactions during gasification of plastics are shown below:

- Oxidation reactions

$$C + \frac{1}{2}O_2 \rightarrow CO \tag{2.1}$$

$$C + \frac{1}{2}O_2 \rightarrow CO_2 \tag{2.2}$$

$$H_2 + \frac{1}{2}O_2 \rightarrow H_2O \tag{2.3}$$

$$C_nH_m + \frac{n}{2}O_2 \leftrightarrow nCO + \frac{m}{2}H_2 \tag{2.4}$$

- Gasification reactions that involves steam

$$C + H_2O \leftrightarrow CO + H_2 \tag{2.5}$$

$$CO + H_2O \leftrightarrow CO_2 + H_2 \tag{2.6}$$

$$CH_4 + H_2O \leftrightarrow CO + 3H_2 \tag{2.7}$$

$$C_nH_m + nH_2O \leftrightarrow nCO + \left[n + \frac{m}{2}\right]H_2 \tag{2.8}$$

- Gasification reactions that involves hydrogen

$$C + 2H_2 \leftrightarrow CH_4 \tag{2.9}$$

$$CO + 3H_2 \leftrightarrow CH_4 + H_2O \tag{2.10}$$

- Gasification that involves carbon dioxide

$$C + CO_2 \leftrightarrow 2CO \tag{2.11}$$

$$C_nH_m + nCO_2 \leftrightarrow 2nCO + \frac{m}{2}H_2 \tag{2.12}$$

- Decomposition of tars reactions and hydrocarbons

$$pC_xH_y \rightarrow qC_nH_m + rH_2 \tag{2.13}$$

$$C_nH_m \rightarrow nC + \frac{m}{2}H_2 \tag{2.14}$$

Kayes & Tehzeeb (2009) reviewed different thermal processes applied to MSW for the generation of electricity. Several methods are reviewed such as thermochemical processes which consist of combustion, gasification, thermal depolymerisation, plasma arc gasification or pyrolysis (see Table 2.3 for main chemical processes). In addition to these thermochemical processes, there are biochemical processes which consist of anaerobic digestion, hydrolysis and mechanical biological treatment. The principle of some of these technologies mentioned above is to use incinerators to burn waste, whereas the rest do not use direct burning to extract energy from waste.

The main focus of waste to energy (WTE) is to use modern technologies to recover energy in the form of electricity and steam from MSW from the conversion of different materials such as paper, biomass, coal or plastic waste. Waste-to-energy technologies can be classified as either biochemical, chemical or thermal process. With regards to combustion, waste is fed continuously in a high temperature furnace where the temperature is constantly maintained around 800 - 1400 °C. Air is added to the combustion chamber to ensure complete combustion of waste (feedstock) until it reaches its natural and stable form of vapour and carbon dioxide (CO_2). The gases produced are later used in boilers to produce superheated steam that will drive turbines to generate electricity. In addition, other products such as steam can be used in district heating.

Table 2.3: Main characteristics of the chemical processes for thermal treatment of solid waste (adapted from Arena, 2012)

	Combustion	Gasification	Pyrolysis
Aim of the process	To maximize waste conversion to high temperature flue gases, mainly CO_2 and H_2O	To maximize waste conversion to high heating value fuel gases, mainly CO, H_2 and CH_4	To maximize thermal decomposition of solid waste gases and condensed phases
Operating conditions	Oxidizing	reducing	Total absence of any oxidant
Reactant gas	Air	Air, pure oxygen, oxygen enriched-air, steam	None
Temperature	Between 850 °C and 1200 °C	Between 550 °C and 900 °C (in air gasification) and 1000-1600 °C generally atmospheric	Between 500 °C and 800 °C
Produced gas	CO_2, H_2O	CO, H_2, CO_2, CH_4	CO, H_2, CH_4 and other hydrocarbons
Pollutants	SO_2, NO_2, HCl, particulate	H_2S, HCl, COS, NH_3, HCN, tar, alkali, particulate	H_2S, HCl, NH_3, HCN, tar, particulate
Ash	Bottom ash can be treated to recover ferrous (iron, steel) and non-ferrous metals (aluminium, copper and zinc) and inert materials. Air pollution control residues are generally treated and disposed as industrial waste	Bottom ash are often produced as vitreous slag that can be utilized as backfilling material for road construction	Often having a not negligible carbon content. Treated and disposed as industrial special waste
Gas cleaning	Treated in air pollution control units to meet the emission limits and then sent to the stack	It is possible to clean the syngas to meet the standards of chemicals production processes or those of high efficiency energy conversion devices	It is possible to clean the syngas to meet the standards of chemicals production processes or those of high efficiency energy conversion devices

2.3   Gasifiers

Selecting a gasifier design that will match the characteristics of the end-use applications is necessary. There are several technologies that are available for the gasification process with a broad range of reactors designed and used. These reactors can be grouped into three (3)

categories: fixed-bed (moving bed) gasifiers, fluidized-bed gasifiers and entrained-flow gasifiers. According to the needs of a specific application, the type of gasifier chosen will depend on:

- The production rate of energy required
- Operating pressure
- Operating temperature and the heating value of the gas: whether it is low or high heating value

2.3.1 Fixed-bed gasifier

Fixed-bed gasifiers as shown in Figure 2.4, are also called moving bed gasifiers and are characterised by a bed in which the feed enters from the top of the gasifier and move slowly downward. The feed is gasified by a counter-current of air or oxygen. The fuel and gas move in the same direction. The produced syngas serves to preheat and pyrolyse the downward flowing feed. Fixed-bed gasifiers are characterised firstly by low oxidant requirements, secondly by relative high methane content in syngas and lastly by the production of liquids such as tar and oils (Belgiorno et al., 2003). The resulting gas is high in temperature and contains almost no tars with a medium calorific value. Fixed bed gasifiers are limited in terms of fuel particle size distribution as well as in moisture content.
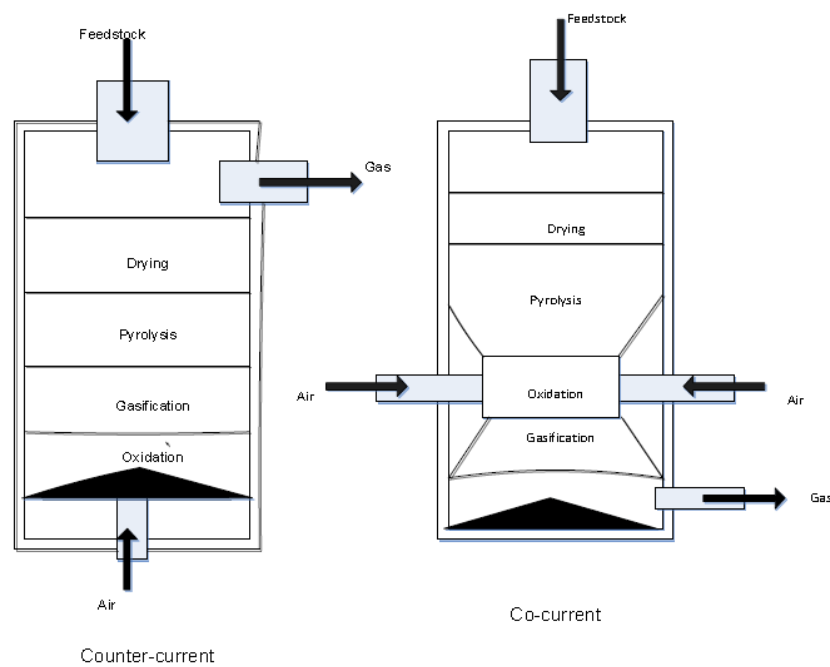
Figure 2.4: Example of fixed-bed gasifier (Akhator, 2014)

2.3.2 Fluidised bed gasifier

The feedstock in a fluidised bed gasifier as shown in Figure 2.5 is dried and introduced near the bottom of the gasifier. It is a gasifier in which new particles are constantly mixed with older, partially gasified and fully gasified particles. The flow of gas into the reactor (oxidant, steam and recycled syngas) has to be sufficient in order to float the feed particles within the bed. The gasified particles will become smaller and lighter and will be entrained out of the reactor. The residence time of the feed in a fluidised bed gasifier is less than that of a fixed-bed gasifier (Belgiorno et al., 2003). Fluidised bed gasifiers are characterised by extensive solid recycling, the temperature is uniform and moderates requirements of steam and oxygen.
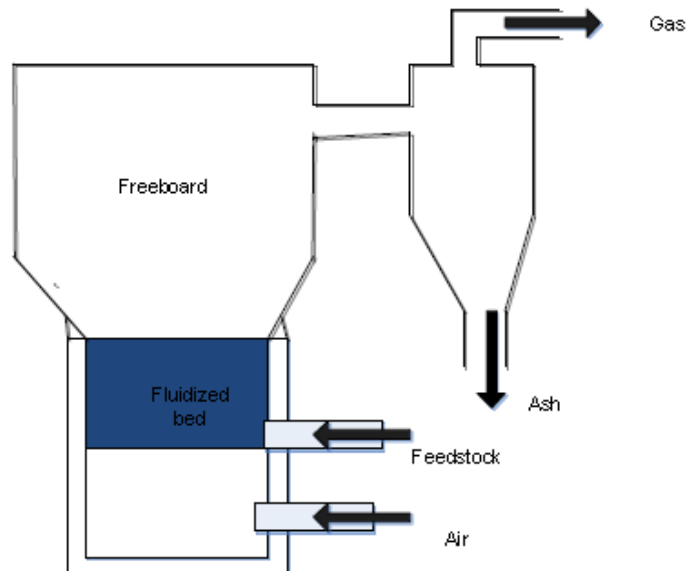
Figure 2.5: Schematic of a fluidized bed reactor (Akhator, 2014)

2.3.3 Entrained-flow gasifier

The feedstock in an entrained-flow gasifier as represented in Figure 2.6 is injected with the air or oxygen in the high. The feed rapidly heats up and reacts with the oxidant while moving downward and the residence time of an entrained flow gasifier is in order or seconds. Due to the short residence time, entrained-flow gasifiers must operate at high temperature in order to achieve high carbon conversion which is one of their characteristics. Entrained-flow gasifiers require relatively large amount of oxygen.
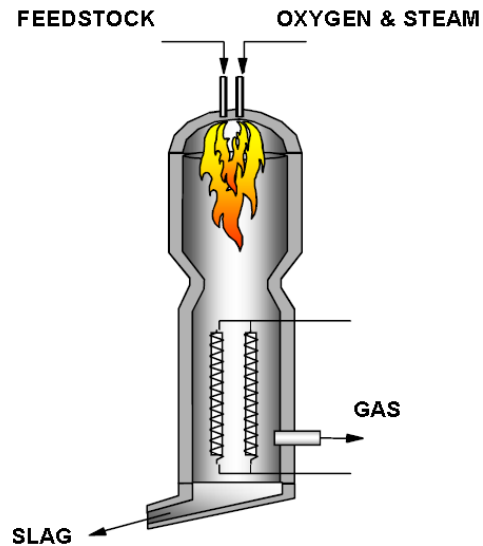
Figure 2.6: Entrained-flow gasifier (Kurkela, 2010)

Toledo et al. (2011) focused on the gasification of 100 wt% of plastic waste (polypropylene) with the objective of studying the effect of some operating variables such as different percentage of olivine in the gasifier bed and the temperature of the freeboard of the gasifier bed. These variables were studied to see the effect on the quality of the raw gas that is produced at the gasifier exit. It was found that the introduction of olivine into the gasifier as a bed material, influenced the gas composition at the exit of the gasifier and the amount of tar released was very low (tar content less than 2 g/m^3 under normal conditions 273.15 K and 1 atm). It was also discovered that the use of 100 wt% olivine in the bed of a fluidized-bed gasifier for plastic waste gasification with air significantly improves the quality of the gas produced.

As gasification is an alternative solution for energy production from plastic waste, several researches were conducted with regard to plastic waste elimination. Aznar et al. (2006) studied the treatment of plastic waste by co-gasification in fluidized-bed with air with feedstock composed with coal, biomass and plastic waste in various percentages respectively. The gas produced has minimum hydrogen content (up to 15 % of hydrogen percentage) and low tar content (less than 0.5 g/m^3_n). It was found that plastic waste could be added to coal or biomass without a change in the process. The elimination of plastic waste is achieved. Furthermore, a chemical recycling is also produced. For co-gasification with air, tar content can be reduced up to 50 %.

To improve the heating values of the gas produced, Pletka et al. (1998) performed experiments by means of indirectly heated gasification by using a pilot-scale fluidized bed gasifier. The method used for the process is an indirectly heated gasifier based on latent heat ballasting in order to produce a gas that contains higher energy compared to classical biomass gasification. The unit was evaporated with and without the latent heat ballast. Results show that the unballasted reactor processes less fuel than the ballasted reactor and the latter can process it more efficiently. Moreover, the pyrolytic gasifier produces a gas quality which is substantially higher than the one produced during air-blown gasification and has a dry gas with higher heating value.

By using an indirectly heated batch reactor, Baggio et al. (2009) implemented a thermochemical equilibrium model to describe the gasification/pyrolysis conversion yields. The experimental model designed for biomass gasification operates at variable pressure (1-7 bars) and set in an external furnace that is capable of reaching temperatures up to 1000 °C. A set of thermocouples were placed inside the reactor to monitor the temperature and several electric resistances were used as heating source with a maximum power of 10.5 kW at 230 V and up to a maximum work temperature of 1000 °C. The thermocouples were insulated by a refractory sheath and inserted into the furnace through the insulation layer. The model was validated by comparing the results of a thermal simulation of the system carried out with experimental measurements performed at atmospheric pressure and at peak temperatures of 600 °C or 800 °C. The internal temperature, the same as the syngas temperature has been assumed as the local conversion temperature used in the equilibrium model and its range in the pyrolysis zone varies from 400 °C and 500 °C and the peak temperature previously mentioned (600 °C or 800 °C). It was noticed that the biomass thermal conversion process starts with a significant production of CO_2, followed gradually by an increase of CO, CH_4 and H_2 in concentrations. The characterization of the pyrolysis and gasification processes are effective and occur between 1500 seconds and 3500 seconds run time and the steam coming from vaporization of water in the biomass feedstock is used for the gasification reactions as an acting agent (gasifying agent).

2.4   Comparison between gasifiers

Table 2.4 gives a summary of different gasifiers taken and adapted from (Bain, 2008).

Table 2.4: Gasifiers comparison

Gasifier	Advantages	Disadvantages
Fixed-bed (updraft)	Mature for heat Small scale applications Can handle high moisture No carbon in ash	Feed size limits High tar yields Scale limitations Producer gas Slagging potential
Fixed-bed (downdraft)	Small scale applications Low particulates Low tar	Feed size limits Scale limitations Producer gas Moisture sensitive
Fluidised bed	Large scale applications Feed characteristic Direct / indirect heating Can produce syngas	Medium tar yield Higher particle loading Excellent mixing characteristics
Entrained-flow	Can be scaled Potential for low tar Can produce syngas	Large amount of carrier gas Higher particle loading Particle size limits Potentially high in sulphur / carbon

2.5   Benefits of gasification

Below is a summary of some advantages of gasification (Arena & Mastellone, 2006; Brems et al., 2013; Arena, 2012; Stiegel & Rusell, 2001; Belgiorno et al., 2003):

- Gasification is environmentally friendly technology that produce low-cost electricity from solid feedstock
- Gasification technology offers both feedstock and product flexibilities
- Gasification generates less solid waste

- Gasification relies on oxygen rather than air
- Gasification can use high pressure and temperature in a reactor
- With gasification of bio-waste, the produced gas can be used directly in a gas turbine provided that the gas is cleaned significantly
- Gasification generates non-hazardous solid residues that can be used in construction materials without added disposal cost or further process to produced value-added products
- Larger molecules such as plastics are completely broken down into simple syngas components
- The resultant product from gasification can be directly used in landfill as it is non-hazardous without added disposal cost
- A wide range of feedstock can be used for plastic waste gasification in a reactor due to its flexibility

2.6   Disadvantages of gasification

Below is a summary of some disadvantages of gasification (Wu & Williams, 2010; Arena, 2012; McKendry, 2002; Consonni & Viganò, 2012:

- A lot of items in the waste are needed to be separated
- Feed size limits depending on the reactor used
- Gas released potentially high in sulphur
- Moisture sensitive
- Syngas treatment

The production of electricity from syngas can be accomplished in several ways with technologies such as combustion engines or gas turbines. Gas turbines are well-known for their high efficiency, low capital cost and especially at small scale application (Bridgwater et al., 2002).

2.7   Feedstock characteristics: Plastics

Plastic waste may possibly be a very good candidate for the gasification process. However, the characteristics of the feedstock determine the pre-processing, the use in a gasifier and as a result its efficiency. Plastic waste have different characteristics, in terms of size, shape, bulk density, energy content, chemical composition, ash melting. Therefore, plastic waste needs to

be resized from regular large sizes to about 5 cm or even less in diameter. The size of the feedstocks into a gasifier could have a large influence on not only the feeding process to run smoothly but also on the gasification performance. The study of thermoplastics, a type of plastics, is one of the focuses of this research project. Thermoplastics constitute in most part of the world the largest portion in the plastic waste stream (Shakya, 2007).

2.8   Syngas

Syngas, also called synthetic gas is a mixture of combustible gases such as carbon monoxide, hydrogen, nitrogen, carbon dioxide and methane (Consonni & Viganò, 2012). It can be used as fuel to generate steam or electricity. Moreover, it can also be used for a large number of applications in the petrochemical and refining industries as basic chemical building block as shown in Figure 2.7.

Luo et al. (2012) investigated the production of syngas by catalytic steam gasification of MSW in a fixed-bed reactor as well as the influence of the reactor temperature, steam to carbon ratio (S/C) and catalyst calcined dolomite (or NiO / $\gamma\text{-}Al_2O_3$) on the gas yield. Results show that the temperature has a significant influence on the catalytic steam gasification of MSW. As temperature increases in the reactor, syngas produced increases rapidly and carbon conversion efficiency. The highest gas yield was achieved at 900 °C. The increase of the gas yield with temperature is due to three factors: the greater production of syngas in the initial pyrolysis which is faster at high temperature, increased rate of endothermic reactions of gasification of char and increase in the steam cracking and reforming of the tars.

To measure the syngas composition and identify optimized conditions for wood gasification Begum et al. (2014) carried out experiments using a pilot scale gasifier. They developed and validated a numerical model using software to study the effect of air-fuel and steam fuel ratio on gas composition with a maximum variation in performance of 3 % between simulation and experimental results in terms of performance. Results showed that by increasing the amount of air, the produced gas H_2 and CO decrease while the volume of N_2 in the syngas increases. It was also shown that the amount of CH_4 remains almost the same while the composition of CO_2 decreases with very small deviation. The air-fuel ratio represents the O_2 quantity that is introduced into the reactor as well as the gasification temperature. The syngas quality can degrade due to an increased oxidation reaction when the air-fuel ratios are high. On the other

26

hand, a higher gasification temperature will mean higher-fuel ratios as well as acceleration in the gasification process with a better product quality. In addition, the concentration of syngas components are respectively 28 %, 20 %, 15 %, 11 % and 2 % for CO, H_2, N_2, CO_2 and CH_4 produced.
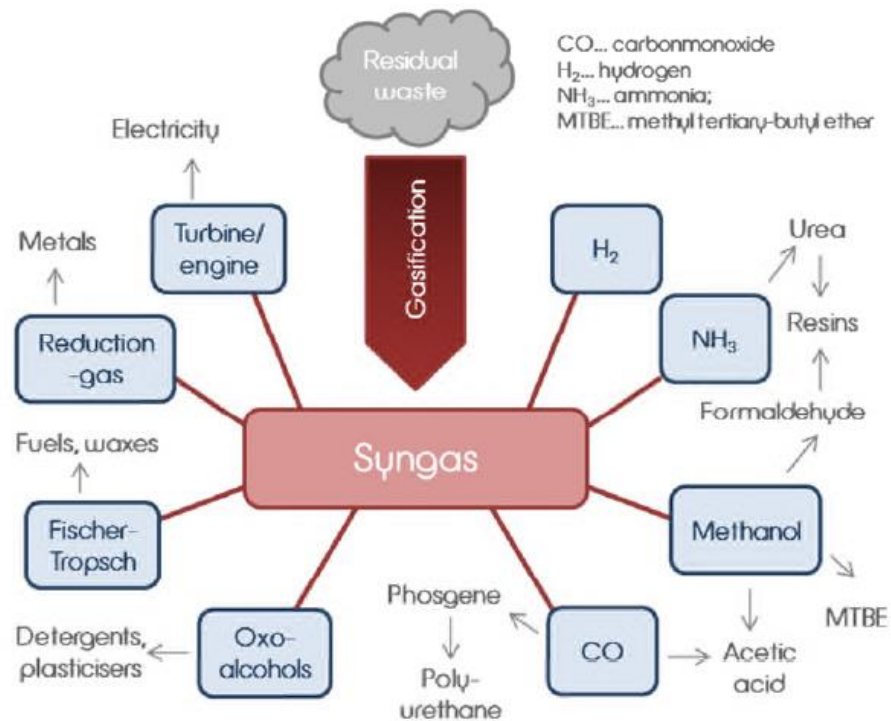
Figure 2.7: Different applications of syngas (Tiefenbacher, 2013)

2.9   Molecular structure of polymers

Polymer is a large molecule consisting of recurring structural units joined together, usually containing more than or at least five units (DMSE, 2015). Those structural units are derived from a compound called a monomer as shown in Figure 2.8:

- Linear polymers: polyethylene, nylon.
- Branched polymers
- Cross-linked polymers
- Network polymers

a) Linear polymers   b) Branched polymers

c) Cross-linked polymers   d) Network polymers
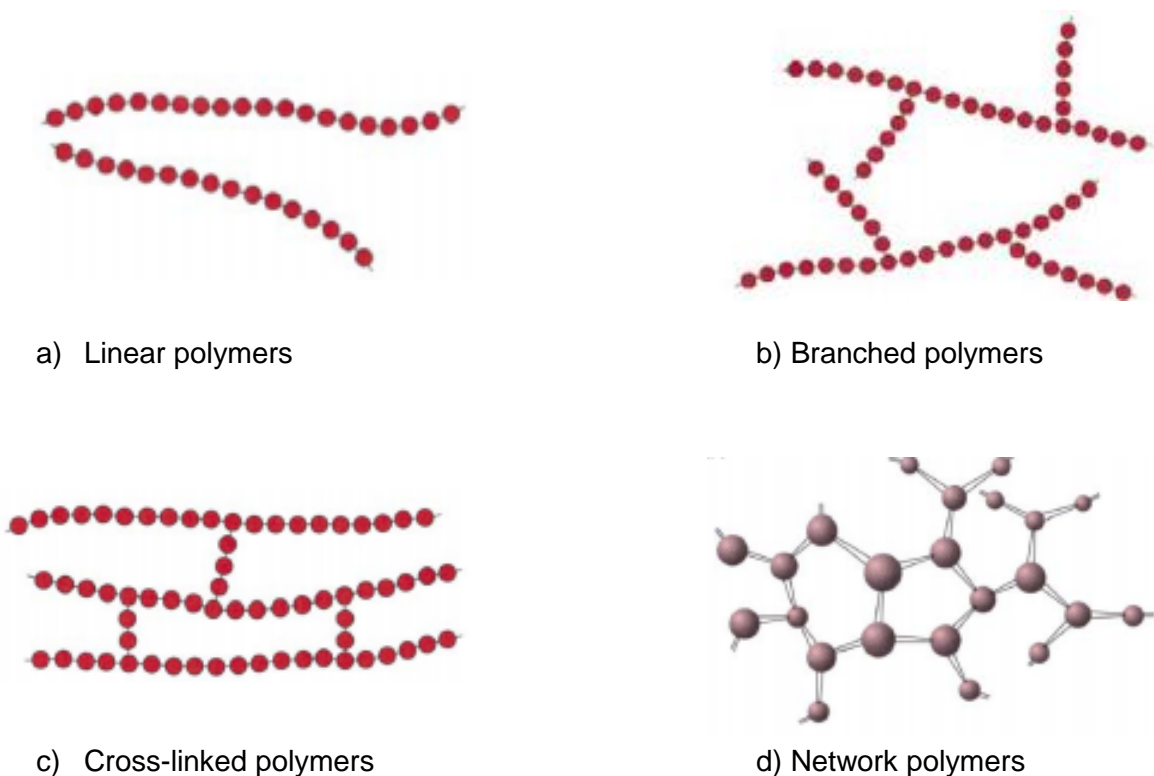
Figure 2.8: Molecular structure of polymers (DMSE, 2015)

With regards to general physical properties, three types of solid polymers are usually identified: elastomers, thermoplastics polymers and thermosetting polymers. Elastomers are rubberlike elastic materials. Thermoplastic polymers, at room temperature, are hard but when exposed to heat they become soft and can be moulded whereas thermosetting polymers at room temperature can be moulded but on heating they become hard.

2.10   Infrared radiation
2.10.1 Drying and freeze drying

Plastics can melt using infrared radiation, a method whereby heat is transferred and absorbed to the material without contact. Typical industrial applications using infrared radiation include curing or baking, drying and product heating. The following is a literature review on the use of infrared radiation.

A study on the effects of far infrared radiation on the freeze-drying of sweet potato in Taiwan was conducted (Lin et al., 2004). The authors noticed that as freeze-drying was an expensive process, other methods were conducted to evaluate a better drying effect on sweet potato within a shorter time. These methods were air-drying, freeze-drying and freeze-drying with far-infrared

radiation with the hypothesis that the utilisation of FIR could increase the drying efficiency, four models were developed. The first model is the Exponential model based on empirical model with Lewis model using the exponential equation whereas the second model is Page model which is an empirical modification of the exponential model by involving an additional exponential component. The third model used for the study was the diffusion model using Flick's equation model in the thin layer drying of foods (Lin et al., 2004). Lastly, the fourth model is an approximation of the diffusion model and it is based on the solution of the first term of infinite series of Flick's second law.

All these four models were developed and their accuracy was also investigated. For the study, a FIR radiator with a maximum power of 200 W and which emits thermal radiations within the wavelength range of 4 – 50 µm was used. The temperature of the heater was measured by K-type thermocouple. Lastly, the experiment was run for at least one hour to reach steady-state condition. Their results showed that freeze-drying with FIR uses less drying time according to the different size of potato cubes than those required by freeze-drying and air drying alone respectively. The authors also acknowledged that the size of sweet potato was an important influencing factor on the drying time and the utilisation of FIR freeze-drying proved a better result compared to freeze-drying and air drying. The latter took more time than the previous two method of drying. Finally, they discussed that FIR radiation provided an efficient heat transfer and agreed on the fact that Page model described properly the drying characteristics of freeze-drying with FIR radiation.

In addition, other researches were conducted with regards to drying technology on biological products (Wang & Sheng, 2004). The authors argued that FIR drying of biological products produces high drying rate when FIR heaters with high emissivity are used. For this reason, a model was developed through comparison of the simulation results with experimental data of black mushrooms. They agreed and suggested that the models for heat transfer and drying rate of biological products in the FIR dryer can be obtained by establishing the equation of radiation and dehydration in between elements. It was then found that the moisture content and drying rate vary. Moreover, the drying rate increases with the electric power that was supplied to the FIR heater and as a result, the temperature of samples also increases.

To develop a model, Wang & Sheng (2004) assumed that the FIR heater is composed of n-elementary surfaces and considered the biological products and any other material as gray body. As a result, equations of modelling of multi-layer FIR dryer were obtained such as the

effective radiation heat associated with the surfaces, the effective heat absorbed as well as the drying rate. K-type thermocouples were used to measure the temperature of FIR heaters and black mushrooms as biological product for the experiment. Results showed that calculated data satisfy the experimental ones within 16.6 % error. In addition, the moisture content and drying rate were not identical on elements of the dryer which is due to the geometry of the heater used. The results were, however, found to be satisfactory.

2.10.2 Radiative curing

To study the behaviour of polyester with triglycidylisocyanurate (TGIG) Vechot et al. (2006) investigated and established the thermal modelling of the cure process and kinetics studies. As background, they studied powder coating as opposed to organic solvent based system which tends to disappear due to regulations. They established some limitations on application of powder coating such as high melting point and the difficult usage on non-metallic support.

As far as modelling is concerned, the thermal behaviour of powder coating during curing is described with characteristics of curing kinetics, physical property and infrared curing efficiency. The latter shows that the efficiency of IR heating relies on the coatings spectral absorption characteristics and the spectral emission of the IR source. In addition, the results obtained described the experimental model of the curing process of polyester +TGIC and as a result, the authors believed the kinetics parameters do not change with the heating rate as from experiments on powder samples applied on identical metallic surface the heating rate didn't change for all IR emitters. It is also believed that medium wave infrared leads to the fastest cure due to the fact that at this wavelength, the IR absorption is significant.

Other applications of infrared heating are ray tracing method. Cosson et al. (2011) studied an infrared heating stage of the thermoplastic in infrared heaters. Ray tracing method is used to simulate radiative transfer. Numerical tools were developed to implement temperature calculation. Results showed that good knowledge of radiative properties of emittance and absorption are needed to get a good estimation of the temperature field.

CHAPTER 3 : A BRIEF THEORY OF INFRARED RADIATION

3.1 Introduction

The discovery of infrared occurred in the eighteen century by English astronomer Sir William Herschel. Herschel's approach was that human kind is warmed up with some "invisible rays", undetectable from human eye coming from the sun. He later on based all his work on these invisible rays also called infrared rays and was soon followed by other peers on the study of rays throughout centuries (Hudson, 2006).

Infrared rays lie under the invisible part of light on the electromagnetic spectrum and are divided into three rays, near infrared, mid-infrared and far- infrared (Hudson, 2006)**.**

The discovery of infrared has led to revolutionary techniques and applications in various domains such as science, technology and industry. It is used in the zone control of food handling and processes (Krishnamurthy et al., 2008), heating and drying applications on fruit (Adonis & Khan, 2008) and rice (Afzal & Abe, 1997).

3.2 Electromagnetic spectrum

Several types of radiation exist and are from diverse forms such as sunlight, heat, X-rays, radio-waves and gamma rays in the electromagnetic spectrum. Infrared rays are classified and described following their position on the electromagnetic spectrum as shown in Figure 3.1. Infrared radiations are organised by wavelength or frequency and following electromagnetic waves they obey the general Equation 3.1:

$$\lambda v = c \tag{3.1}$$

Where *c* represents the velocity of light, *v* the frequency and *λ* is the wavelength. Electromagnetic waves propagate at the velocity of light but are different in frequency and wavelength from one another.
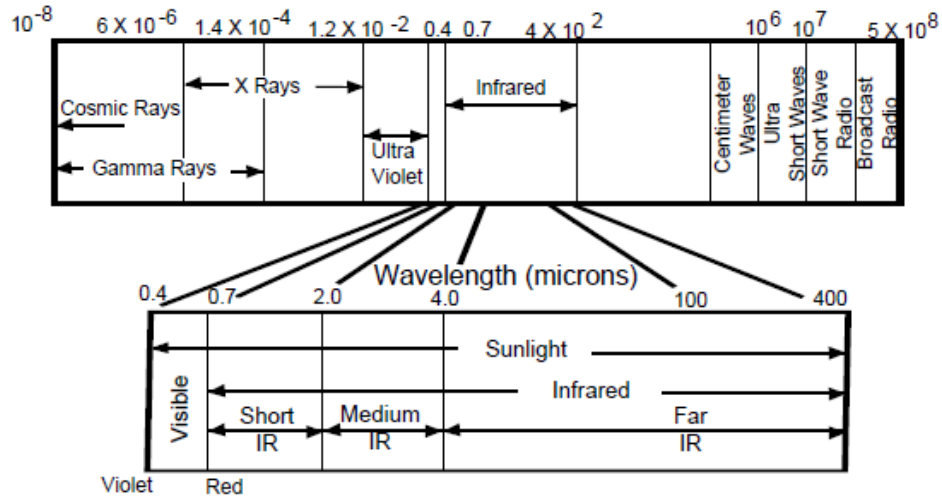
Figure 3.1: Electromagnetic wave spectrum (Watlow, 1997)

3.3 Modes of heat transfer

Heat transfer is the process by which energy moves from a hot source to a cold sink. Heat is transferred via three modes: conduction, convection and radiation. Conduction takes place when heat diffuses through a solid or a fluid which is not in motion within molecules and when a temperature gradient exists (Long, 2009). Convection takes place within molecules of fluid in motion. Heat transfer by radiation occurs when the energy is transmitted without the need of a medium and this is done by electromagnetic phenomenon. Heat transfer by thermal radiation takes place in the range of wavelength 0.1 µm to 100 µm. Although this phenomenon happens daily no one is aware of it as it takes place in the invisible part of light. Infrared radiation is divided in three subparts on the electromagnetic spectrum:

▪ Near Infrared (NIR): 0.76 – 2 µm
▪ Middle Infrared (MIR): 2 – 4 µm
▪ Far Infrared (FIR): 4 – 100 µm

The use of thermal radiation has become a dominant mode of heat transfer in low pressure because it does not require the use of medium to transfer energy (Bejan, 2003).

3.3.1 Conduction

Heat is transferred by conduction at a molecular level from one material to another and the material may be solid or fluid. Conduction heat transfer takes place when the temperature gradient exists in a medium (Long, 2009). Heat transfer by conduction is explained by Fourier's

law and is expressed in terms of heat flux Q, the temperature gradient $\frac{dT}{dx}$, the area A and the thermal conductivity k:

$$Q = -kA\frac{dT}{dx}$$
(3.2)

Or

$$q = -k\frac{dT}{dx}$$
(3.3)

The temperature gradient $\frac{dT}{dx}$ is always negative because the heat flows from high temperature to low temperature hence, down the temperature gradient. Moreover, the heat transfer by conduction is also characterised by its thermal diffusivity. Thermal diffusity describes the capability of a material to transfer thermal energy in relation to its capability to keep that energy (Long, 2009). The Equation 3.4 defines the thermal diffusivity as:

$$\alpha = \frac{thermal\ conductivity}{thermal\ capacity} = \frac{k}{\rho c}$$
(3.4)

Where:

ρ is the density, kg/m^3 of material and C_p is the specific heat capacity $J/kg\ K$

3.3.2 Convection

Heat transfer by convection is accomplished by motion of fluid. Newton's law of cooling rate expresses the convection heat transfer between a surface and a fluid.

$$Q = h_c A(T_1 - T_2)$$
(3.5)

Convection can be expressed in two ways depending on the nature of the flow as natural convection and forced convection. Figure 3.2 below is an illustration of it.
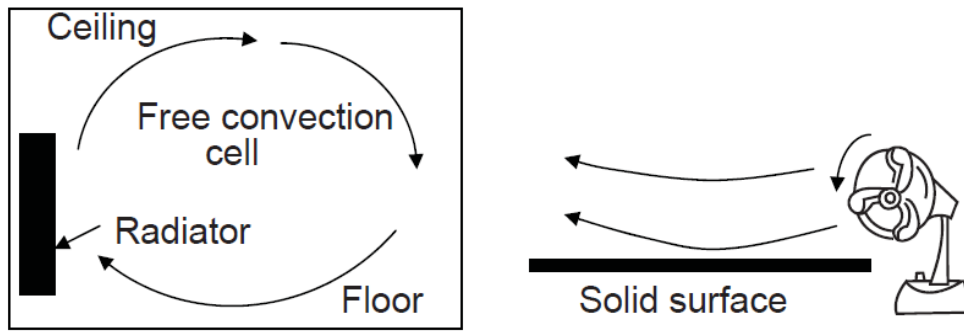
Figure 3.2: (a) Natural convection. (b) Forced convection (Long, 2009)

3.3.3 Thermal radiation

Thermal radiation is the rate of energy transferred from a surface to another by means of electromagnetic waves or photons. These photons are known to propagate through any medium at high velocity called the speed of light (Modest, 2003). The latter depends on the medium through which it travels. Thermal radiation does not require the use of a medium between elements as opposed to heat transfer by conduction and convection (see Figure 3.3). Thermal radiation is also proportional to the difference of temperature to the fourth power as expressed in Equation 3.6:

$$q \propto (T^4_1 - T^4_2) \tag{3.6}$$
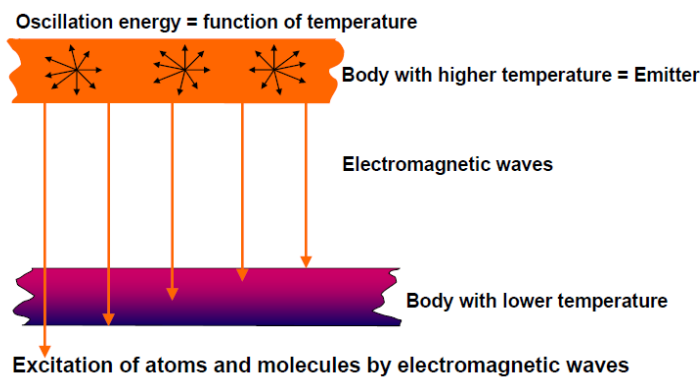
Figure 3.3: Heat transfer by IR Radiation (Heraeus, n.d.)

Infrared radiation as mentioned before can be classified into three ranges such as, near-infrared (NIR), mid-infrared (MIR) and far-infrared (FIR). The heat transferred to a surface is done by electromagnetic radiation and incident radiation may be absorbed, transmitted or reflected as shown in Figure 3.4.
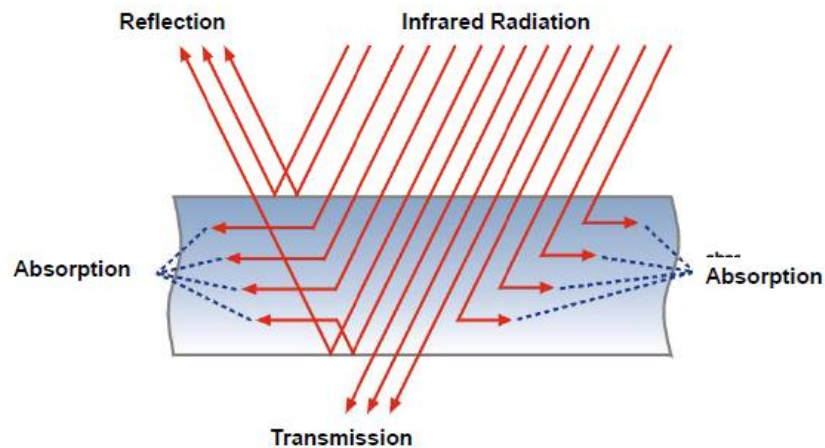
Figure 3.4: Absorption, transmission and reflection of Infrared radiation (Heraeus, 2011).

All materials have basic physical constants and thermodynamic properties. These constants are used in the evaluation of the materials and in heat energy calculations. The following constants and properties are used most often.

- **Specific heat,** C_p: it is the quantity of heat energy or thermal capacity of a certain material. All materials have or absorb heat energy in different amounts. The specific heat of most materials is constant at only one temperature and usually varies to some degree with temperature.
- **Thermal conductivity,** k: it is the ability of a material to transmit heat energy by conduction (see Figure 3.5 for range of thermal conductivity for various phases).
- **Thermal resistivity** R: it is the inverse of thermal conductivity. Insulating materials are rated by "R" factors. The higher the "R" factor, the more effective the insulation.
- **Heat of vaporization**: it is the energy requirements or amount of energy required from a material to change from liquid to gas (or reverse) at the same temperature.
- **Heat of fusion**: it is the energy requirements or the amount of energy required from a material to change from solid to liquid (or reverse) at the same temperature.
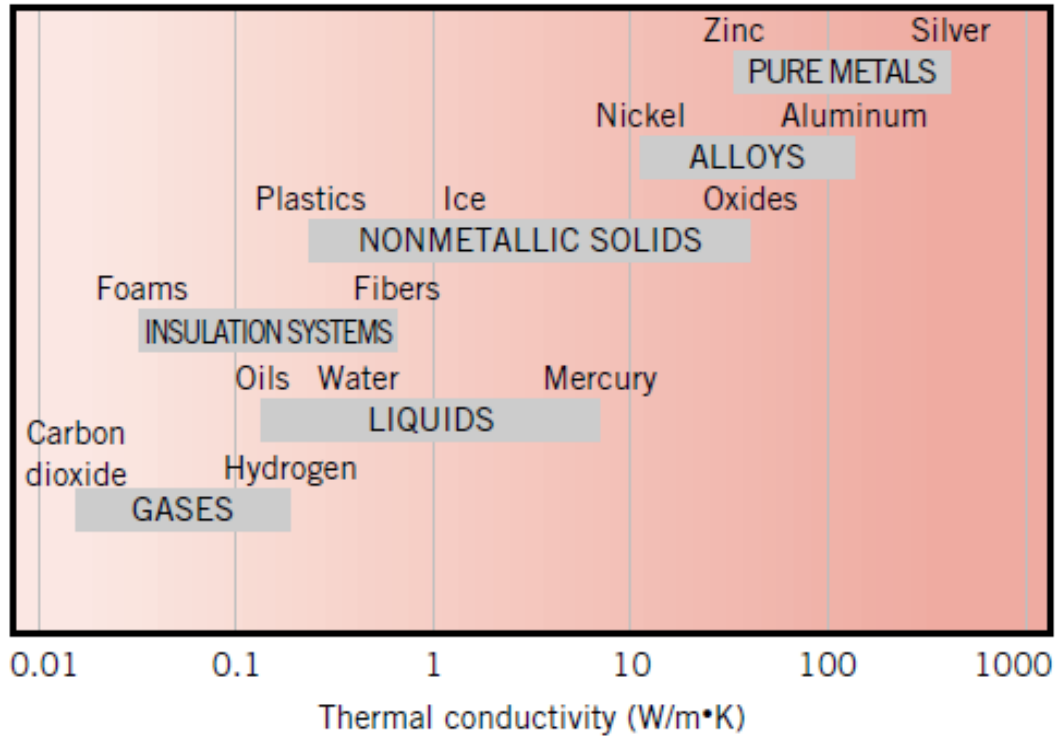
Figure 3.5: Range of thermal conductivity for various phases of matter at normal temperatures and pressure (Moran et al., 2003)

3.4 Characteristics of thermal radiation

3.4.1 Concept of blackbody

A blackbody may be viewed as an object that absorbs completely radiant energy. It is an ideal body that allows all the incident radiation to pass unto it and it absorbs all the incident radiation as illustrated in Figure 3.6. In other words it is a perfect absorber as it does not reflect nor transmit energy (Siegel & Howell, 1992).
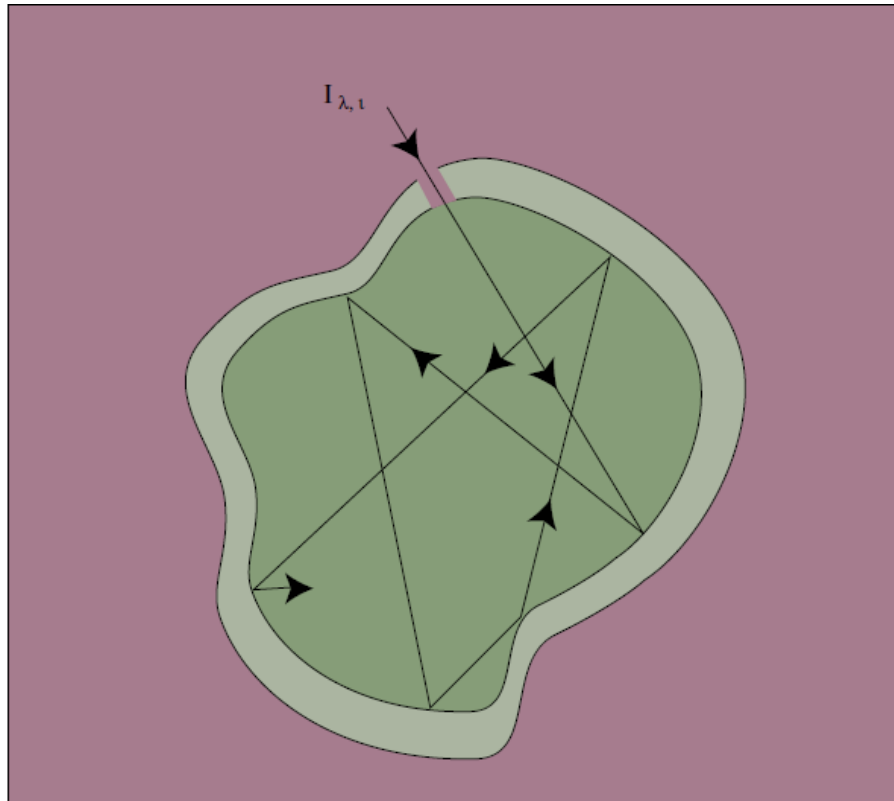
Figure 3.6: An Isothermal Blackbody Cavity (Omega, 1998)

3.4.2 Energy balance

Incident radiation may be absorbed, reflected or transmitted. The radiation energy balance (see Figure 3.7) expressed in a body is given in Equation 3.7 as:

$$\alpha + \tau + r = 1 \tag{3.7}$$

For opaque medium, $\tau = 0$ and $\alpha + r = 1$. The total emissivity for ceramic varies from $\varepsilon: 0.6 - 0.9$.
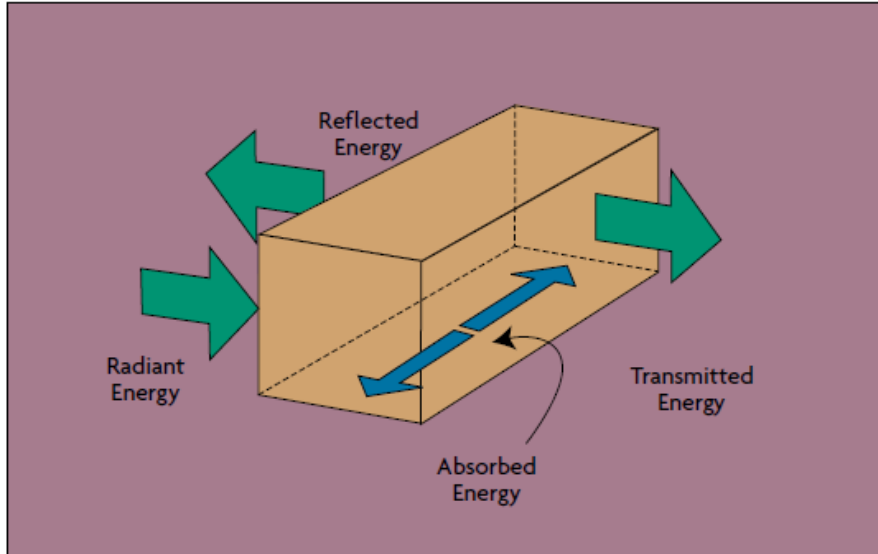
Figure 3.7: Radiation energy balance (Omega, 1998)

3.4.3 Planck's law

The heat transfer emitted by radiation or the emissive power (see Figure 3.9) from a blackbody stated in Equations 3.8 and 3.9 as:

$$E_b = \sigma T^4 \tag{3.8}$$

$$E_{\lambda,b}(\lambda, T) = \frac{C_1}{\lambda^5 (e^{C_2/\lambda T} - 1)} \tag{3.9}$$

Where
$$C_1 = 2\pi h C_0^2 = 3.7418 \times 10^8 \; W.\mu m^4/m^2$$

And
$$C_2 = \frac{hC_0}{k} = 1.4388 \times 10^4 \; \mu m.K$$

- The speed of light:
$$C_0 = 2.998 \times 10^8 \; m/s$$
- Planck's constant (see Figure 3.8):
$$h = 6.626 \times 10^{-34} \, J/s$$
- Boltzmann's constant :
$$k = 1.3806 \times 10^{-23} \, J/K$$
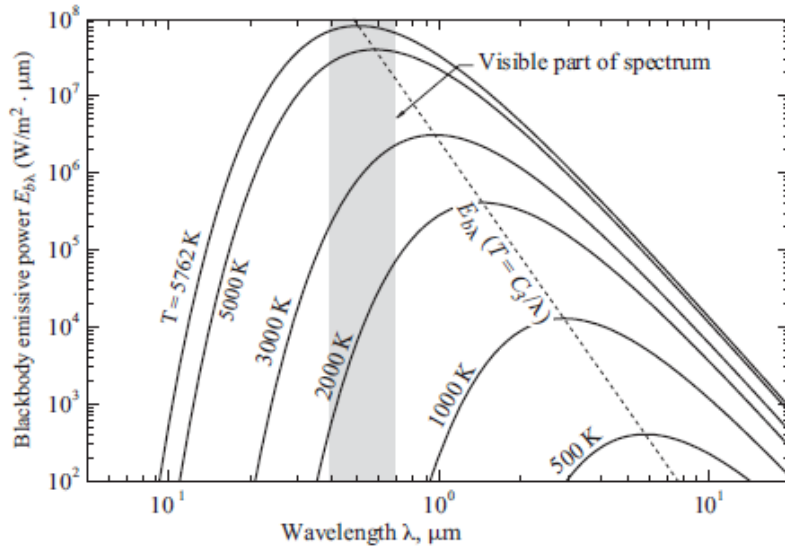
Figure 3.8: The Planck's distribution for a blackbody (Adrian Bejan, 2003)
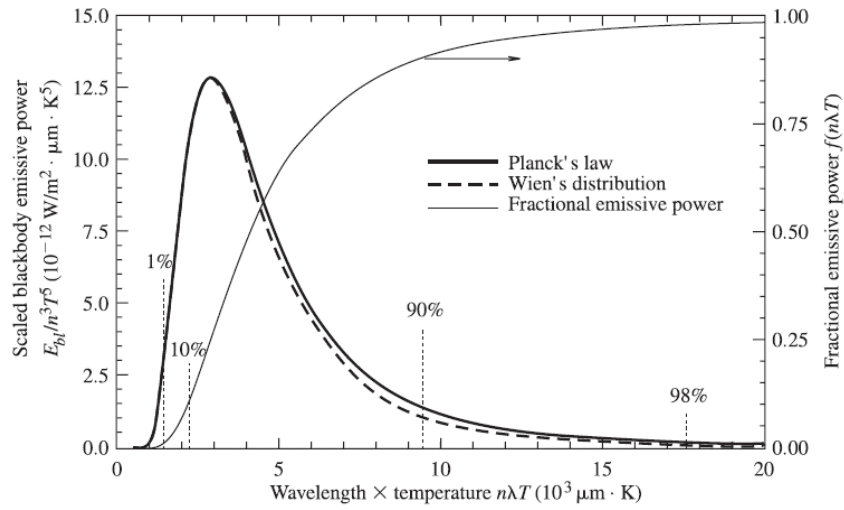
Figure 3.9: Normalized blackbody emissive power spectrum (Bejan & Kraus, 2003)

3.4.4 Wien's displacement law

Wien's displacement law is the wavelength at which the emissive power $E_{\lambda,b}$ (see Figure 3.10) is maximum.

$$\lambda_{max}T = 2897.8 \, \mu m.\,K \tag{3.10}$$

Radiative interchange between two blackbodies at T_1 and T_2

$$E_{b,1-2} = \sigma(T_1^4 - T_2^4) \tag{3.11}$$

Where $\sigma = 5.670 \times 10^{-8}\, W/(m^2.K^4)$, is the Stephan-Boltzmann constant

3.4.5   Emissivity, absorptivity, transmissivity, reflectivity

Emissivity: $\varepsilon = \dfrac{radiation\ emitted\ by\ actual\ surface}{radiation\ emitted\ by\ a\ blackbody} = \dfrac{E}{E_b}$ $\tag{3.12}$

Reflectivity: $r = \dfrac{portion\ of\ radiation\ reflected\ by\ the\ surface}{total\ irradiation} \cong \dfrac{G_{\lambda,ref(\lambda)}}{G_\lambda(\lambda)} \cong \dfrac{G_{ref}}{G}$ $\tag{3.13}$

Absorptivity: $\alpha = \dfrac{portion\ of\ radiation\ absorbed\ by\ the\ surface}{total\ irradiation} \cong \dfrac{G_{\lambda,abs(\lambda)}}{G_\lambda(\lambda)} \cong \dfrac{G_{abs}}{G}$ $\tag{3.14}$

Transmissivity $\tau = \dfrac{portion\ of\ radiation\ transmitted\ by\ the\ surface}{total\ irradiation} \cong \dfrac{G_{\lambda,tr(\lambda)}}{G_\lambda(\lambda)} \cong \dfrac{G_{tr}}{G}$ $\tag{3.15}$
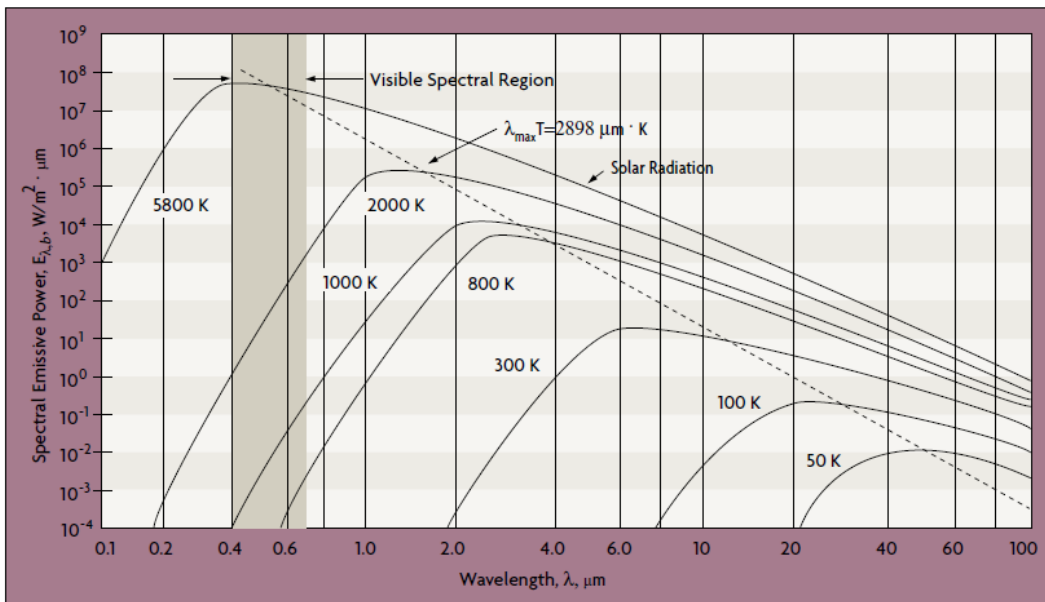
Figure 3.10: Planck prediction of blackbody emissive power (Omega, 1998)

3.5 Spectral absorption of some plastics

The wavelength produced by the heat source is dependent of the heat source temperature. The temperature can be adjusted and thus the peak wavelength to match spectral absorption rate (or wavelength) of plastics. For infrared energy absorption by plastics, it can be determined the wavelength corresponding provided that the element temperature is known.

$$°C = \frac{2897}{\mu} - 273 \tag{3.16}$$

Then the desired wavelength can be determined:

$$\mu = \frac{2897}{273+°C} \tag{3.17}$$

The emissivity factor describes how well a material absorbs infrared. Figure 3.11 to Figure 3.14 show the spectral absorption rate of different plastics such as PP, PS, PE, and PVC. The emissivity/conversion ratio of ceramic heater is from 90 % which means that the infrared energy produced by the ceramic infrared heater is absorbed during the process.
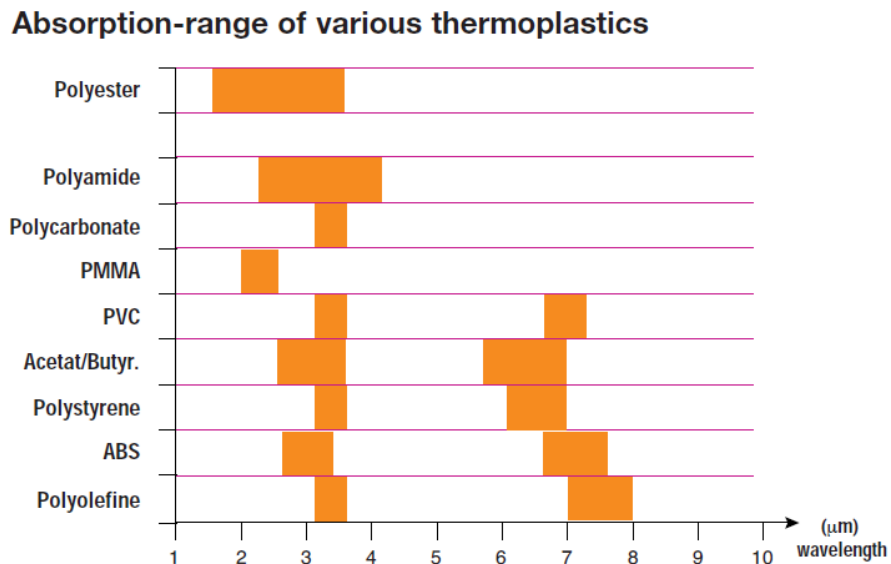
Figure 3.11: Absorption range of various thermoplastics (Krelus Infrared, 2011)
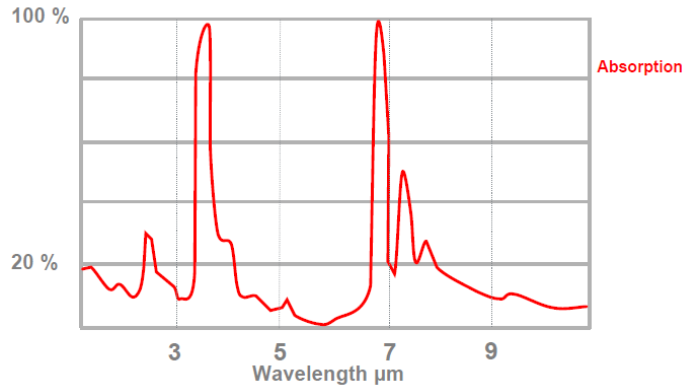
Figure 3.12: Spectral absorption of Polyethylene 0.1 mm (Heraeus, n.d.)
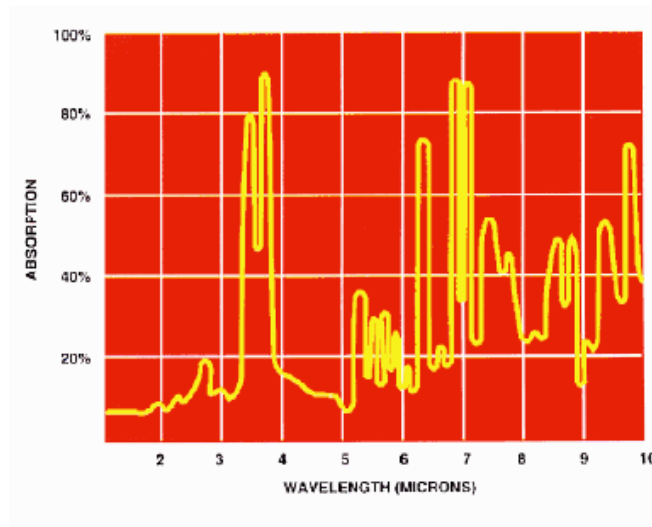
Figure 3.13: Spectral absorption of Polystyrene (Deltat, n.d.)
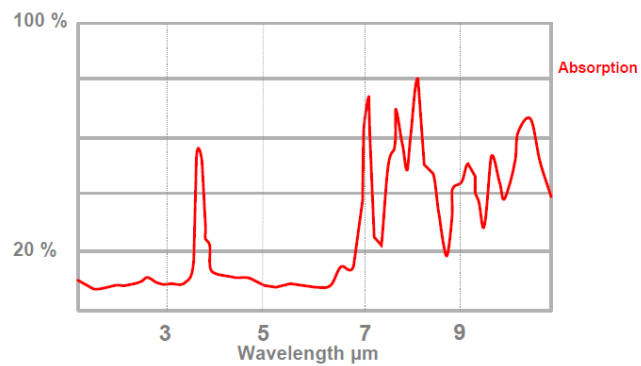
Figure 3.14: Spectral absorption of Polyvinyl Chloride 0.02 mm (Heraeus, n.d.)

42

3.6 View factor

The view factor is the fraction of radiation emitted from one surface that is incident to another surface.

$$F_{ij} = \frac{1}{\pi A_i} \int_{Aj} \int_{Ai} \frac{\cos\theta_i \cos\theta_j dA_i dA_j}{r^2} \tag{3.18}$$

The symmetry between the surfaces i and j gives:

$$F_{ji} = \frac{1}{\pi A_j} \int_{Ai} \int_{Aj} \frac{\cos\theta_i \cos\theta_j dAj dA_i}{r^2} \tag{3.19}$$

The reciprocity rule is expressed as:

$$A_i F_{ij} = A_j F_{ji} \tag{3.20}$$

The summation rule is expressed as:

$$\sum_{j=1}^{N} F_{ij} = 1 \tag{3.21}$$

The net radiation leaving a surface i is expressed as:

$$Q_i = A_i(J_i - G_i) \tag{3.22}$$

Using the definition of emissivity: $J_i = r_i G_i + \varepsilon_i E_{b,i}$

For opaque solid surface, $\tau = 0, r = (1 - \alpha) = (1 - \varepsilon)$

Therefore $\qquad \dfrac{Q_i}{A_i} = \dfrac{E_{b,i} - J_i}{\frac{1-\varepsilon_i}{\varepsilon_i}}$ $\qquad\qquad$ (3.23)

The total radiation falling on the surface i due to irradiation from all other surfaces

$$A_i G_i = \sum_{j=1}^{N} F_{ij} A_i J_j \tag{3.24}$$

$$Q_i = J_i - \sum_{j=1}^{N} F_{ij} J_i \tag{3.25}$$

Heat flow in term of radiosity is:

$$Q_i = A_i \sum_{j=1}^{N} F_{ij} (J_i - J_j) \tag{3.26}$$

The spectral irradiation is the degree at which the radiation of wavelength λ is incident on surface per unit per area:

$$G_\lambda(\lambda) = \int_0^{2\pi} \int_0^{\frac{\pi}{2}} I_\lambda(\lambda, \theta, \phi) \cos\theta \sin\theta \, d\theta d\phi \tag{3.27}$$

$$G = \int_0^\infty G_\lambda(\lambda) \, d\lambda \tag{3.28}$$

3.7 Classifications of infrared heaters, industrial heaters and module

Electric infrared heaters produce radiant heat through the ohmic heating effect of an electric current that flows through a spiral coil of wire such as a tungsten filament or a suitable heating element alloy (Heraeus, 2011). The surface temperatures of heaters are in the range of 400 °C to 2200 °C.

Electric ceramic heaters normally operate within a surface temperature range of 300 °C to 700 °C. The large emitting area of ceramic infrared heaters allows an important proportion of the input power to emerge as heat by convection to the surrounding air. Ceramic heaters have an embedded coiled heating element usually of nickel chrome alloy and their glazed ceramic body protects against thermal shock as well as prevents attack by atmospheric oxygen. Ceramic heater life span is in the order of several years and the radiated energy is in the long wave band on the wavelength spectrum with it peak emission between 3 and 5 microns.

CHAPTER 4 : IR REACTOR DESIGN AND NUMERICAL MODEL DEVELOPMENT

This chapter introduces the concept of a small laboratory scale gasification plant including the infrared reactor design as well as the numerical model development. Several industries are using infrared heating technology for diverse applications such as food processing, drying, paint curing and in prevention of hypothermia with premature infants (Roongprasert et al., 2013).

Thermochemical processes require appropriate models that consider diverse working conditions for simulation and optimization of suitable reactors. The model developed describes the proof of concept of the IR reactor for the gasification of plastic waste and the total heat change or accumulated heat of the system which is given with regards to the generated, heat conducted and heat convected throughout the volume of the reactor.

4.1 Small laboratory scale gasification plant

The gasification plant is aimed for power generation. The plastic feedstock (LDPE or HDPE) is put in IR reactor built with four infrared heaters through a feeding tube where the temperature is maintained at 600 °C to ensure a rapid gasification. The reactor is airtight, the syngas produced from the gasification (H_2, N_2, CO and CO_2 mainly) is sent to a catalytic water gas shift (WGS) stage to enhance the hydrogen production by concentrating the syngas thermal energy in the form of hydrogen and carbon dioxide with partial oxidation for fuel cell application and electric power generation. Part of the power produced will be used for the plant sustainability. The present project is limited to the IR reactor optimization.

Gasification enables the use of waste being available locally and converts it into fuel gas. The latter can be utilized with better efficiency than converting it with direct combustion. The gasification performance depends on the reactor technology as well as on the reactants type and the operating conditions such as temperature and pressure (Mastellone & Zaccariello, 2013).

The design of the gasification plant as referred in Figure. 4.1 is based on a process that is able to generate fuel / energy from waste plastic material using infrared reactor composed of ceramic heaters to gasify the waste in order to generate syngas. The syngas is then processed in order to generate pure hydrogen to be stored in a fuel cell with the following emphasis:

- Syngas production for use in gas turbine: Gas produced from the gasifier should be subjected to further analysis in order to quantify and identify the constituents. The syngas generated from the IR reactor can be fed directly to a gas turbine to generate power. The exhaust gases from the turbine (hydrogen and carbon dioxide) can be captured. The hydrogen can be used for the fuel cell whilst the CO_2 can be sequestered or liquefied depending on the purity thereof.

- Energy / heat optimization of the entire process: This is done by using the IR reactor exhaust (syngas) to generate steam for the process. A required amount of the steam will be feed to the reactor whilst the excess steam can be fed to a steam turbine/engine.

- Hydrogen production for storage: The hydrogen will be produced via a water gas shift (WGS) reactor which converts the carbon monoxide (CO) from the produced syngas to H_2 and CO_2. The reactor is a packed bed reactor that will be packed with a high performance catalyst. The operating conditions of the reactor have to be optimized in order to generate a high yield of hydrogen for storage. The hydrogen will potentially be stored in a storage canister. Before storage the product gas must be subjected to a GC analysis.
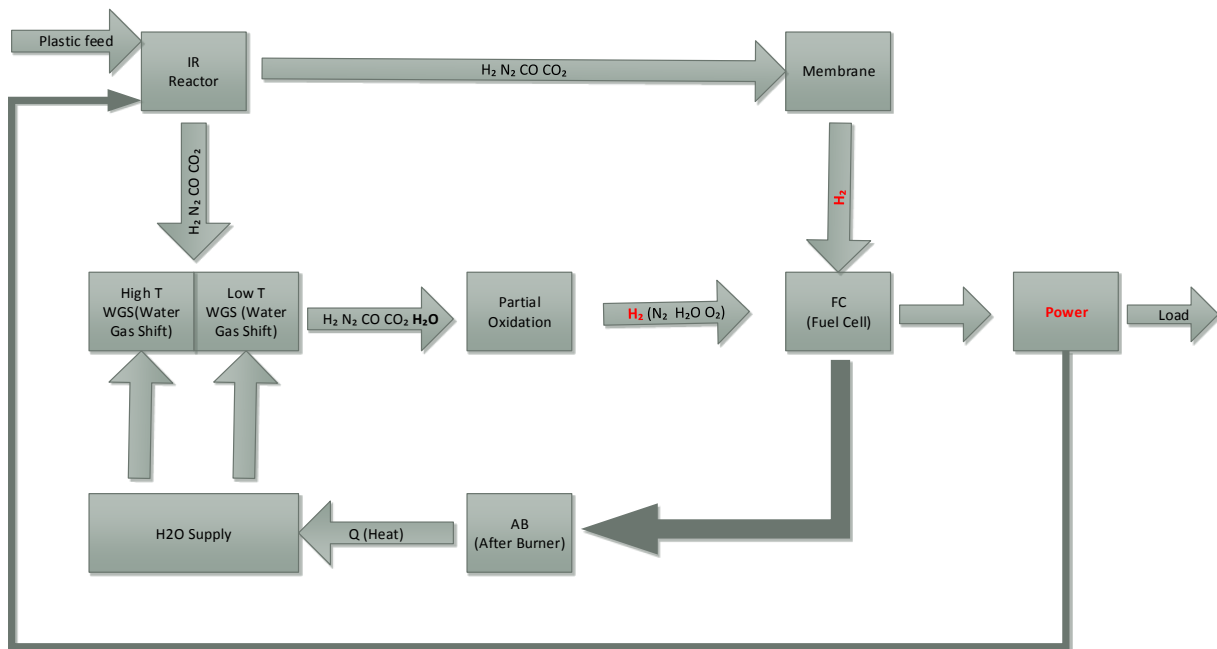
Figure 4.1: Gasification schematic diagram

Gasification application offers opportunities for electricity generation and may be a profitable opportunity for commercial exploitation of biomass and waste. There are current projects pursuing sustainable gasification systems for the generation of several forms of energy as described in Table 4.1. However, the level required for syngas purity differ extensively for different downstream applications. In this perspective, for power generation, syngas quality required is lower than other applications.

Table 4.1: Electrical efficiency of gasification plant (adapted from (Di Gregorio, 2013))

Energy conversion device	Net electrical efficiency of gasification plant	Level required for gas cleaning
		Tar
Steam turbine	15 – 24 %	Not limited
Organic Rankine plant	15 – 18 %	Not limited
Gas engine	13 – 28 %	< 50 mg/m^3_N
Gas turbine	20 – 30 %	< 10 mg/m^3_N

4.2   Classification of infrared heaters

IR heaters are generally classified into three categories according to their radiation wavelength: short, medium and long wave. However, due to boundary not being precise between the categories, it is difficult to determine their fixed range with regards to their wavelength as they overlap. Electric infrared heaters produce radiant heat through the ohmic heating effect of an electric current that flows through a spiral coil of wire such as a tungsten filament or a suitable heating element alloy (see Figure 4.2). The surface temperatures of heaters are in the range of 400 °C to 2200 °C.

- **Short-wave infrared heaters**: they emit energy between 1 and 1.2 microns with energy densities between 100 and 310 kW per square meters.
- **Medium-wave infrared heaters**: they emit energy between 2.4 and 4 microns.
- **Long-wave infrared heaters**: they emit energy between 4 and 6 microns with their energy densities between 5 to 23 W per square meter.

All heaters (emitters) have three different constituents:

- The source of the energy which may be the coil, foil or filament wire.

- The reflector or source support that directs the heat or supports the filament
- The face that electrically insulates the source and acts either as a window to allow all primary radiation to pass through or as an absorber that will absorb the heat and release that heat as secondary radiation (Solar Products Inc., The Infrared Heater Company, 2007).

Electrical energy is produced by filament wire and converted into thermal energy

Thermal energy in filament wire is transferred to heater surface by conduction

Thermal energy from heater is transferred to surroundings in the reactor via Convection / Radiation
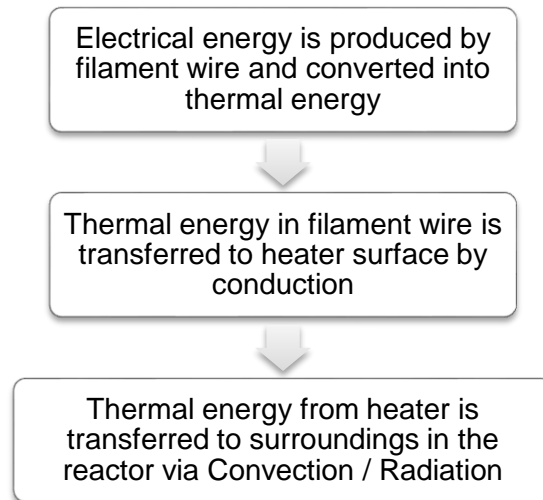
Figure 4.2: Heating process of infrared heater

Any infrared emitter has its own distinctive sets of properties meaning radiant efficiency, physical strength, and heat-up and cooling times, maximum temperature and colour sensitivity and maximum radiant wavelength). Those properties are defined as:

- **Radiant Efficiency** is the total amount of energy emitted from the source as infrared radiation, the rest of the energy from the sources is transferred via convection and conduction and / or radiation.
- **Physical Strength** is the mechanical strength of an emitter. A high rating indicates a very durable source that can withstand physical shock.
- **Heat-up / cool down** time is the amount of time required for the emitter to rise up to operating temperature and cool down to room temperature.
- **Maximum Temperature** is the maximum operating temperature of an emitter.
- **Colour sensitivity** is the ability of a material to absorb the spectral radiation emitted from a source based on the colour of the material. It occurs more often with short wavelength emitters. The shorter the wavelength emitted from a source the more colour

sensitive a load will be to the sources spectral radiation. Medium and longwave heaters are not colour sensitive.

4.2.1 Quartz lamp heaters

The filament temperature of quartz lamp heater shown in Figure 4.3 can be greater than 2000 °C with an output power that can range from 0 to 7874.02 Watts per meter and this depends on the input voltage. The heater lamp has sealed ends and it is filled with inert gas that surrounds the tungsten filament. The latter is suspended so that there is no contact with the quartz. The heating response time is within few seconds.
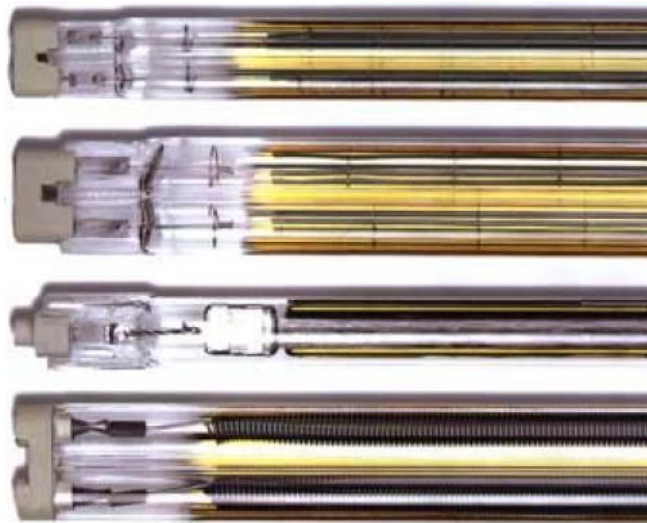
Figure 4.3: Quartz lamps (Heraeus, 2011)

4.2.2 Quartz tube radiant heaters:

Quartz tube radiant heaters as shown in Figure 4.4 are generally used for bathroom heating, cooking and in the medical field. Their operating temperature is 950 °C. Compared with the quartz lamp heater, quartz tubes have a maximum operating temperature that will depend on the heating wire coil (nichrome) which has open ends. There is a minimal contact between the filament wire and the quartz tube inner wall. The heater output power ranges from 0 to 1968.50 watts per meter and this is dependent on the input voltage. The input power is converted into

radiant heat at an efficiency of approximately 60 %. The heating response time is within 120 seconds with a peak wavelength that is around 2.5 μm.

Figure 4.4: Quartz tubes (Heraeus, 2011)

4.2.3 Panel heaters

Panel heaters (Figure 4.5) are mounted in channels on the rear side of a quartz window and the whole assembly is contained in a steel case. The temperatures are in the range of 500 to 950 °C from a uniform distribution of heat obtained across the emitting surface. Power intensities are about 40 kW/m^2. Panel heaters have heating and cooling times rather slower which can be as long as 5 to 15 minutes due to their large mass.
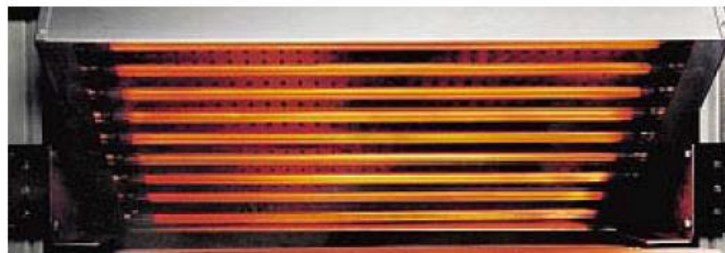
Figure 4.5: Panel heaters (Heraeus, 2011)

4.2.4 Metal sheathed heaters

Metal sheathed heaters as shown in Figure 4.6, use tube-shaped rods, commonly used as boiling rings and grill elements on electric cookers. The resistive heating elements are spiral mounted inside a tubular metal sheath and made of nickel-chrome. An electrical insulation is between the two parts of the heater. As a result, the sheath can operate safely at ground potential. Metal sheathed heaters have an operating temperature of 850 °C, although it is

recommended to operate the heaters at a temperature of 750 °C to maintain a long operating life. Table 4.2 presents heater specifications at various wavelengths and temperatures.

Figure 4.6: Metal sheathed elements (Heraeus, 2011)

Table 4.2: Heater comparisons adapted from (Heraeus, 2011) and (Anon., n.d.)

Characteristics parameters		Quartz lamps	Quartz tube heater	Radiant panel heater	Metal sheathed element	Ceramic heater
Coiled heating element		Tungsten filament wire	Nickel Chrome Spiral winding	Fe-Cr-Al	Nickel chrome	Nickel chrome alloy
Radiated energy		Shortwave	Medium wave band	Long wave band	Medium wave band	Longwave band
Radiation emission efficiency		72 - 86 %	40 - 60 %	88 %	45 - 56 %	96 %
Operative temperature		1649°C - 2204°C	760°C - 950 °C	500 - 950 °C	Up to 850 °C	300 – 700 °C
Luminous Emission colour		Bright white	Cherry red	No visible light	Dull red	No visible light
Peak Energy wavelength range		1.15 – 1.5 microns	2.3 - 2.8 microns	3.2 – 6 microns	2.8 - 4 microns	3.3 – 5.7 microns
Qualitative response time	**Heat up**	Seconds	Minutes	Slow: 5 – 15 minutes	Minutes	Slow: 3 – 4 minutes
	Cool down	Seconds	Seconds	Several minutes: 5 - 15 minutes	Minutes	Several minutes: 3 - 4 minutes
Power rating			Up to 8 kW			125 – 1000 W
Input power conversion		72 – 86%	60 %	20 – 50%	45 – 53%	Up to 95%

Emissivity of the unit		0.8			0.9
Applications		Drying, solder reflow, curing, moisture removal…	Drying in paper mills, wallpaper production	Paint curing, moisture removal, cooking…	Drying, preheating…

4.2.5 Electric infrared ceramic heater

Electric IR ceramic heaters are designed with a coiled heating element wire such as iron, chrome or aluminium alloy with high emissivity; they are also designed according to their shape, and also depending upon the presence or absence of reflectors. They are manufactured to pass electric current across the filament and the large emitting area of the heaters allows an important proportion of the input power to emerge as heat by convection to the surrounding air. The filament determines the energy characteristics and efficiency for ceramic heaters. IR ceramic heaters normally operate within a surface temperature range of 300 °C to 700 °C. The wire is embedded inside the ceramic materials to protect against thermal shock as well as to prevent any attack by atmospheric oxygen. The whole system is conceived to prevent any damage and oxidation and corrosion (Das & Das, 2010). IR heaters are energy efficient with efficiency of about 95 % and can radiate from medium-wave to long-wave spectrum. It is found in the literature (Das & Das, 2010) that peak values of radiation vary between 3.3 and 5.7 µm. A ceramic heater life span is in the order of several years.

4.3 Infrared reactor gasifier
4.3.1 IR reactor description

The developed IR reactor is a packed bed reactor equipped with four electric infrared ceramic heaters. The heater dimensions are 125x125 mm, model UHI-LYTHTS-0250 from ELSTEIN. The IR reactor consists of a tube and the whole length is 336 mm. The external diameter of the inlet and outlet is 300 mm and 330 mm respectively. The whole reactor is made of stainless steel material. The tubes are separated with heat insulation fibre blanket that can withstand high temperatures up to 1300 °C. A plastic pellet holding tray at the bottom of the tube is removable and made of fine wire mesh. The tray is a cylinder of 200 mm diameter and 250 mm height. The heaters are operating at a maximum temperature of 900 °C individually. The gasification process takes place at standard atmospheric pressure and the reactor is airtight.

The different schematic views of the gasifier design can be seen in Figure 4.7 to Figure 4.9. The visual views of the reactor with ceramic heaters are in Figures 4.10 and Figure 4.11 and the reactor mesh that holds the plastics during experiment is shown in Figure 4.12. The top of the reactor has a smoke filter for the yield gases that will be possible during the gasification process and can be connected to the purification plant shown in Figure 4.13.
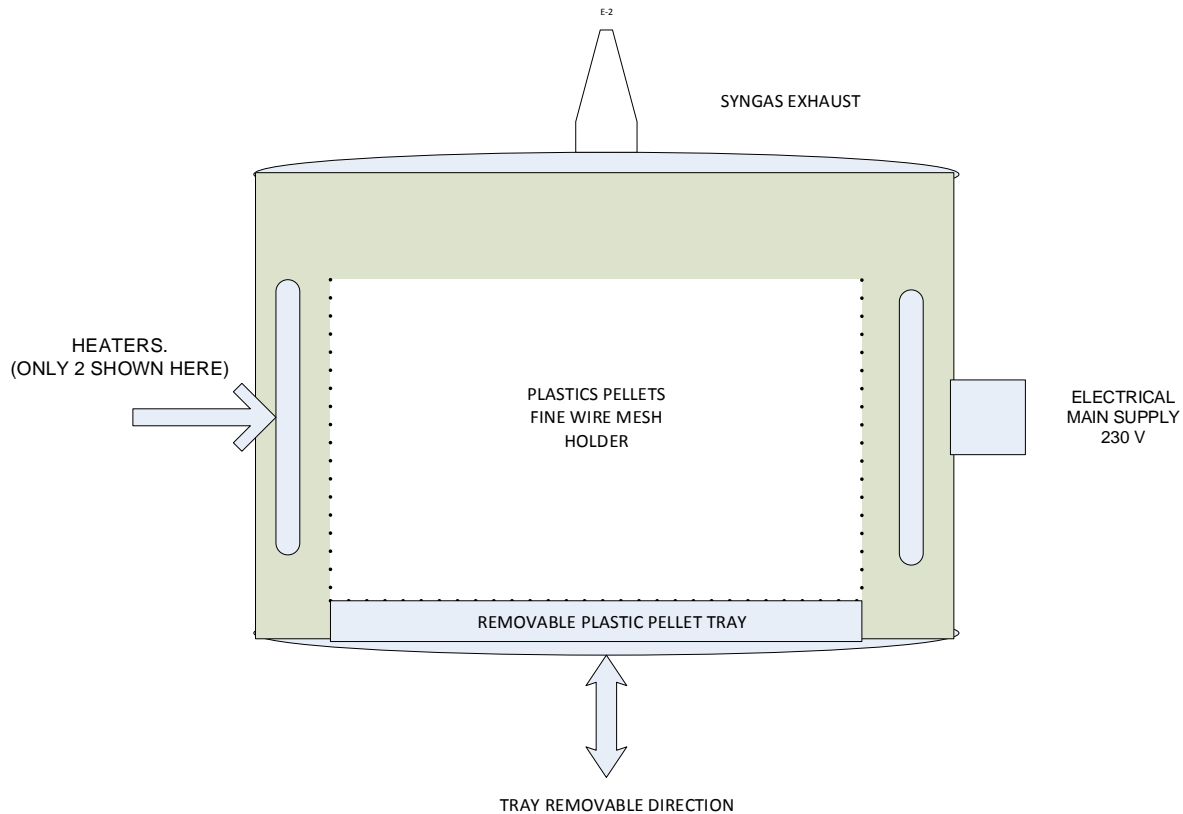
Figure 4.7: IR Reactor side and internal view

E-2

SYNGAS EXHAUST

ELECTRICAL
MAIN SUPPLY
230 V
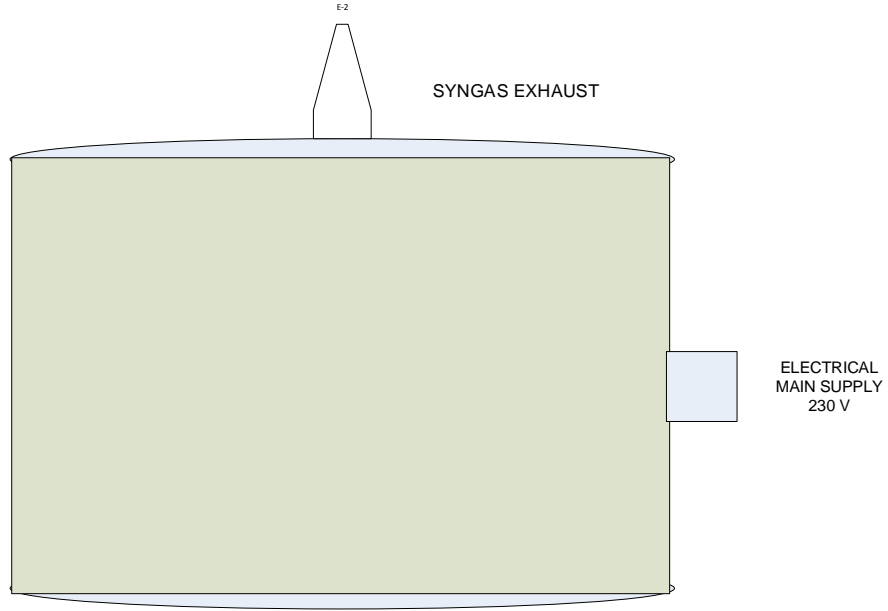
Figure 4.8: IR reactor side view

INNER CYLINDER

Ceramic
Heater
125 x
125
mm

Wire mesh holder
for plastics pellets

Ceramic
Heater
125 x
125
mm

Ceramic
Heater
125 x
125
mm

HEATER
ELECTRICAL
CONNECTION
TO THE SUPPLY

OUTER CYLINDER

SYNGAS EXHAUST

HEAT INSULATION

Ceramic
Heater
125 x
125
mm
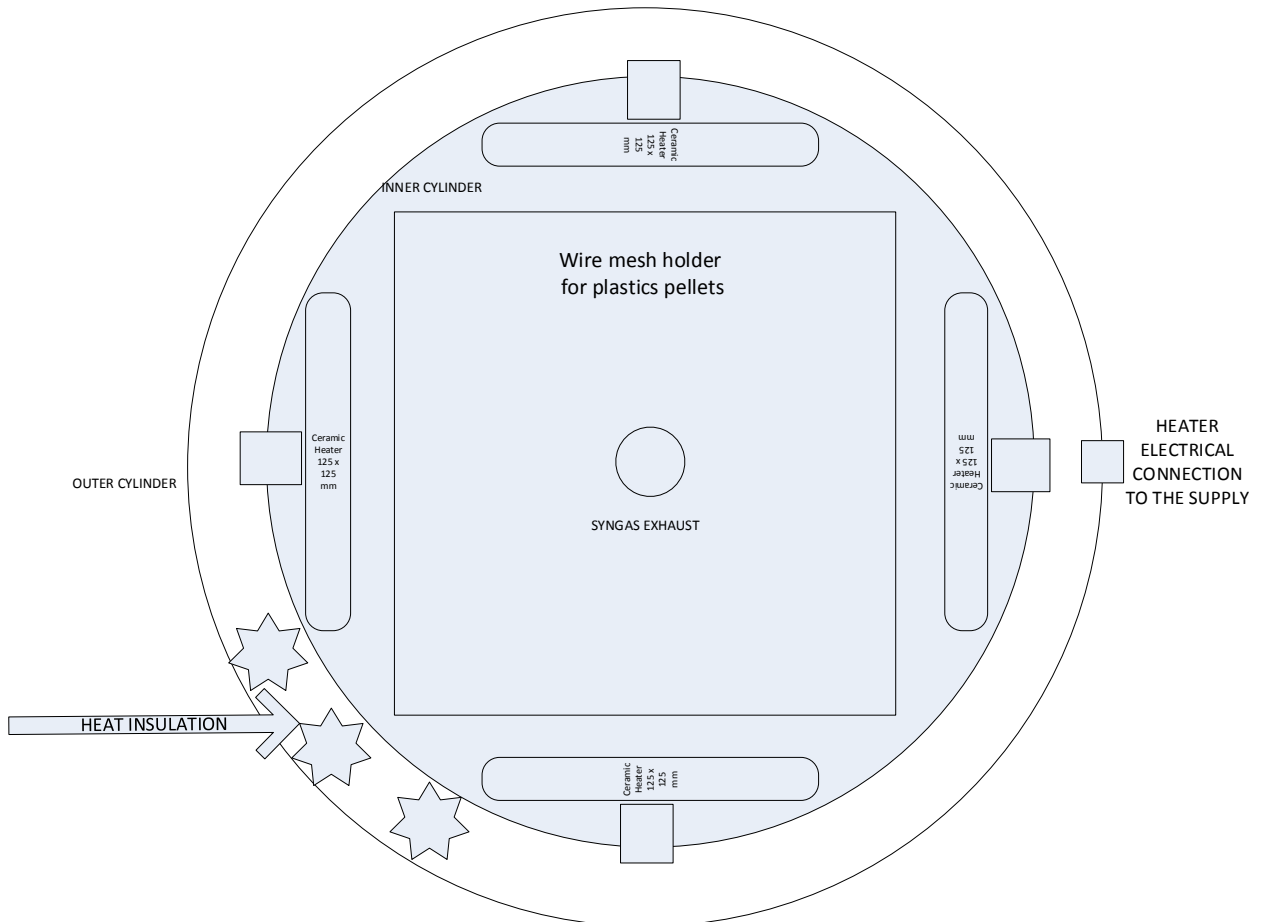
Figure 4.9: Schematic of IR reactor: top view

The following dimensions presented in Table 4.3 have been used to design the IR reactor:

Table 4.3: Reactor description

Description	Size (mm)
Reactor Length	300
Reactor Height	336
Material thickness	2
Heater	125*125
Smoke Hole diameter	20
Mesh bucket diameter	178
Mesh bucket length	270
Reactor exhaust diameter	25.4

Figure 4.10: IR reactor top view

Figure 4.11: IR reactor inside view

Figure 4.12: The reactor mesh

Figure 4.13: The actual gasification purification plant

4.3.2 Insulation fibre for the reactor

The insulation for the IR reactor is a fibre blanket made of thread compound of a ceramic material, usually alumina and silica and it is used in light weight units for electrical, thermal and insulation, filtrating at high temperature, packing and reinforcing other ceramic material. The fibre blanket is used in the heater to prevent heat loss on the outside diameter of the reactor. This fibre blanket as shown in Figure 4.14 has a classification temperature of 1300 °C and its continuous used temperature is 1150 °C which will depend on the application. A fibre blanket presents the following benefits (Morgan Advanced Materials, 2011):

- Better thermal insulating performances
- Exempt of binder or lubricant
- Thermal stability
- Low heat storage
- Flexible and resilient
- Resistant to thermal shock
- Doesn't react with alumina based bricks in application in the range of the typical use temperature
- Cleared from any cancer-causing classification under nota Q of directive 97/69 EC

Figure 4.14: Reactor fibre insulation blanket (Morgan Advanced Materials, 2011)

4.4 Numerical development of IR reactor

Several heaters are commercialised to meet client specific needs. Heater applications may vary from drying, heating in food industry or in household applications, to boiling, and furnace application for commercial building (Roth & Brodrick, 2007). In addition, as the temperature increases so does the filament resistivity which as a result, reduces the amount of current and power consumed by the heater.

In order to study the reactor a schematic of the heater used was developed and it is shown in Figure 4.15. The radiation heat transfer described is similar to the one suggested by (Pettersson & Stenstrom, 2000) as they assumed that radiation is to be diffuse and the model for radiation exchange will have to be non-grey for simplification purpose. For the geometry of the ceramic heater, a symbol is allocated on each surface with regards to the radiosity J_i and irradiation G_i.
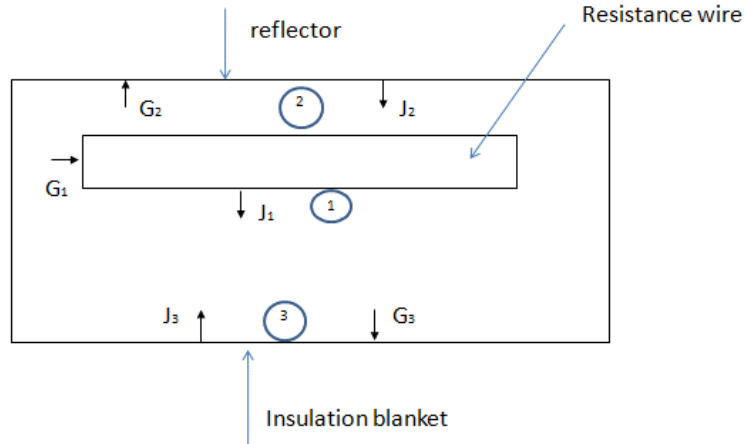
Figure 4.15: Schematic of IR heater (Mbourou & Adonis, 2012)

The temperature rising in the resistive filament is the result of conduction heat transfer to the surrounding and is expressed in Equation 4.1.

$$i(t) = \frac{U}{R}\left(1 - e^{k_1}\right) + c_2 e^{k_2} k_{1,2} = -\frac{1}{2RC}\left[1 \pm \sqrt{1 - \frac{4R^2C}{L}}\right] \qquad (4.1)$$

Where c_2 is constant and

$$k_1 = \frac{R}{L} \qquad (4.2)$$

$$k_2 = -\frac{1}{RC} + \frac{R}{L} \qquad (4.3)$$

Heat transfer by conduction is the mechanism involved in ceramic heaters from the resistive filament to the ceramic body. To calculate the heating rate of the heater, a Fourier equation is determined by Equation 4.4:

$$T = T_1 + (T_0 + T_1)e^{\frac{2Na_t^2}{r_0}} \qquad (4.4)$$

Where $a = c_p\lambda$ is the diffusivity that is equal to the product of the heat capacity of the heater, the density and thermal conductivity of the insulating sheath.

- N represents the heat transfer coefficient characterizing heat exchange with the medium, r is the depth of penetration of the heat pulse
- T is the running temperature of the surface of the heaters after the time t

- T_o, the initial temperature of the heater
- T_1 is the temperature of the medium

The extent to which the heater remains constant over its service of life determine the heating reliability and stability:

$$\xi = \xi_0 \exp\left[-\frac{Q}{RT}\right]$$ (4.5)

Where ξ_0 is a constant that depends on the method of production of the material, of the conducting phase, the electrical insulator, on the composition and Q is the energy of activation of the aging process which is dependent on the ambient conditions and the thermo-mechanical stability of the material of the heater. T represents the heater operating temperature.

The following assumptions with regards to the modelling and simulation of IR reactor are made:

- Infrared source, ceramic reflector and surface to be irradiated are all considered as grey bodies.
- Heat loss through the IR reactor is negligible.
- The heaters are parallel to the chamber surface where plastic pellets are irradiated.
- Insulation blanket inside the IR reactor prevents heat loss. Hence there is no re-radiation.

4.5   Energy balance

4.5.1   Governing equations

The energy balance is defined as the rate at which energy is transferred from the heater surface to the target surface and it is expressed in Equation 4.6 as:

$$E_{out} - E_{in} = 0$$ (4.6)

Due to the passage of an electrical current (I), the filament wire inside the ceramic heater, initially in thermal equilibrium, will be opposed by a resistance. The variation of the filament wire temperature is equal to the power lost by the filament through convection and radiation from the surface of the heater. Steady state is reached when the current passing through that filament has become constant, in other words, when the derivative of the temperature is equal to zero ($\frac{dT}{dt} = 0$). The variation of the filament temperature during the passage of current developed

using the first law of thermodynamics to a certain system with a wire of length L is given by Equation 4.7:

$$E_g - E_{out} = E_{st} \tag{4.7}$$

This equation involves E_g the internal energy generation due to electrical current through the wire, E_{st} a change in energy storage and E_{out} the energy outflow. The energy generation due to the electric resistant heating is expressed (Equation 4.8) as:

$$E_g = I^2 R_e L \tag{4.8}$$

The electrical energy generated is being converted to heat at a rate of $I^2 R$.

The outflow energy due to the net radiation that leaves the heater surface is expressed by:

$$E_{out} = \varepsilon \sigma (\pi D L)(T^4 - T_{sur}^4) \tag{4.9}$$

The change of energy storage due to the temperature change is expressed by Equation 4.10:

$$E_{st} = \frac{dU}{dt} = \rho c V \frac{dT}{dt} \tag{4.10}$$

Where ρ and c are the density and specific heat, respectively of the filament wire material and V represents the volume of the wire:

$$V = \left(\frac{\pi D^2}{4}\right) L \tag{4.11}$$

By substituting the rate equations into the energy balance equation, it results in Equation 4.12:

$$I^2 R_e L - \varepsilon \sigma (\pi D L)(T^4 - T_{sur}^4) = \rho c \left(\frac{\pi D^2}{4}\right) L \frac{dT}{dt} \tag{4.12}$$

Therefore the time rate of change of the filament wire temperature of the heater is:

$$\frac{dT}{dt} = \frac{I^2 R_e L - \varepsilon \sigma (\pi D)(T^4 - T_{sur}^4)}{\rho c \left(\frac{\pi D^2}{4}\right)} \tag{4.13}$$

4.5.2 Output power of heater

The heater output power is expressed from the resistance of the filament wire by:

$$P = IV = \frac{V^2}{R} \tag{4.14}$$

With $R = \rho\left(\frac{l}{A}\right)(\Omega)$ (4.15)

Where R = resistance (Ω), l = length, A = area, ρ = resistivity and V = voltage (220 single phase)

The overall heat transfer rate is expressed as

$$Q = \frac{P_{tot}}{V}$$ (4.16)

With P_{tot} is the total heater output power and V is the volume.

4.5.3   Runge Kutta method

The dynamic of system behaviour is important to derive a mathematical model. An electrical or electronic system may be expressed with a voltage or current and with derivatives of the latter, whereas for a thermal system it can be expressed with temperature, temperature gradient and thermal conductivity. In general, mathematical models derived to describe such dynamic systems imply the use of unknown parameters to help solve and understand the behaviour of these dynamic systems.

When an equation has more than one derivative, it is called a differential equation. Differential equations can be classed in two categories: differential equations with initial conditions and differential equations with boundary conditions. The method used to solve the differential equations developed for this project is the fourth of order of Runge Kutta method. In Matlab it is represented as ODE standing for Ordinary Differential Equation. The order of this equation depends on the highest degree of the derivative. Runge Kutta method is expressed as in the following Equation 4.17 to Equation 4.20:

$$k_1 = h.f(y_i, t_i)$$ (4.17)

$$k_2 = h.f\left(y_i + \frac{k_1}{2}, t_{i+1/2}\right)$$ (4.18)

$$k_3 = h.f\left(y_i + \frac{k_2}{2}, t_{i+1/2}\right)$$ (4.19)

$$k_4 = h.f(y_i + k_3, t_{i+1})$$ (4.20)

The solution of the differential equation is given with the following Equation 4.21:

$$y_{i+1} = y_i + \frac{1}{6}.(k_1 + 2.k_2 + 2.k_3 + k_4)$$ (4.21)

Where $h = 0.1s$ and $0 \le t \le 100$ seconds. These values are used for the simulation in Matlab script. (see Appendix D).

The equation given is a first order differential equation and it was computed in Matlab and Simulink using the Fourth-order Runge Kutta method to obtain the heating response. The Simulink model for this equation as well the LabVIEW model are shown in Figure 4.16 and Figure 4.17. The models are simulated under the conditions that the ambient temperature and the surrounding temperature are equal and are at 22 °C or 295.15 K.
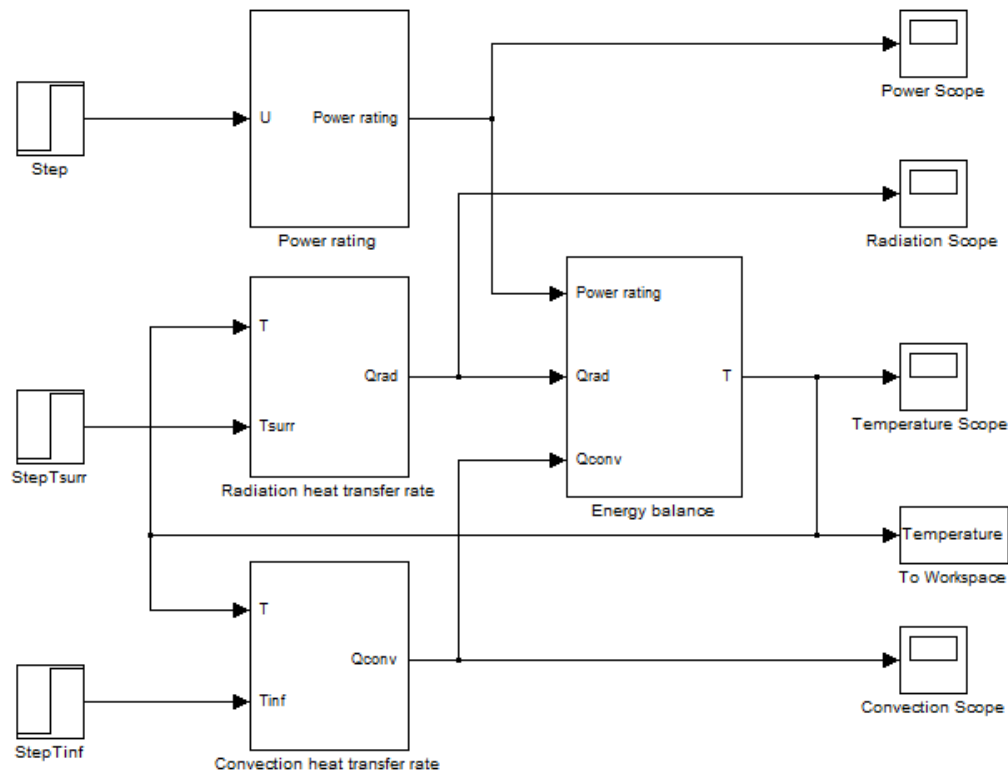
Figure 4.16: Simulink model of temperature of the heated filament of an infrared heater
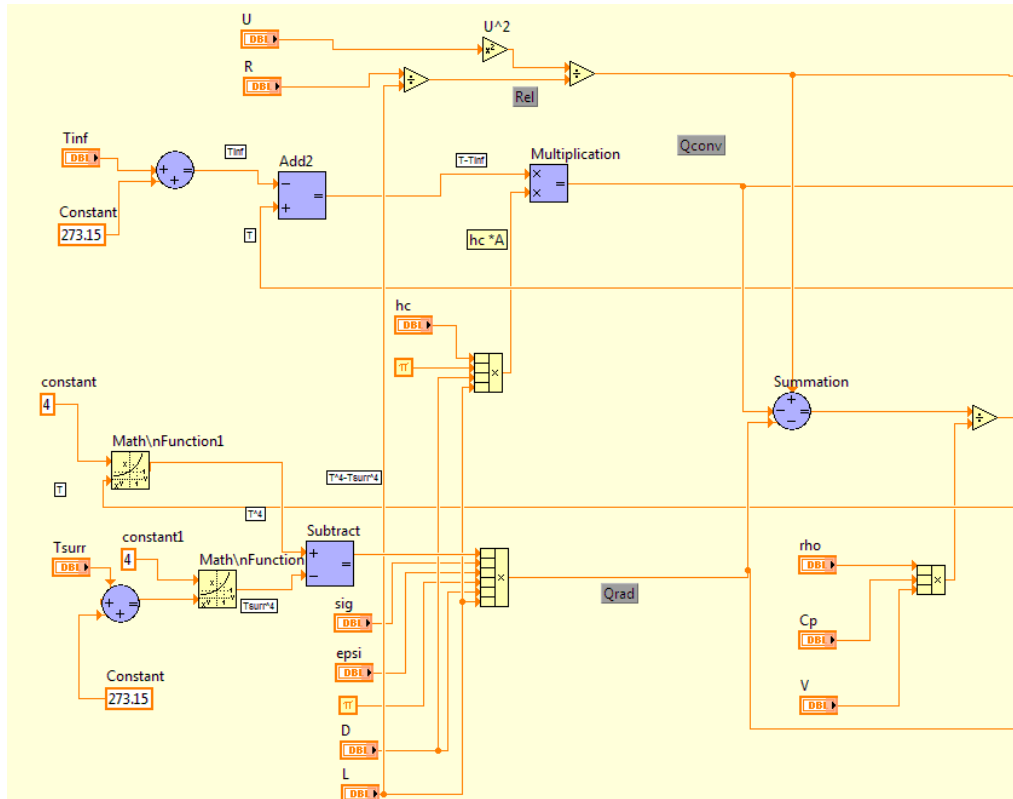
Figure 4.17: LabVIEW block diagram representing the heating stage

4.6   IR reactor: heater enclosure

The radiation heat exchange between surfaces depends on the orientation of surfaces (see Figure 4.18) relative to each other and which is defined as the view factor. View factor is a purely geometric quantity that is independent of the temperature and surface properties. The view factor ranges are between 0 and 1. There are two types of view factors:

- **Diffuse view factor**: it is a view factor that is based on the hypothesis that the surfaces are diffuse emitters and diffuse reflectors.
- **Specular view factor**: it is a view factor that is based on the hypothesis that the surfaces are diffuse emitters but specular reflectors.
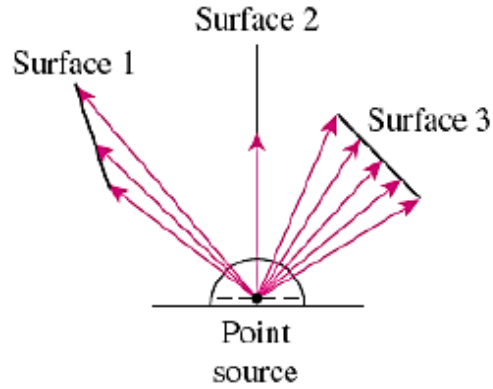
Figure 4.18: Example of radiation heat transfer to surrounding surface (Kanoglu, 2011)

The IR reactor has a cylindrical shape and plastic pellets to be gasified are in a spherical form. The total radial heat flow *Q(r)* considering the cylindrical shape of the IR reactor is expressed in Equation 4.22 as

$$Q(r) = -\lambda \cdot 2\pi r H \cdot \frac{dT}{dr} \ (W) \tag{4.22}$$

By considering the basic case of constant λ and no further complications with the heat flow Q being independent of *r*, the temperature distribution inside the reactor cavity can be expressed in Equation 4.23 as (Rao & Schott, 2012):

$$T(r) = T_i + (T_o - T_i)\frac{\ln\left(\frac{r}{r_i}\right)}{\ln\left(\frac{r_o}{r_i}\right)} \tag{4.23}$$

Where T_i and T_o are the temperature at the inner surface and the outer surface respectively and r_i and r_o represent the radii of the inner surface and the outer surface respectively of the reactor and *r* is the radius.

The total energy or heat change is expressed in Equation 4.24 as:

$$dQ = \rho C_p \frac{\partial T}{\partial t} \tag{4.24}$$

Where ρ and C_p are the specific mass and the thermal conductivity respectively.

4.7   Plastic pellets

The unique aspects related to the thermal treatment of plastic waste are the following (Mastellone & Zaccariello, 2015):

- The very low content of ashes
- The very low content of char
- The low specific heat volume of the solid polymer
- The stickiness of the molten polymer

After the plastic pellets are fed into the reactor; a very fast heat transfer mechanism leads the external surface of the pellet to soften. The necessary time to reach the softening stage can be evaluated by methods of the dynamic energy balance on a single plastic pellet. The polyethylene properties for the energy balance as well as the thermos-optical parameters are shown in Tables 4.4 and Table 4.5 respectively.

$$m_{fuel} \cdot C_p \cdot \frac{dT}{dt} = A \cdot h_{bed} \cdot (T_{bed} - T_{melting}) - r_{melting} \cdot \Delta H_{melting} \qquad (4.25)$$

Where m_{fuel} is the mass of the fuel, C_p is the specific heat of the fuel, T the temperature of the pellet surface which is time depending, A is the external pellet surface, h_{bed} is the heat transfer coefficient between the bed and the plastic pellet, T_{bed} is the bed temperature, $T_{melting}$ is the temperature at which the plastic pellet melts, $r_{melting}$ is the rate of melting, $\Delta H_{melting}$ is the latent heat of melting.

Mastellone & Zaccariello (2015) expressed the general solution of the energy balance in Equation 4.26 as:

$$T(r) = T_{bed} + (T^{\circ} - T_{bed}) \cdot exp(-h_{bed} \cdot {}^{A}\!/_{m \cdot C_p}) \qquad (4.26)$$

With $h_{bed} = Nu \cdot {}^{k_{fuel}}\!/_{d_{fuel}}$ \qquad (4.27)

and Nu is the Nusselt number, k_{fuel} is the fuel conductivity and d_{fuel} is the fuel pellet diameter

They reported that the necessary time for a plastic pellet to soften its external surface is about 1 second.

The convection by the surrounding gas produced in the IR reactor is given by:

$$H_{conv} = \propto A(T - T_g) \qquad (4.28)$$

Where:

- T is plastic temperature in Kelvin
- T_g is the outlet gas temperature in Kevin
- $\propto$ is the convective heat transfer coefficient
- A is the surface area in m²

Table 4.4: Polyethylene (PE) properties for the energy balance adapted from (Mastellone & Zaccariello, 2015)

Parameter	Value	Units
Temperature (T)	To be determined in simulation	°C
Gas viscosity (μ)	4.91E-05	Ns/m²
Gas density (ρ)	0.315	kg/m³
Gas conductivity (k)	0.016	cal/s m°C
Fuel diameter (d_{fuel})	0.005	m
Density of fuel (ρ_{fuel})	950	kg/m³
Specific heat of fuel (C_p)	0.55	kcal/°C kg
Melting heat of fuel ($\Delta H_{melting}$)	23.8	kcal/kg
Softening temperature of fuel	135	°C
Conductivity of fuel (k_{fuel})	0.46	cal/s m °C

Table 4.5: The thermo-optical parameters

Properties	HDPE	LDPE
$C_p(J/KgK)$	3640	3180
$\rho(g/cm^3)$	0.96	0.92
$k(W/mK)$	0.49	0.34
$H(J/Kg)$	0.801	0.572

CHAPTER 5 : SYSTEM SIMULATION

There are several analytical solutions for radiation heat transfer problems that have been developed in the literature (Toskov et al., 2013; Baggio et al., 2009; Dupleix et al., 2013). Computer simulation has allowed engineers and researchers to optimize modelling and process efficiency as well as to study new designs and at the same time reducing time and costly experiments.

5.1 COMSOL Multiphysics ©

Simulation software is based on the process of modelling a real or physical phenomenon with a set of mathematical formulas. As discussed in chapter three and four, three modes of heat transfer are identified: conduction, convection and radiation heat transfer. Two methods are identified for problem solving in the present study: theoretical method and the software package used for the simulation is COMSOL Multiphysics, (version 5.0), a three-dimensional numerical solver software that applies finite element method to simulate the temperature distribution in the reactor. COMSOL uses numerical calculations and simulations, to model and analyse several engineering problems such as electromagnetic field, structural mechanics, fluid flow and heat transfer (Ngabonziza & Delcham, 2014) which has been used for simulations in this project.

COMSOL software can be used as a standalone product through a flexible graphical user interface (GUI) which does not require an in-depth knowledge of numerical analysis or mathematics. In addition, conventional models for one type of physics can be easily extended into Multiphysics models that solve coupled physics phenomena simultaneously. The software can also be used as an application by using the Application builder (for version 5.1 and above), or by script programming using Java environment or the MATLAB language. Several types of studies can be done with COMSOL software such as:

- Stationary and time-dependent also called transient studies
- Linear and nonlinear studies
- Eigen frequency, modal and frequency response studies

There are several application modules in COMSOL Multiphysics. The most common ones are as follow:
- AC/DC Module
- Acoustics Module

- CAD Import Module
- Chemical Engineering Module
- Earth Science Module
- Heat Transfer Module
- Material Library

COMSOL Multiphysics software also offers optional modules that are optimized for specific application area as shown in Figure 5.1. These modules include interfacing modules such as CAD Import Module and bidirectional interfaces such as the LiveLink products.

COMSOL Multiphysics can be used in the following area:

- Acoustics
- Bioscience
- Chemical reactions
- Corrosion and corrosion protection
- Diffusion
- Electrochemistry
- Electromagnetics
- Fluid dynamics
- Fuel cells and electrochemistry
- Geophysics and geomechanics
- Heat transfer
- Microelectromechanical systems (MEMS)
- Microfluidics
- Microwave engineering
- Optics
- Particle tracing
- Piezoelectric devices
- Photonics
- Plasma physics
- Porous media flow
- Quantum mechanics
- Radio-frequency components
- Semiconductor devices
- Structural mechanics

- Transport phenomena
- Wave propagation
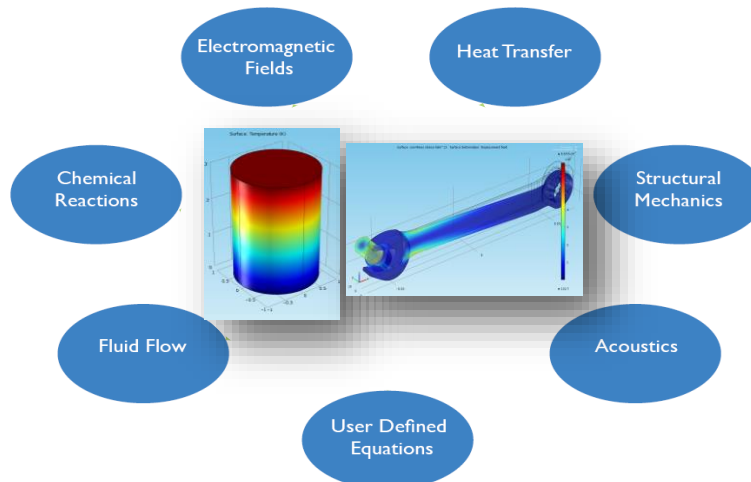
Figure 5.1: COMSOL Multiphysics

COMSOL Multiphysics software is designed for drawings as well as for physical analysis with the different models. Although the software is easy to use with no required specific knowledge of numerical algorithms, when using the heat transfer module to stimulate the heat transfer process, the following steps can be used

- **Defining parameters**: Parameters are user-defined and are usable throughout the model. They define geometric dimensions as well as specify mesh element sizes and a parameter expression may contain numbers, built-in constants, built-in functions with parameters expressions such as arguments, unary and binary operators

- **Geometry**: COMSOL Multiphysics has many geometric primitives that can be found in the in the CAD tools. It also contains operation for modelling the geometry in 1D, 2D, and 3D

- **Materials:** built-in COMSOL library or can be uploaded by the user. Each material includes a number of physical properties with the values or functions which describes the model material.

- **Physics**: the physics can be coupled depending on the model complexity. The governing equations can be included by user that may describe a material property; COMSOL however has a wide range of built-in equations even a set of partial differential equations (PDEs). The physics menu contains two settings which are subdomain and

70

boundary settings determined by user. The subdomain setting is to set the material property as well as initial conditions. The boundary settings is to set the boundary conditions in two parts such as to set the boundary conditions on the interface of different materials and secondly and to set boundary conditions on the interface between material and the environment

- **Mesh:** is the discretization of the geometry into small units of simple shapes. The mesh generator discretizes the domains into *tetrahedral*, *hexahedral*, *prism*, or *pyramid* mesh elements several mesh element shapes and size: fine, coarse…
- **Studies**: transient or steady state, etc.
- **Post-processing:** data can be exported to Excel datasheet.

In order to study the heat distribution in the reactor by software simulation, three stages can be identified:

- Theoretical method knowing the governing equations to represent the physical model taking place and this can be implemented by COMSOL directly
- COMSOL modelling with a model representation of physics to be simulated by using the library software for simulation
- The model is validated by experiments and therefore evaluating the error margin between implementation as shown in Figure 5.2.
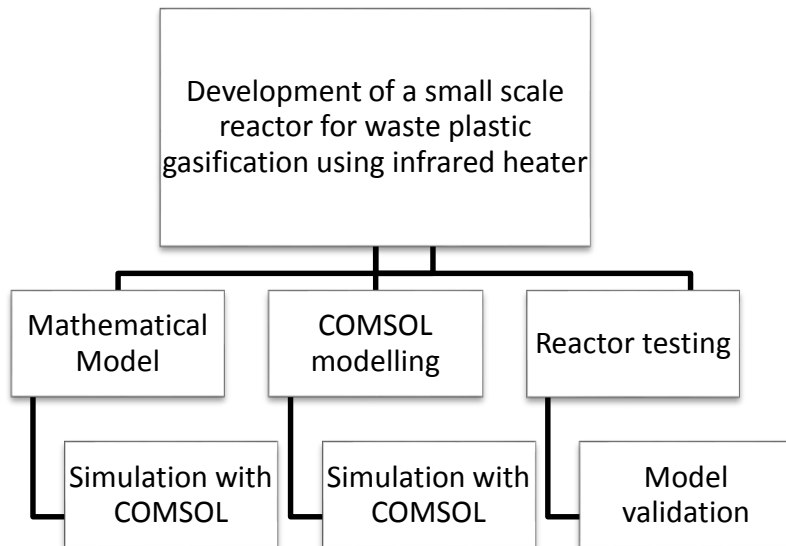
Figure 5.2 : Options used by software system simulation

5.2   Heat transfer module

In order to do an estimation of the temperature distribution within a system, it is necessary to determine the heat exchange between the model and the environment which will depend on the temperature difference between media, the surroundings and the reactor. Standard values have been set for boundary temperatures such as for air at 22 °C or 295.15 K.

The heat transfer module, used to determine the temperature distribution in the reactor, heat flux propagation and heat loss, is one of the optional modules offered by COMSOL Multiphysics. It is based on the study of the balance of energy in a system. The influences to this energy balance originate from conduction, convection, and radiation, but also from heat sources, and heat sinks. The module contains modelling tools to simulate all fundamental mechanisms related to heat transfer such as conduction, convection and radiation. Simulations can be run for different conditions in 1D, 2D and 3D coordinate systems respectively. The heat transfer equations are defined automatically and their formulations can be visualized in detail for validation and verification purposes.

The associated features of the heat transfer module are:
- Surface-to-ambient radiation which is based on the radiosity method that assumes that the ambient surroundings in view of the surface have a constant temperature T_{amb} and that the ambient surrounding behaves as a blackbody; this means that the emissivity and absorptivity are equal to 1 and the reflectivity is equal to 0. The irradiation is therefore expressed in Equation 5.1 as:

$$G = \sigma T_{amb}^4 \tag{5.1}$$

  The net inward heat flux for surface-to-ambient radiation is expressed in Equation 5.2 as:

$$q = \varepsilon \sigma T_{amb}^4 - T^4 \tag{5.2}$$

- Surface-to-surface radiation which combines heat transfer in fluids or solids, including conduction and convection with surface-to-surface radiation. The surface-to-surface radiation model also takes into account the dependency of surface properties on the spectral bands.
- External radiation source;
- Radiation in participating media which takes into account the absorption, emission, and scattering of radiation by the fluid present between radiating surfaces.

5.3 Model implementation

As a result of the complexity of the reactor design, the use of only theoretical considerations is unlikely to provide a complete and realistic behaviour of the heat transfer in the system. Therefore, numerical investigations are expected to present a more realistic representation of the heat transfer.

There are mostly three research fields (Xion, 2010) which can be identified as:

- How to increase the heat transfer rate
- How to decrease the heat transfer rate
- How to keep the temperature within a certain range

5.4 COMSOL model development method

5.4.1 Model assumptions

In order to simulate the heat transfer in the reactor chamber during gasification and due to the difficulties to implement such a model in COMSOL, the following assumptions have been made:

- The gasifier is assumed to have a cylinder shape, top feeding of plastics and air/oxygen.
- All gases are assumed to behave ideally.
- All particles are assumed to have the same temperature and same velocity.
- Plastic pellets are assumed to have spherical shape.
- Slag, char formation and deposition are not taken into account in the model.

5.4.2 Geometry

Before starting the geometry modelling, it is important to determine the parameters to be used for simulation. The model was developed based on a 1000 W rated power reactor that is built with four infrared heaters in parallel with 250 W rated power for each heater individually. The geometric model is hollow cylinder with an enclosure at the back (see Figure 5.3). For simplification purpose, heat power generated was assumed to be 1000 W. Table 5.1 to Table 5.3 show properties of reactor description, heaters properties and materials used respectively.

The properties listed below modelled to be temperature-independent over the range of temperature considered for this project.

Table 5.1: IR reactor size

Description	Outer cylinder value (mm)	Inner cylinder value (mm)
Radius	150	135
Height	336	336

Table 5.2: Heater parameters

Name	Expression	Description
T_wall	295.15 [K]	Temperature, wall
Cp_heater	460 [J/(kg*K)]	Heat capacity, heater
e_heater	0.88	Surface emissivity, heater
rho_heater	8300 [kg/m^3]	Density, heater
k_heater	17 [W/(m*K)]	Thermal conductivity, heater

Table 5.3: Materials parameters used for IR reactor – stainless steel

Name	Value	Unit
Heat capacity at constant pressure	475[J/(kg*K)]	J/(kg*K)
Thermal conductivity	44.5[W/(m*K)]	W/(m*K)
Density	7850[kg/m^3]	kg/m^3
Electrical conductivity	4.032e6[S/m]	[S/m]
Coefficient of thermal expansion	12.3e-6[1/K]	[1/K]

Some parameters were kept constant for simplification. Material considered for simulation is stainless steel type AISI 4340. The model established is a 3D model of transient analysis:

- The reactor made of stainless steel and the thermal conductivity was given directly by the software which is 44.5 W/(m*K).

- The heat generated from the heaters was set to 1000 W assuming they are placed right by the inside cylinder
- The temperature at the bottom of the reactor plate was kept constant at 295.15 K
- The boundary condition at the reactor wall was defined as fixed in the model.
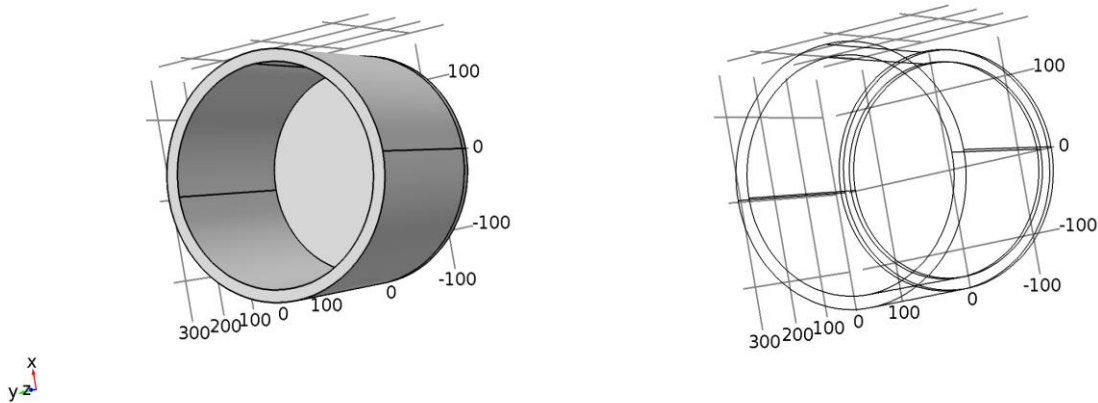
Figure 5.3: IR reactor 3D model

5.5.3   Initial value and boundary conditions

The initial temperature of the reactor is the same as the surrounding area which is the ambient temperature T_{amb}= 22 °C as shown in Figure 5.4b (or ht.Tinit =295.15 K according to software notation). The second boundary was assumed to be the inside reactor wall as shown in Figure 5.4a considering that heaters are placed against the inside cylinder wall. For simulation purpose the final temperature was set to be at T= 1200 K (or ht.T0 = 1200 K according to software notation). The heat source is equal to P= 1000 W which is the total operating temperature of the four heaters placed inside the reactor chamber. Table 5.4 shows a summary of simulation boundaries as noted by COMSOL, the initial and final temperatures.

Table 5.4: Initial and final temperatures for simulation

Name	Expression	Unit	Description	Selection
ht.Tinit	295.15	K	Initial Temperature	Domains 1–3
ht.T0	1200	K	Final Temperature	Boundaries 6, 8–9, 11–13, 16–19

(a)   (b)
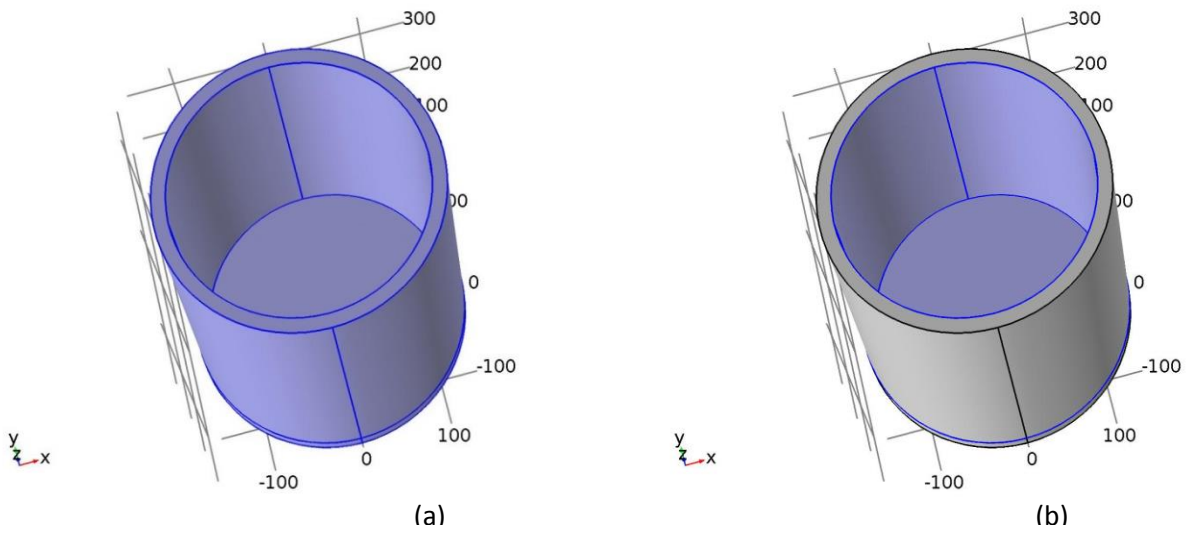
Figure 5.4: Boundaries for initial and final temperatures a- initial b- final

5.5.4   Thermal insulation

The boundaries selected for IR reactor thermal insulation are shown in Figure 5.5 below.
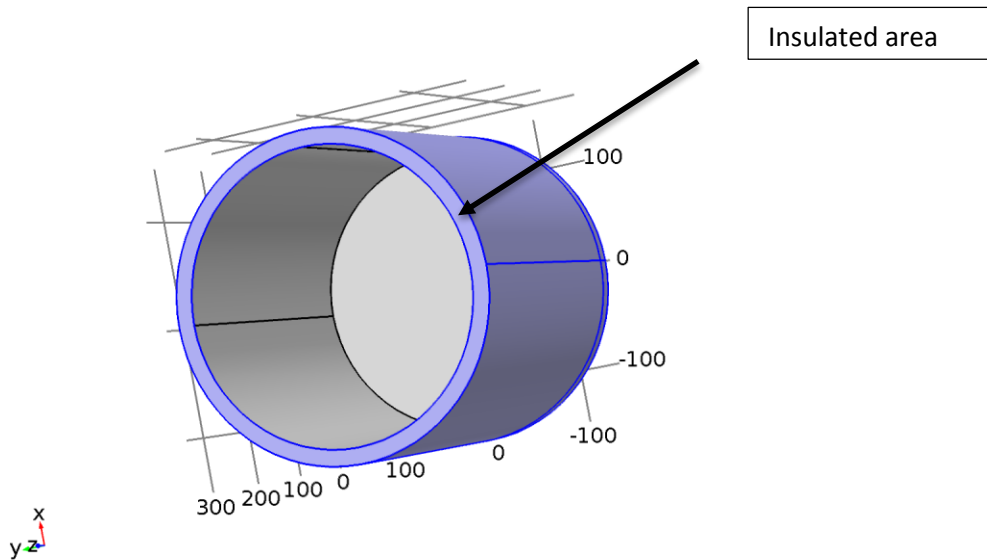
Insulated area

Figure 5.5: Insulated area: boundaries 1–5, 7, 10, 14–15, 20–21

5.4.5 Governing equations

The problem addressed was to determine the effects to change in heat transfer. The model has been implemented to evaluate the temperature distribution in the reactor as well as heat flux propagation. With regards to the Heat Transfer Module, the fundamental law governing is the first law of thermodynamics which expressed in terms of temperature, T, as Equation 5.3:

$$\rho C_p \left(\frac{\partial T}{\partial t} + u.\nabla T \right) = \nabla.(k\nabla T) + Q \tag{5.3}$$

Where:

- ρ is the density, kg/m^3
- C_p is the specific heat capacity at constant pressure, J/(kg·K)
- T is absolute temperature, K
- u is the velocity vector, m/s
- k is the thermal conductivity, W/(m·K)
- Q is a heat source (or sink) [W/m^3]

If the velocity vector is equal to zero, Equation 5.4 for pure conductive heat transfer therefore becomes:

$$\rho Cp \frac{\partial T}{\partial t} + \nabla \cdot (-k\nabla T) = Q \tag{5.4}$$

This equation is the one COMSOL Multiphysics uses for running simulations and were carried out for a better understanding of the experimental stages. The simulations present the temperature profiles and heat flux give more details of changes that are taking place as the system becomes more complex.

Radiation interacts with conductive and convective heat transfer through the source term in the heat flux and boundary heat source boundary conditions. The source is defined as the difference between incident radiation and radiation leaving the surface and it is expressed according to Equation 5.5 given by:

$$q = G - J \tag{5.5}$$

Where

- G is the irradiation or incoming radiative heat flux in W/m²
- J is the radiosity or the total outgoing radiative flux in W/m²

At a given point the irradiation G in the modelled geometry can be expressed as a sum according to Equation 5.6:

$$G = G_m + G_{amb} \tag{5.6}$$

Replacing G_{amb} by its expression in Equation 5.7, it gives

$$G = G_m + F_{amb}\sigma T_{amb}^4 \tag{5.7}$$

Where

- G_m is the mutual irradiation that is coming from other boundaries in the model (W/m²)
- G_{amb} is the ambient radiation
- F_{amb} is an ambient view factor

The radiosity J, is the sum of the reflected irradiation and the emitted irradiation. For diffuse-gray surfaces J is defined by Equation 5.8:

$$J = \rho G + \varepsilon e_b(T) \tag{5.8}$$

- Where ρ is the surface reflectivity which is equal to 1-ε for diffuse-gray surfaces. ε is the surface emissivity ranging from 0≤ε≤1 and is independent on the radiation wavelength and that is the hypothesis corresponding to diffuse-gray surfaces
- $e_b(T) = n^2\sigma T^4$ is the blackbody hemispherical total emissive power
- n is the transparent media refractive index
- σ is the Stephan-Boltzmann constant with $\sigma = 5.670 \times 10^{-8}\, W/(m^2.K^4)$
- T is the surface temperature (K)

5.5.6 Mesh

Once the boundary conditions are created and applied, the model is now ready to be meshed. Meshing a model is to break down this model into smaller pieces that are called elements, which are connected by nodes. Each element is then solved individually which creates a simpler way to obtain an approximate solution of the problem studied.

Moreover, a finer mesh, meaning a mesh that has more elements will give more accurate solution. However, a finer mesh will take more time to compute such solution. For this reason,

determining an appropriate balance between the computational time and also the accuracy level becomes necessary. The mesh was created in COMSOL Mulptiphysics © by selecting free tetrahedral for 3D models with its size set to "coarse" in the setting. This also will depend on the time it takes to solve the problem. The reactor mesh can be seen in Figure 5.6 with 2232 elements created.
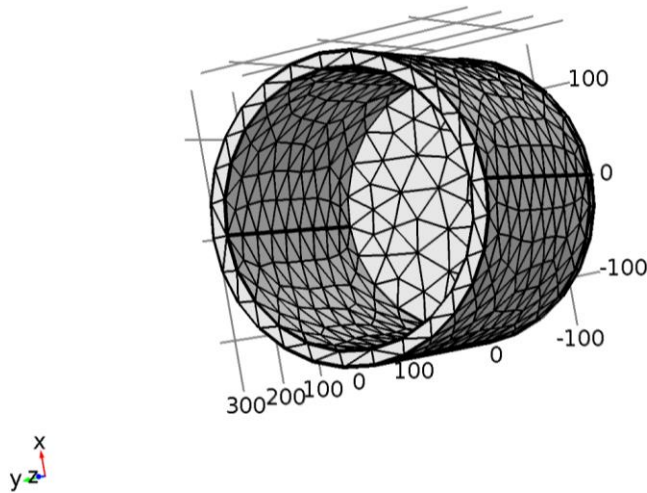
Figure 5.6: Meshing of the reactor model

Table 5.5: Mesh statistics

Description	Value
Minimum element quality	0.03334
Average element quality	0.5602
Tetrahedral elements	2232
Triangular elements	1624
Edge elements	236
Vertex elements	24

5.6 Simulation results

Once the mesh is created the model is ready to run. It was decided to simulate the system under transient conditions which reflects the gasification problem as a function of time. The

times in which the results are expected are assigned. Using heat transfer module, simulate and save the results every 10 seconds starting from zero to 1200 seconds (20 minutes). This is done through COMSOL specific syntax:

1. In the **Model Builder** window, click on **Study> Step 1: Time Dependent**. This is solving for transient.
2. In the **Settings** window, locate the **Study Settings** section and type *range (0, 10, 1200)* in **Times** edit field.
3. Click on **Study 1**.

Click the **Compute** button in the upper toolbar. Wait for COMSOL to compute the results. Results are shown on Figure 5.7 to Figure 5.14.
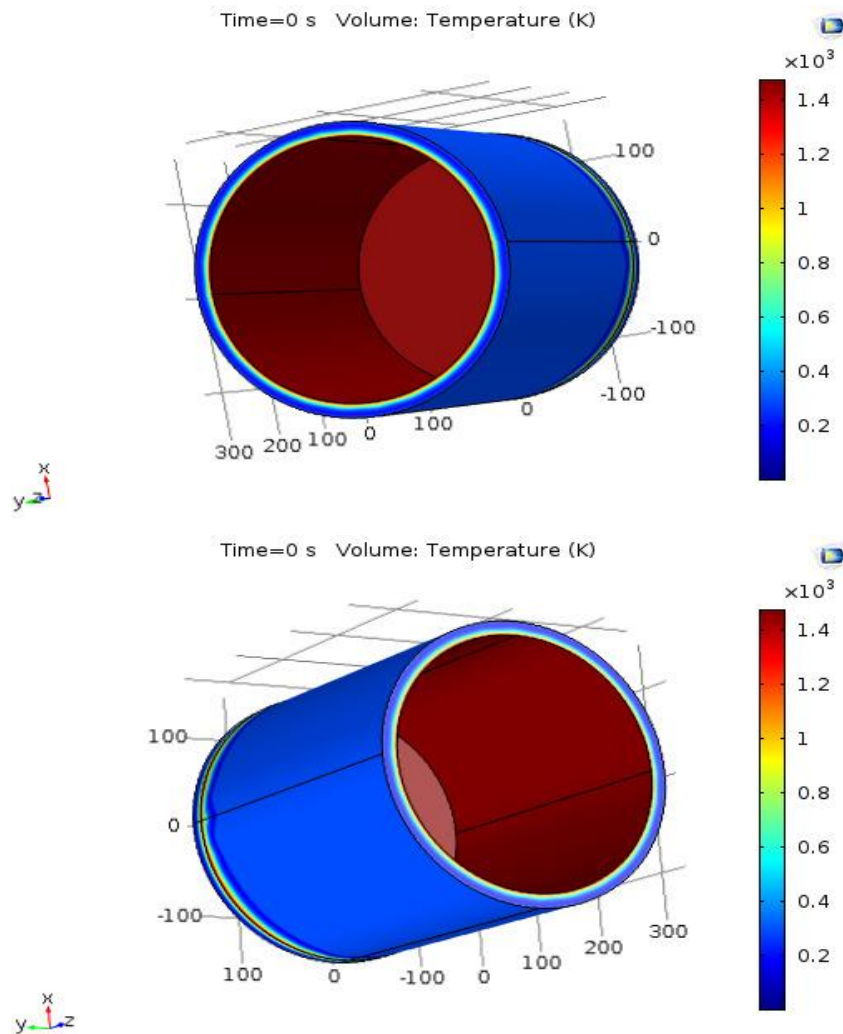
Figure 5.7: IR reactor temperature distribution
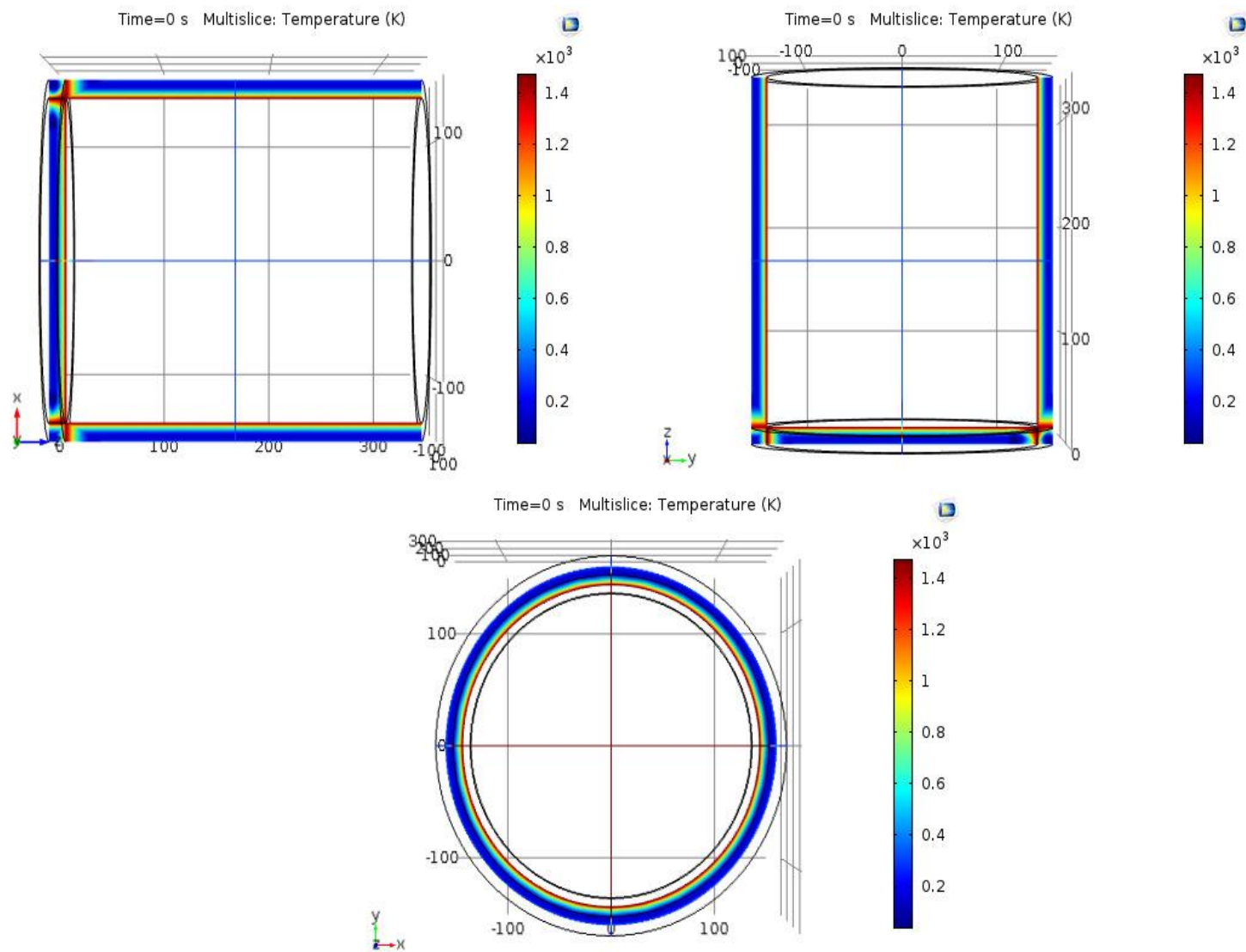
Figure 5.8: IR reactor temperature distribution - 2D plot sectional view

81
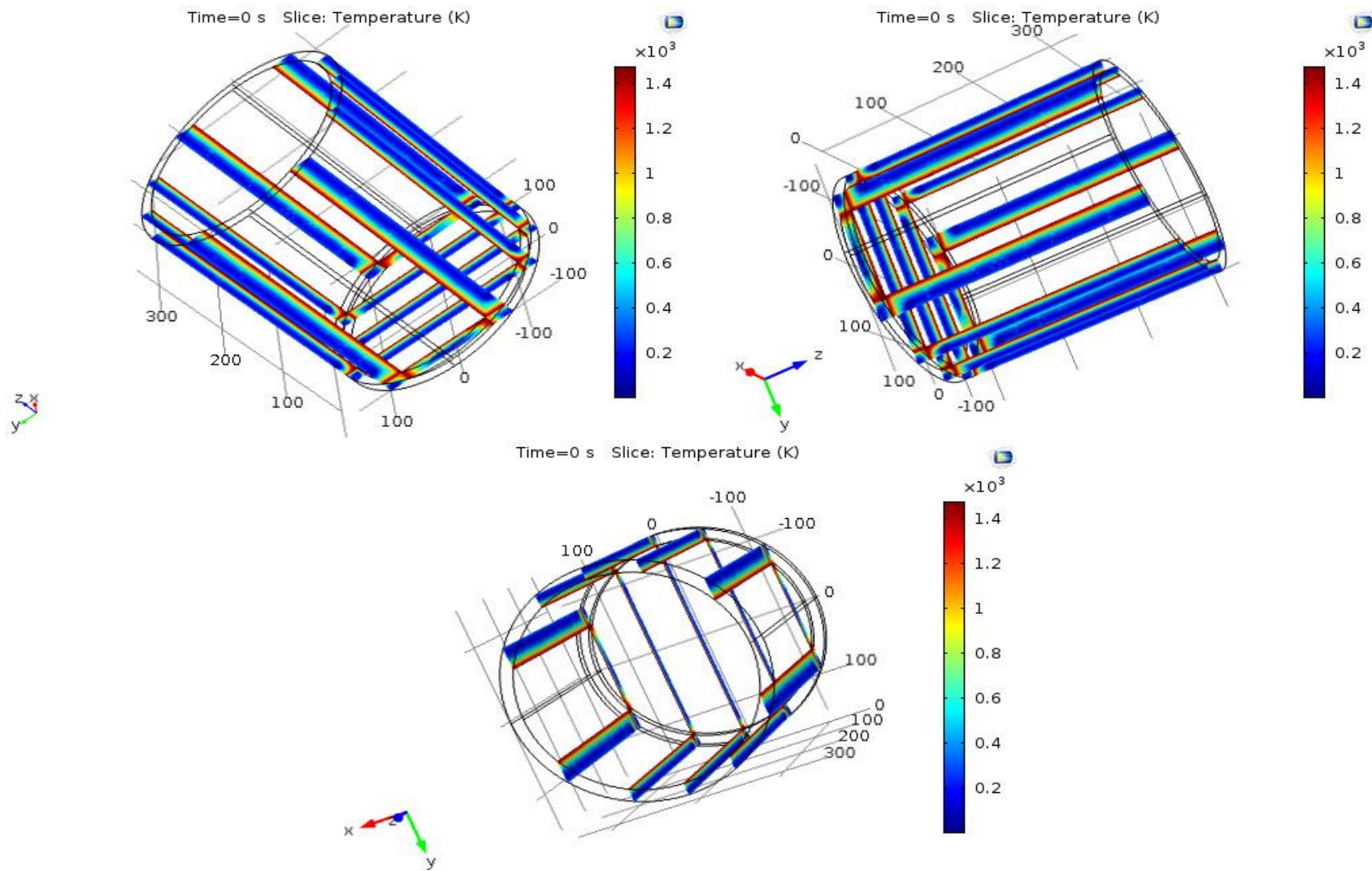
Figure 5.9: Temperature distribution – multisection
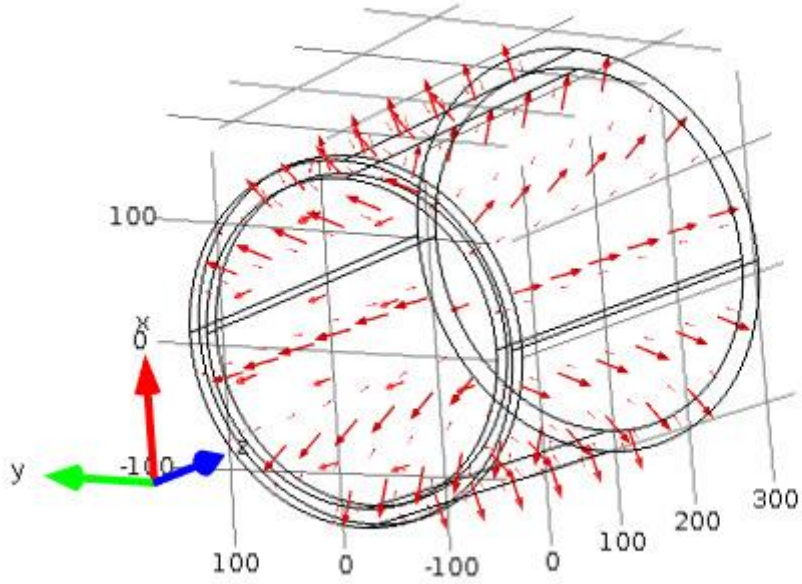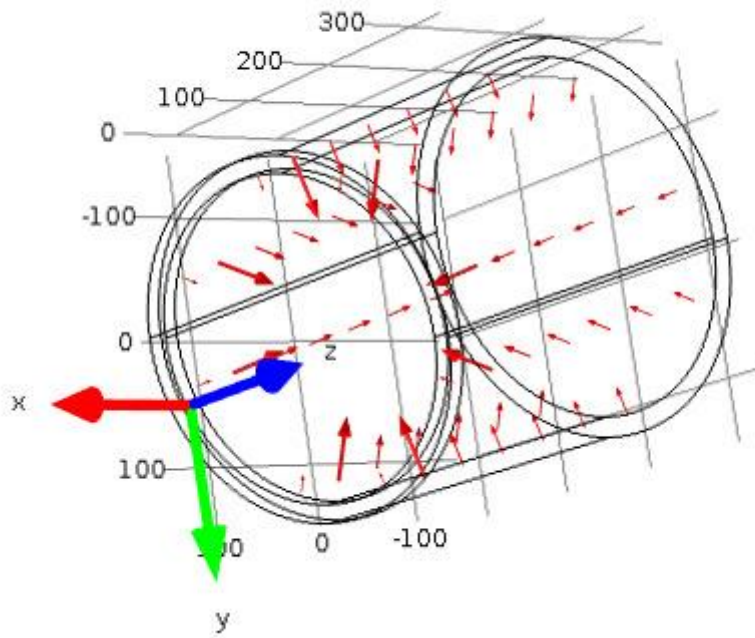
Figure 5.10: Heat flux direction
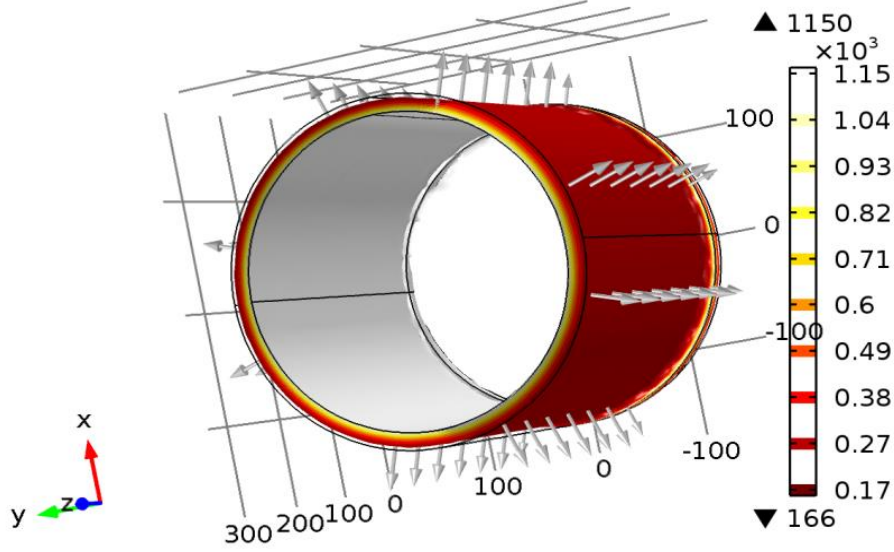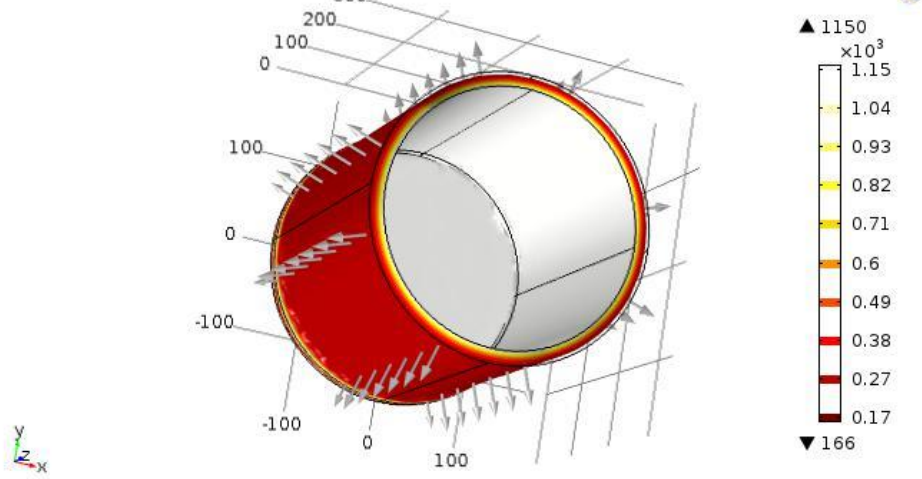
Figure 5.11: Total heat flux and heat distribution
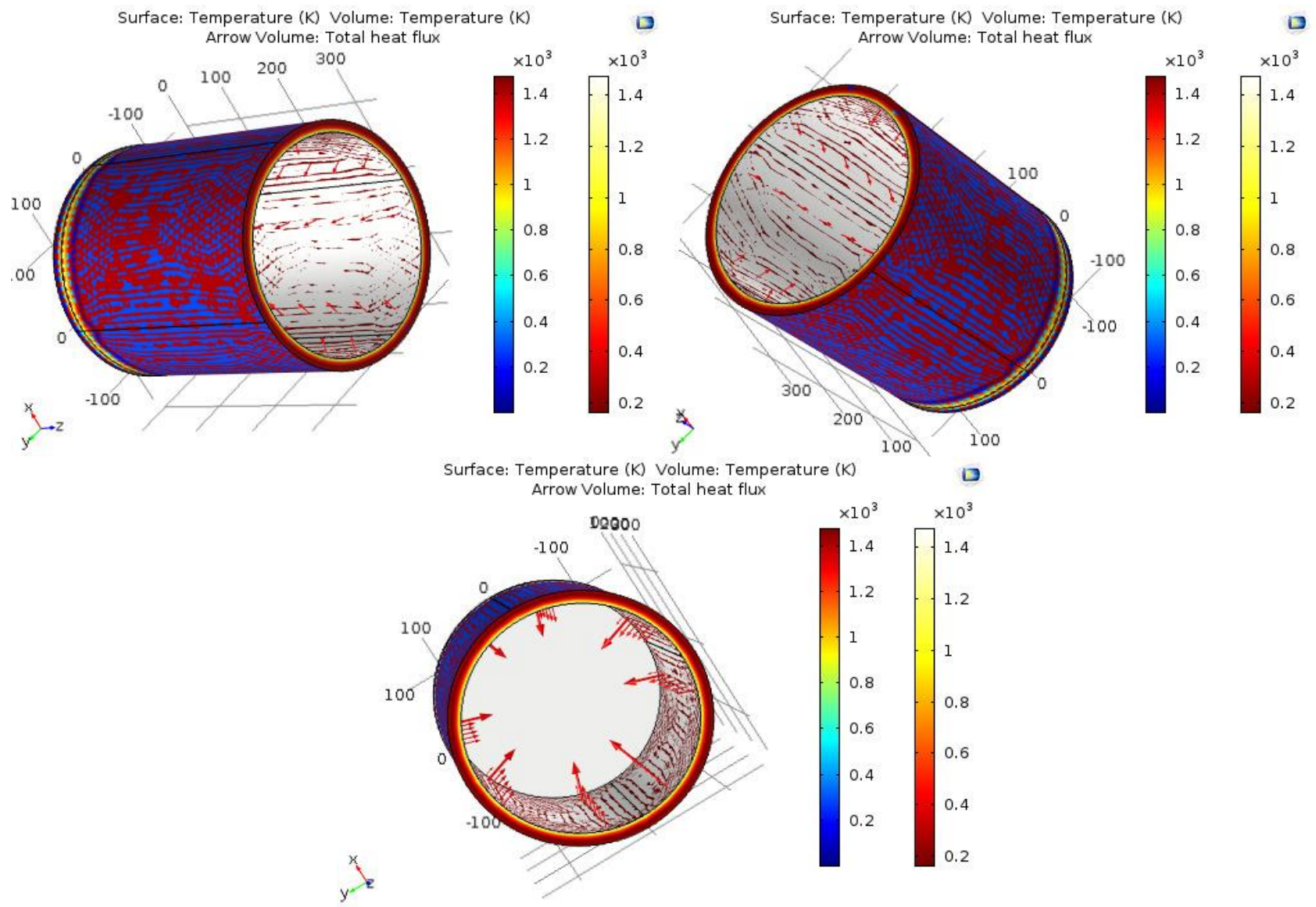
Figure 5.12:   Total heat inward heat flux with streamline
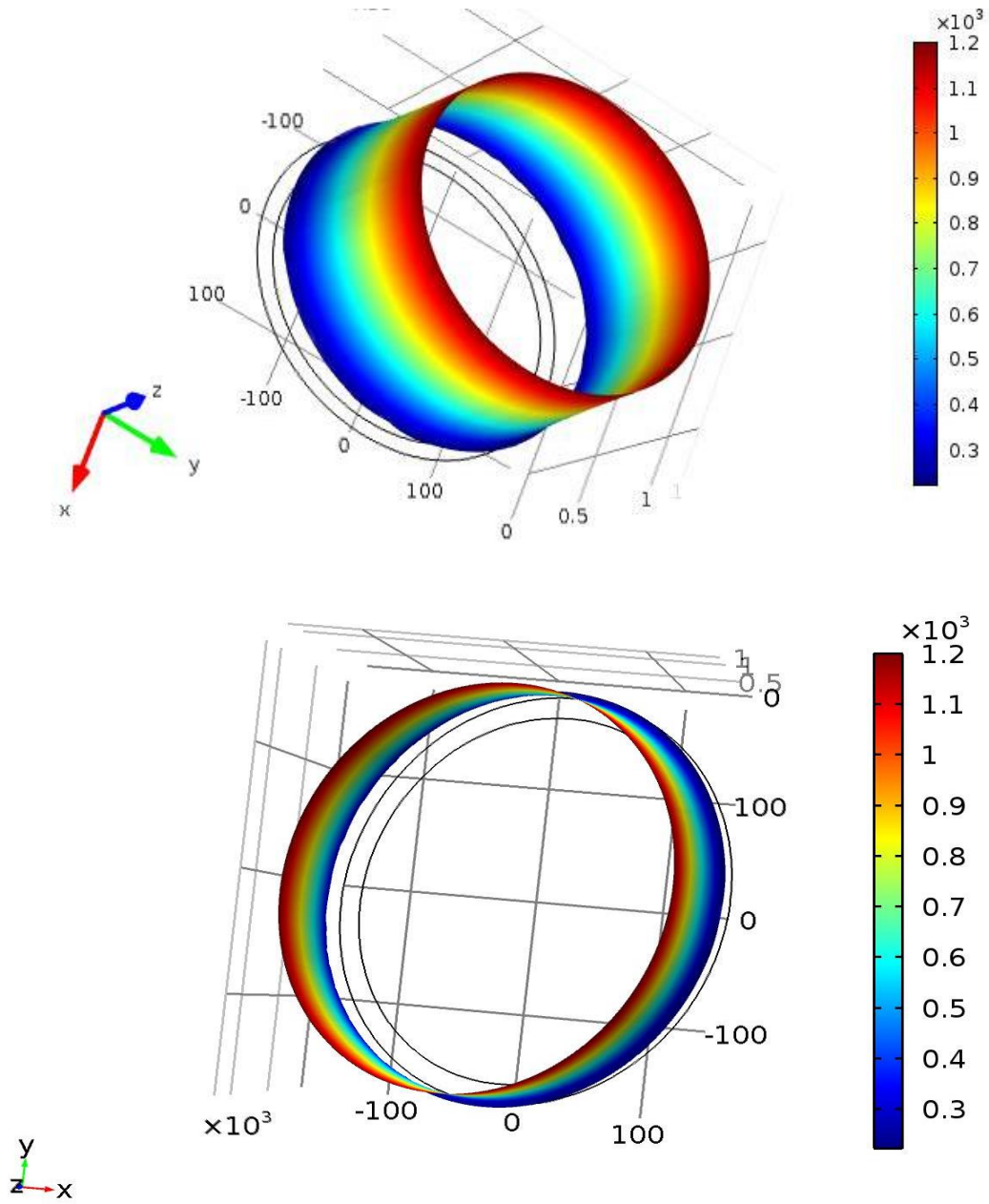
Figure 5.13: 3D cut of heat distribution
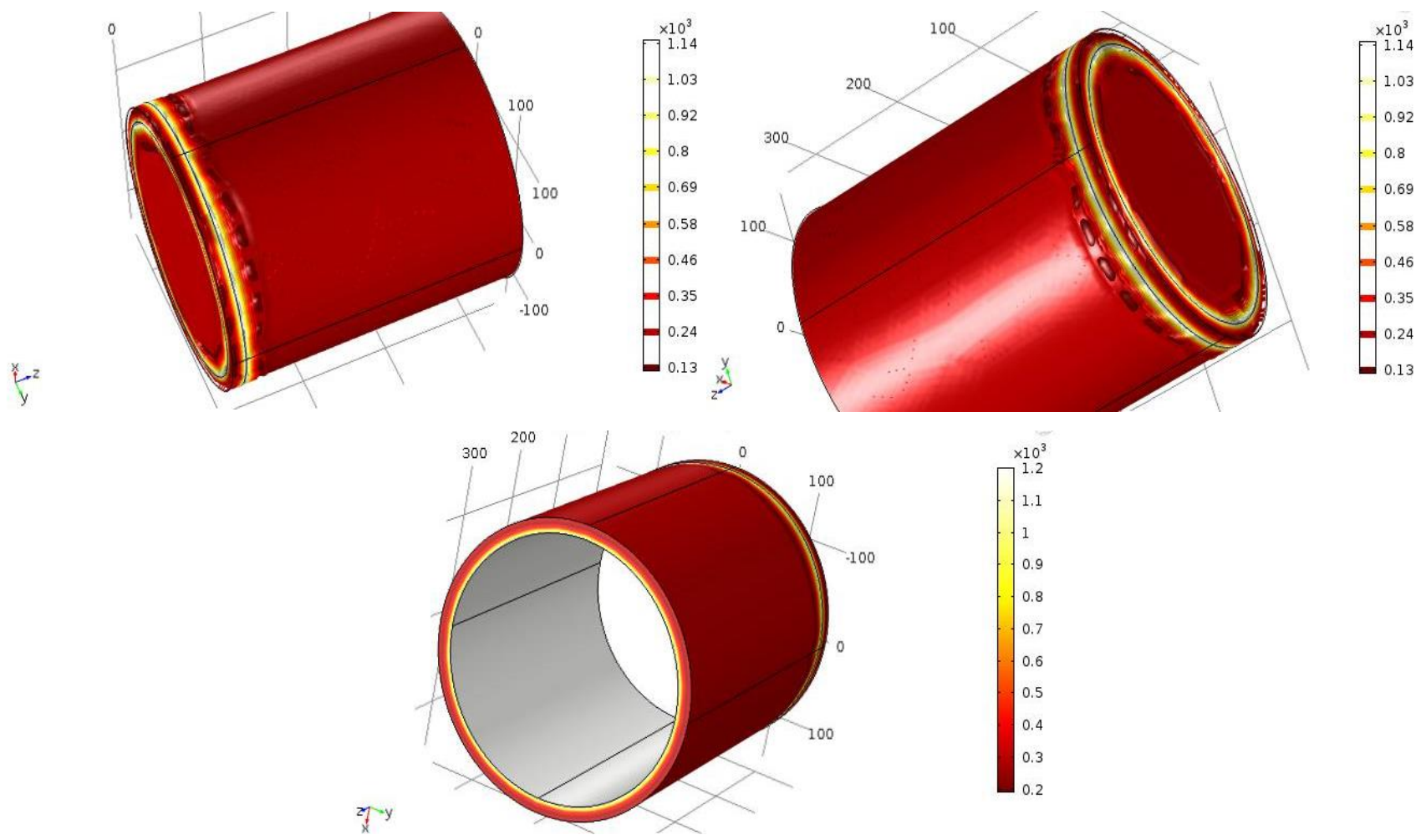
Figure 5.14: Effect of heat at bottom of reactor

In order to better understand the temperature distribution within the IR reactor, a 3D IR reactor model was built using the COMSOL Multiphysics © software version 5.0. As Temperature is an important parameter related to heat transfer within the IR reactor and it could affect the conversion reaction of feedstock, the model was therefore simulated at a maximum temperature of 1473.15 K or 1200 °C. Surface to surface radiation is applied to simulate the heat transfer of the IR reactor.

Figure 5.7 presents an overall temperature 3D distribution within the IR reactor from inside and on the reactor wall with the temperature of the heated reactor was set at 1473.15 K. The results presented indicate that the lowest and highest temperatures are observed on the inside (200 K) and on the wall part of the reactor (1400 K), respectively. This observation shows that the reactor is heated up on the inside by infrared heaters representing the reactor heat source.

To see the inside distribution of temperature, 2D slice plot as well as 3D multi-slice plot are presented in Figure 5.8 and Figure 5.9 respectively. The small arrows in Figure 5.10 indicate the direction and magnitude of the heat flux vector. Figure 5.11 shows the surface plot of the temperature field on the reactor and the heat distribution from the highest temperature (1150 K) to the lower temperature (166 K) while the arrow plot shows the total heat flux and heat distribution in the reactor. Heat flux in Figure 5.12 is visualised through streamlines that show the velocity field of the air that flows inside the reactor. The streamlines are curves through the reactor domain that are such that the heat flow is always constant between two consecutive curves. The streamline colour displays the velocity norm and the arrows predict the main flow direction of heat. The more the streamlines lie together, the heat flow activity is more intense in those regions which is not the case for regions where the distance between consecutive streamlines is larger.

As it is shown in Figure 5.13 with an illustration of 3D cut of heat distribution, the temperature inside the reactor is around 1200 °C or 1400 K. An important point to note is that the temperature at the reactor wall remained constant at 295.15 K for simplification purpose which was not the case during experiments conducted since the temperature at the reactor was higher when manually measured and it is further discussed in chapter 7 as temperature varied throughout time. This could be attributed to the material conductivity of the reactor made with stainless steel, the reactor blanket not withstanding temperatures beyond 1200 °C (its continuous temperature is 1150 °C) as well as the influences of natural and forced convection.

Assuming good thermal isolation for the simulation, the only source of heat loss is via convection at the bottom surface wall of the reactor (see Figure 5.14) due to the reactor bottom bed cover is situated at the back and was not totally insulated.

.

CHAPTER 6 : MATERIAL CHARACTERIZATION AND EXPERIMENTAL SETUP

This chapter introduces the analysis of samples to be gasified and the performance testing of the infrared reactor with its embedded thermocouples. Polymer identification analysis uses several methods to determine the melting range, density as well as infrared spectrum (Sarker & Rashid, 2013). These methods are very fast and accurate for the analysis and quality control of polymers. Different analyses were conducted on low density polyethylene samples.

6.1 Experimental setup for gasification tests

Before feeding plastic samples in the reactor and observing the workability of the system, it is important to determine the temperature profile of the sample to be studied as well as the equipment that constitutes the system. The IR reactor is connected to a 230 V supply through a wall socket and heating temperatures are recorded using a data acquisition (DaQ) device. The temperatures read from the DaQ are directly retrieved from the heater embedded thermocouples placed in the reactor chamber and the process is monitored and recorded with a personal computer (PC) to display and record those temperatures read from the DaQ. Plastic pellets constitute the feedstock for the gasification experiment as shown in Figure 6.1.
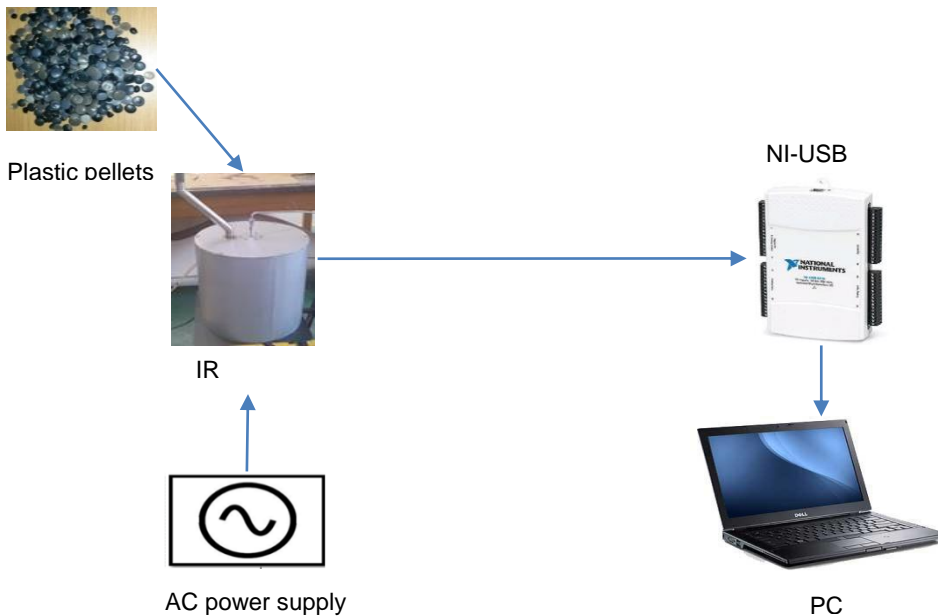
Figure 6.1: Experimental procedure

Temperatures at start-up stages were also recorded (from the time the unit is switched on until sample was fed into the reactor) the following steps can be used as basis in the IR reactor test operation:

- Reactor ready for test: all electrical connections are checked (heaters connected in parallel), thermocouples connected to NI-USB 6211 DaQ in four different gates as analogue inputs for temperature to be retrieved. Several void test runs were conducted to test the reactor performance in terms of temperature profiles before conducting further tests.
- Prepare weighing scale and set to 0 and measure three LDPE samples of 5 g and three LDPE samples of 3 g respectively to be weighed in as batch of 5 g per run and 3 g per run. The first load of sample was done at operating temperature (650 °C). Only a small amount of plastic waste was considered as laboratory scale study.
- Gasification start-up time was recorded as soon as sample was loaded into the reactor.
- The gas emitted from the reactor was recorded until no gas was longer visible coming out from the reactor. This was assumed to be total gasification.

The ash was collected and weighed when possible and results are further discussed in chapter 7. Lastly, prior to the gasification experimentation, experiments with thermogravimetry analyzer, calorimeter and elemental analyzer have been carried out in order to observe the thermal decomposition of plastic waste samples used.

6.2   Data Acquisition

6.2.1   NI-USB 6211 DAQ

A NI-USB 6211 (see Figure 6.2) is a data acquisition device (DAQ) that is connected to a PC and it measures an electrical or physical phenomenon such as voltage, current, temperature, pressure, or sound. It receives input from the heater thermocouples in this case and gives the output signals displayed on the PC screen. The DAQ is an M Series multifunction which combines analogue input, analogue output, counter/timers and digital I/O on a single device. The DAQ to communicate with the PC uses SignalExpress a data logging software from National Instruments which optimizes virtual instrument for design by offering instant interactive measurements and does not require any programming. SignalExpress can be used to acquire, generate, analyse, compare, import and save signals.

Figure 6.2: NI-USB 6211 device

The NI-USB 6211 data acquisition device specifications are the following:

- Maximum sample rate: 250 kS/s
- Maximum voltage +/- 10 VDC
- Resolution: 16-Bits
- Analog input: 8 Diff, 16 single ended
- 2 12-Bit analog outputs (0-5 Volts, 150 updates/sec maximum)
- 12 digital I/O lines

6.2.2 Analogue signal acquisition using the interface USB-6211

The DaQ has more than one analogue input channel. In the "Measurement & Automation" tool which is a part of the software LabView, a list of all interfaces can be seen whether are plugged in presently or previously used. A name is assigned to the interface once it is first plugged into the PC and the name of the interface is also followed by the name of the channel where the analogue signal is connected to. Four analogue inputs were used to connect the four thermocouples accordingly and samples are taken at regular time intervals, 1000 samples over a period of 1ms and results:

- Thermocouple 1: Dev1/ai3

- Thermocouple 2: Dev1/ai4
- Thermocouple 3: Dev1/ai5
- Thermocouple 4: Dev1/ai6

Whereas

Dev1 refers to device 1 (USB 6211, only one device is connected to the PC)

Ai3, ai4, ai5, ai6 refer to analogues inputs 3, 4, 5 and 6 respectively.

6.2.3 LabVIEW SignalExpress © Software

LabVIEW SignalExpress is data-logging software from National Instruments which collect, process, analyse and generate and store signals from the NI-USB 6211.

6.3 Current measurement

A clamp multimeter, ISO-TECH© model IPM 138 was used to measure the current during experiment. The multimeter has several features such as power and power factor measurement, AC and DC RMS (root mean square) reading. Table 6.1 shows some basic specifications of the clamp multimeter.

Table 6.1: Clamp multimeter specifications

Description	Range
DC/AC Voltage	60V, 600V, 1000V DC and 60V, 600V, 750V AC
DC/AC Current	600A
Watt	4KW
Power factor	-1 to 1
Resistance	600 Ω, 6Ω, 20 kΩ

6.4 Material characterization procedures

6.4.1 Thermal decomposition LDPE sample

Thermal analysis refers to a group of techniques used to determine the physical or chemical properties of a substance when it is heated, cooled or kept at constant temperature. When heat

treatment is applied to a sample in the first measurement it may cause physical and chemical changes. Those changes can be investigated by cooling the sample and then measuring it a second time in the same instrument (Toledo, 2013).

6.4.2 Differential Scanning Calorimetry

Differential Scanning Calorimetry (DSC) is a technique that measures the heat flow to and from a sample and then as the sample is heated, cooled or maintained at constant temperature - with Indium as reference material and is measured as a function of temperature or time. The measurement signal expressed in mW is the energy absorbed by or released by the sample.

6.4.3 Thermogravimetric Analysis

Thermogravimetric Analysis (TGA) measures the weight of a sample as function of temperature. It is a technique which provides an understanding of sample decomposition behaviour during heating. It allows to detect the mass of a sample, whether gain or loss and evaluates by step the changes in mass and this will be represented as a percentage of the initial mass. Afterwards, TGA determine temperatures that characterize a step in the mass gain or in the mass loss curve.

6.4.4 Infrared spectrometry

Fourier Transform Infrared Spectrometry (FT-IR analysis) is an analytical technique that is used to identify organics such as wine polymeric and inorganic materials. An infrared spectrum is usually obtained by passing infrared radiation through a sample and determining what portion of the incident radiation is absorbed and passed through at a particular energy (Stuart, 2004; Patz et al., 2004).

IR spectrometers can use ATR technique which is based on the Fourier transform sampling technique to characterize materials. This technique is non-destructive as there is no need for the material to be grinded or dissolve before testing. The sample is then confirmed by comparing the peaks in a specific region in a wavelength to the ones in a reference spectrum that constitute a database. The resulting spectrum represents the absorption and transmission which is the molecular fingerprint of the sample studied. If the resulting peaks match, a report is produced. However, if it does not, the ATR analysis will be reported as inconclusive.

The ALPHA © spectrometer from Bruker shown in Figure 6.3 was used at Stellenbosch University facility (Institute for Wine Biotechnology) for wavelength identification. It is a compact spectrometer used in combination with a diamond ATR (Attenuated Total Reflection) unit and it is able to measure even very hard plastics. The ATR technique is an FT-IR sampling method for both solids and liquids (Lowry & Bradley, 2011). Its diamond crystal is brazed into tungsten carbide hard metal as shown in Figure 6.4. This assembly allows the application of very high pressure on sample to get its IR measurement when brought into contact with the ATR crystal. Table 6.2 shows the ALPHA spectrometer specifications.
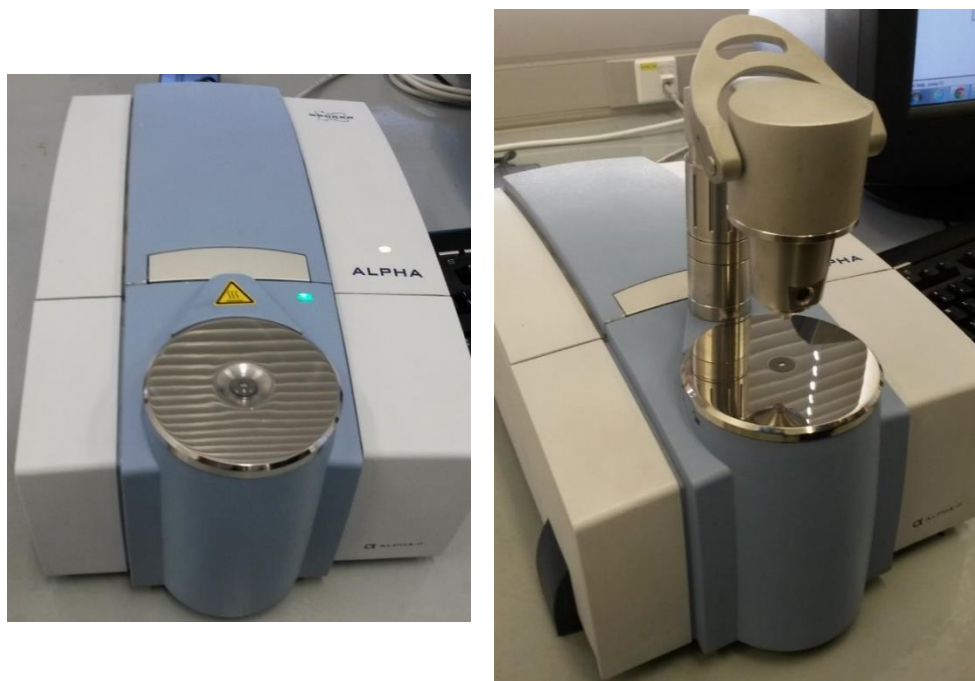
Figure 6.3: ALPHA FT-IR spectrometer

Figure 6.4: IR radiation and spectroscopy (Bruker, n.d.)

Table 6.2: Bruker Alpha spectrometer specifications (Bruker, 2012)

Description	Specification
Weight	7 kg
Dimension (w*d*h)	22*33*26 cm
Operating system	Windows XP, Windows 7
Computer interface	Ethernet, remote control via W-LAN
Accessory recognition	Automatic accessory recognition, automatic performance test and automatic setting of appropriate measurement parameters
Mobility	Rechargeable battery pack, car battery connector, slate tablet PC
Electrical requirements	100 – 240 VAC, 50 – 60 Hz, 20W
A/D converter	True 24 bit dynamic range
Temperature stability 100% line	<1% per °C

Wave number accuracy	< 0.05 cm⁻¹ at 2000 cm⁻¹
Spectral range	375 – 7500 cm⁻¹
Signal-to-noise ratio	typically > 50000:1 (1 min measurement time)
Spectral resolution	> 2 cm⁻¹, freely adjustable from 0.8 cm⁻¹ to 256 cm⁻¹
Wave number accuracy	< 0.05 cm⁻¹ at 2000 cm⁻¹

6.5   Temperature measurement

The gasification process takes place at standard atmospheric pressure and the reactor is relatively airtight. As the project is laboratory scale, it has a limited capacity for processing plastic feed rates. Pelletized LDPE samples of 5 g and 3 g were used throughout the experiments.

At the start-up of each experiment, the reactor was heated up to around 650 °C, the input voltage of the reactor was 230 volts and the rated current was 4.2 A. Once the temperature has reached uniformity in the chamber, pellets were fed manually into the reactor through a feeder inlet.

Results show that recorded temperatures of individual heater are 700 °C which is reasonable to provide sufficient energy to heat and gasify pellets inside the reactor chamber. The overall temperature inside the reactor chamber is 900 °C.

Temperatures measurement were taken inside the chamber and recorded with the DaQ by reading the temperatures directly from the embedded type k thermocouple. The outside temperatures of reactor (reactor wall) were taken using a thermal imager, Fluke © Ti20. The maximum temperature inside the reactor chamber collectively could reach 1200 °C. The maximum operating temperature from each heater is 900 °C, it was therefore advised to switch the reactor off in order to preserve the heaters life span as they are mounted facing each other.

Temperatures recorded were proved sufficient enough to melt the pellets. The melting point of LDPE sample was noted around 114 °C - 115 °C in the literature (Shnawa et al., 2011) and high temperature inside the reactor chamber provided enough heat to let the pellets convert from solid to gas. The char is manually removed from plate before the next experiment feed load.

Only a small amount of liquid plastic falls down on the plate that is the char collector shown in Figure 6.5.

Figure 6.5: Ash residue and char after gasification

CHAPTER 7 : EXPERIMENTAL RESULTS AND DISCUSSION

This chapter discusses the various test results in order to validate the functionality of the reactor. Preliminary results involved determining thermal modelling validation and temperature profiles length measurement sample, infrared spectroscopy experimental results as well as. Several samples of plastic waste were tested in terms of absorptivity and transmitivity in order to determine the exact wavelengths at which low density polyethylene and high density polyethylene perfectly absorb infrared radiation.

Once the results of the abovementioned tests were completed, experimental test was done. Tests were conducted independently on each stage and the results were compared to an expected outcome. For this, each stage was based on the basis of four heaters on, two heaters on and three heaters on.

7.1   Mathematical model simulation

In this section, the heat phase is investigated and the results discussed include only the simulation of the filament wire. The model is simulated under the conditions that the ambient temperature and the surrounding temperature are equal at 22°C and that to verify the validity of the mathematical model of the heating phase of the filament.

The results obtained represent the validation of the IR heater model analysis with a constant ambient temperature and surrounding of T = 295.15 K. Figure 7.1 shows the rising of temperature in the heating rate simulation as expected and it reaches its maximum temperature as mentioned by the manufacturer (AB, 2003) . Steady state is reached quickly as the dynamic is very fast within 30 seconds. The maximum temperature expected for the IR-heater is 1200°C for a power rating of P = 1000 W, which confirms the simulation.
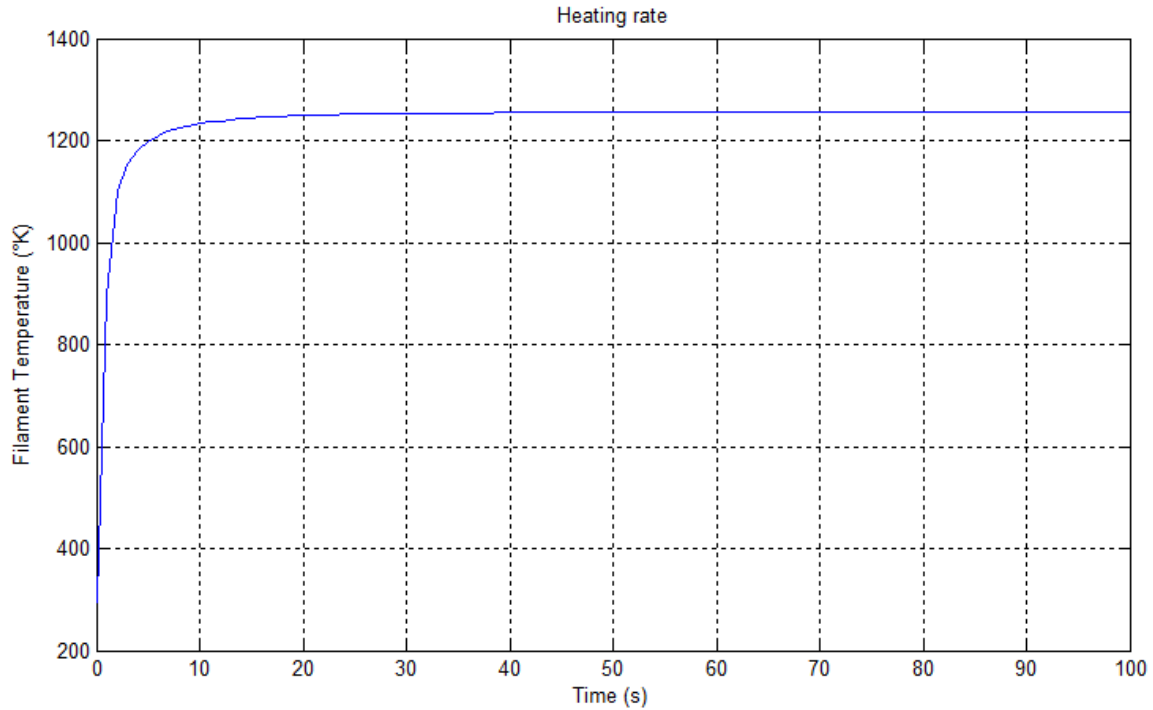
Figure 7.1: Heating phase of filament wire

7.2 Thermogravimetric analysis and wavelength measurements

Differential Scanning Calorimetry (DSC) and Thermogravimetric Analysis (TGA) on LDPE sample were conducted at University of Western Cape using an apparatus which combines both TGA and DSC techniques. The STA6000 from PerkinElmer© collects simultaneously DSC heat flow data and TGA data weight loss and results are shown in Figure 7.2 and Figure 7.3 and Table 7.1.

Table 7.1: TGA process

Sample type	Mass at start-up	Heating stage	Cooling stage	Gas injection	Results
LDPE	39.89 mg	30°C - 600°C at	600 °C to 30 °C	Argon	Gasification starts at 450 °C
Rate	N/A	10 °C/min	10 °C/min	5 ml/min	N/A

The LDPE thermogravimetry results are shown in Figure 7.2 below. These curves represent the weight reduction with time and that is associated with the temperature increase. The experiment stopped at 600 °C and then cooling start from 600 °C to 30 °C/min at a rate of 10 °C/min and the data recorded represent the weight reduction with time during cooling.
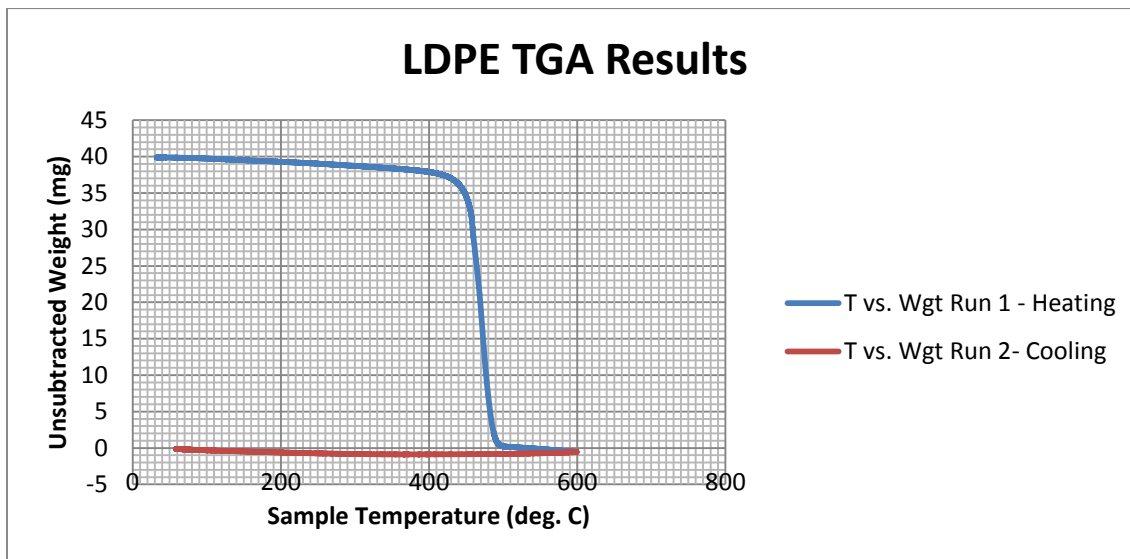
Figure 7.2: LDPE TGA sample results: LDPE sample weight reduction with time
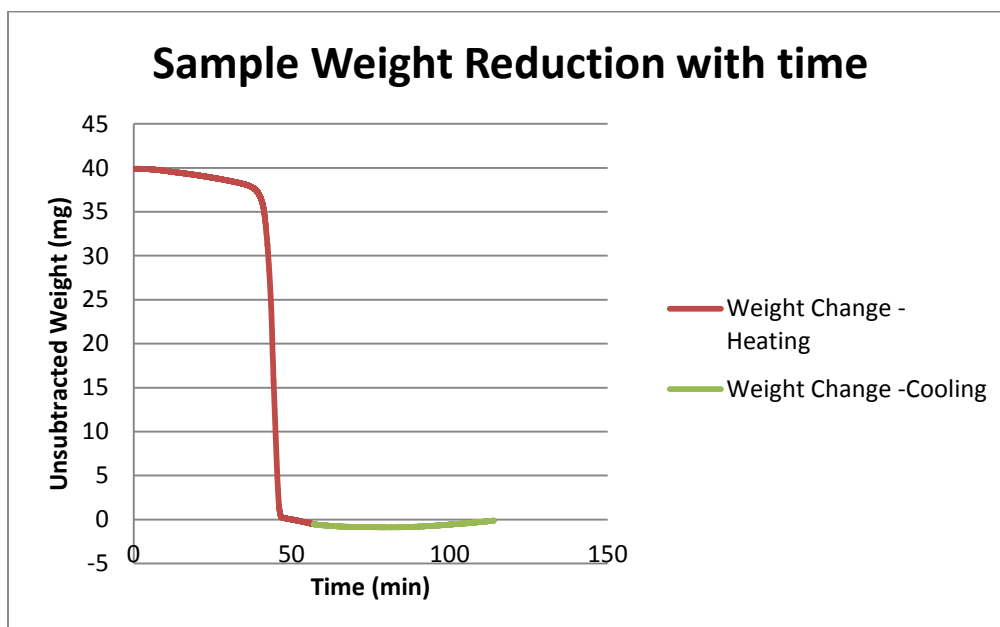
Figure 7.3: Sample weight loss during heating and cooling

The DSC results show the heat flow versus temperature during heating and cooling stages and as a function of time. It was observed that heat flow significantly decreases at around 450 °C as shown in Figure 7.4. It is the corresponding temperature where the LDPE sample was completely gasified which is evidenced from the TGA analysis which shows a marked reduction in mass.
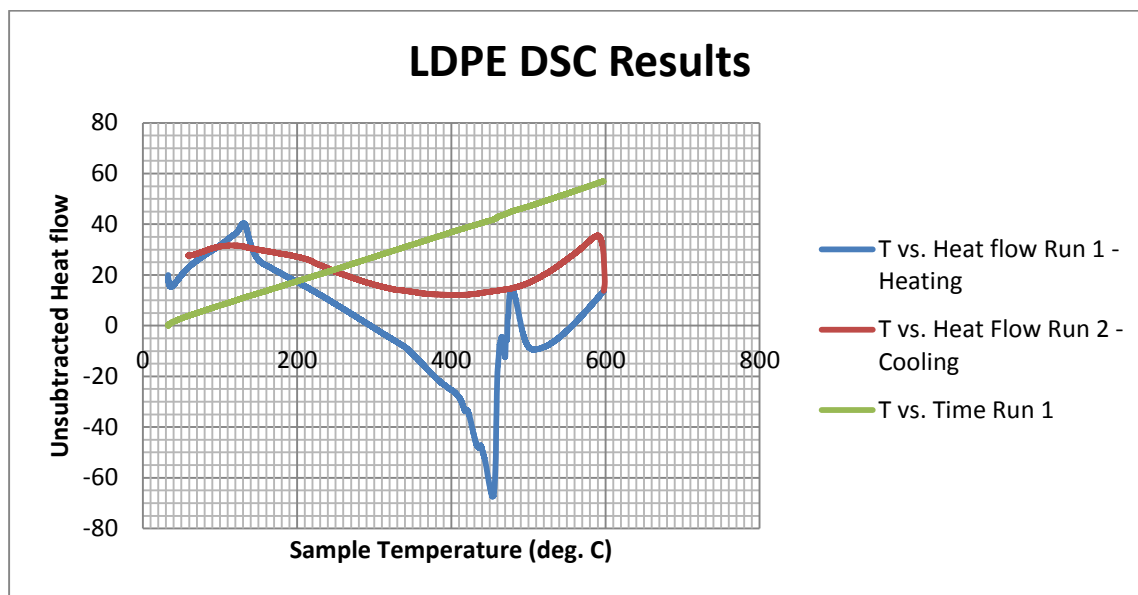
Figure 7.4: LDPE sample DSC results

7.3 Procedures for sample measurements

IR-Spectrometry was used to identify the plastic wavelength and spectra obtained after measurement from each LDPE sample, separated according to their colour, and were compared against a standard database of spectra for polymers (Anon., n.d.; Bruker, 2010) in order to choose the relevant infrared heater. Each sample measurement was done within seconds and displayed using OPUS (v. 7.0) software. The following procedure was adopted before measurement:

- Diamond platform to be mounted on an in-compartment through plate using a millimeter square 45° diamond crystal
- Set the resolution to 4 cm^{-1}
- Temperature measurement ranged from 29.8 °C - 30.1 °C
- Set the number of scans to 64 for the sample

- Number range 4000 – 400 cm^{-1}
- Ensure plate and diamond are clean
- Background measurement 64 scans
- Name the sample
- Start sample measurement

Sample data is collected and results plotted according to XY axis where X axis represents the absorptivity in percentage and the Y axis represents the wavenumber in cm^{-1}.

Absorbance measurement of LDPE sample using an ALPHA spectrometer was conducted and results are shown according to their different colours in Figures 7.6 – 7.11 to determine the IR absorption wavelength. Results also show that the absorption of LDPE may depend on the sample tested as well as its thickness due to the fact that pellets were of different sizes. Some LDPE pellet samples have 0.5 mm thickness and others have 1 mm thickness as shown in Figure 7.5.

Figure 7.5: LDPE sample
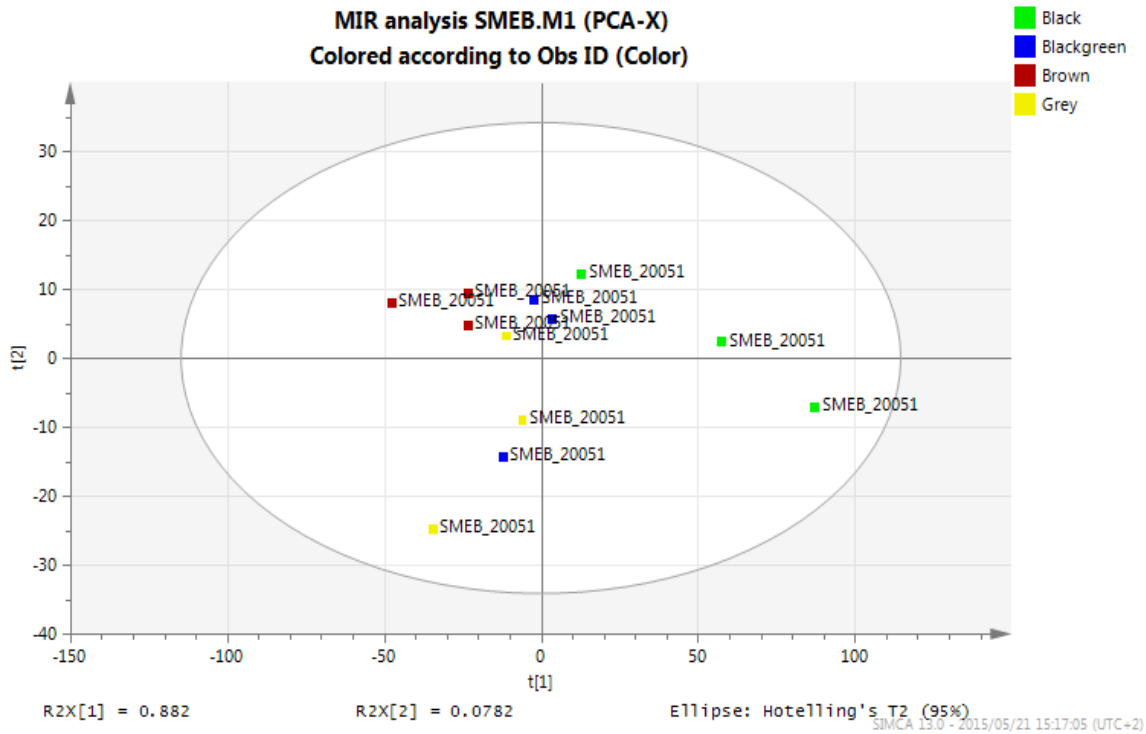
Figure 7.6: Principal Component Analysis (PCA) of LDPE sample
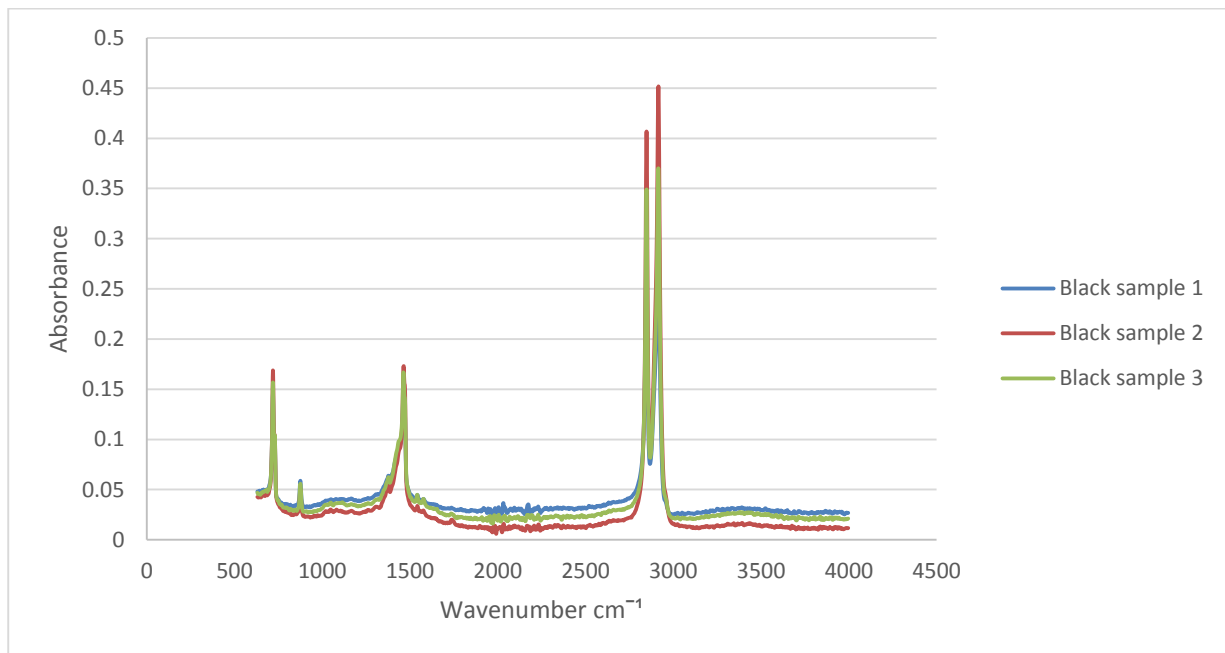
Figure 7.7: Absorptivity of low density of polyethylene – black sample

104
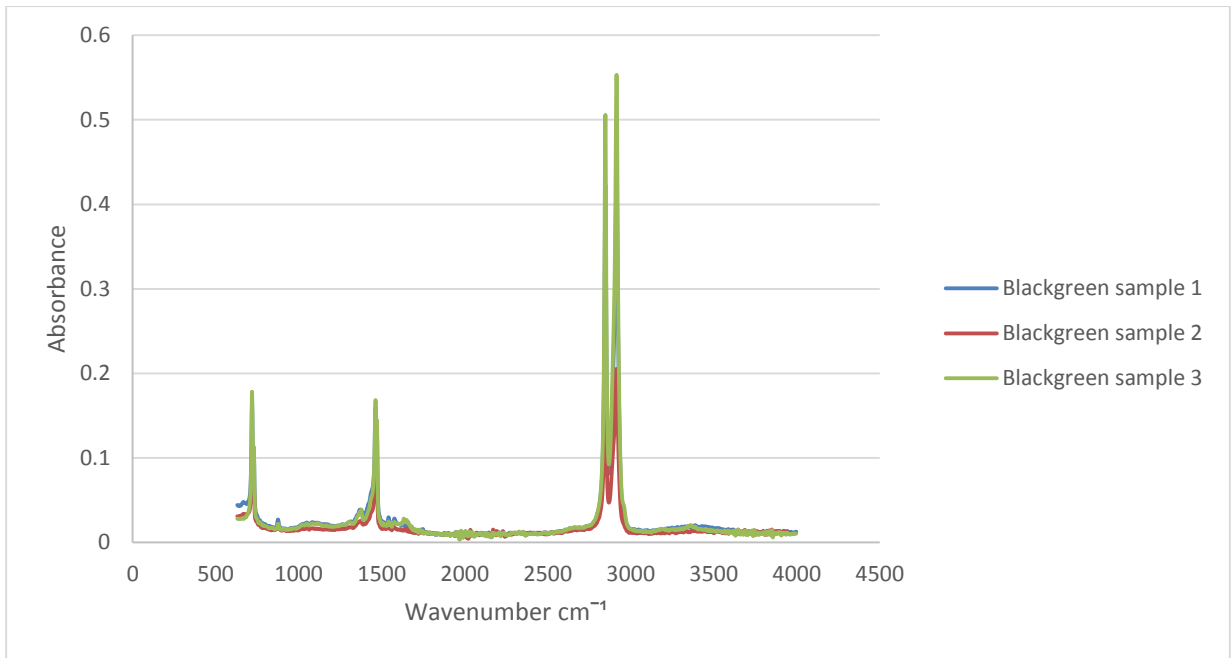
Figure 7.8: Absorptivity of low density of polyethylene – black-green sample
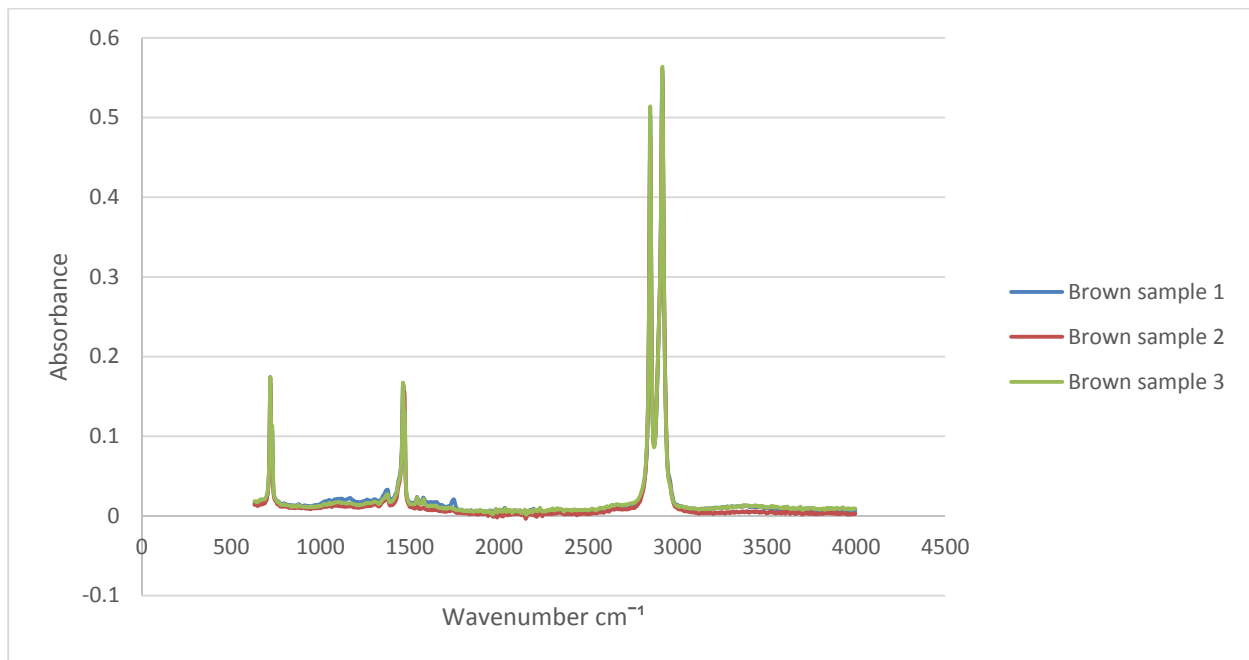
Figure 7.9: Absorptivity of low density of polyethylene – brown sample
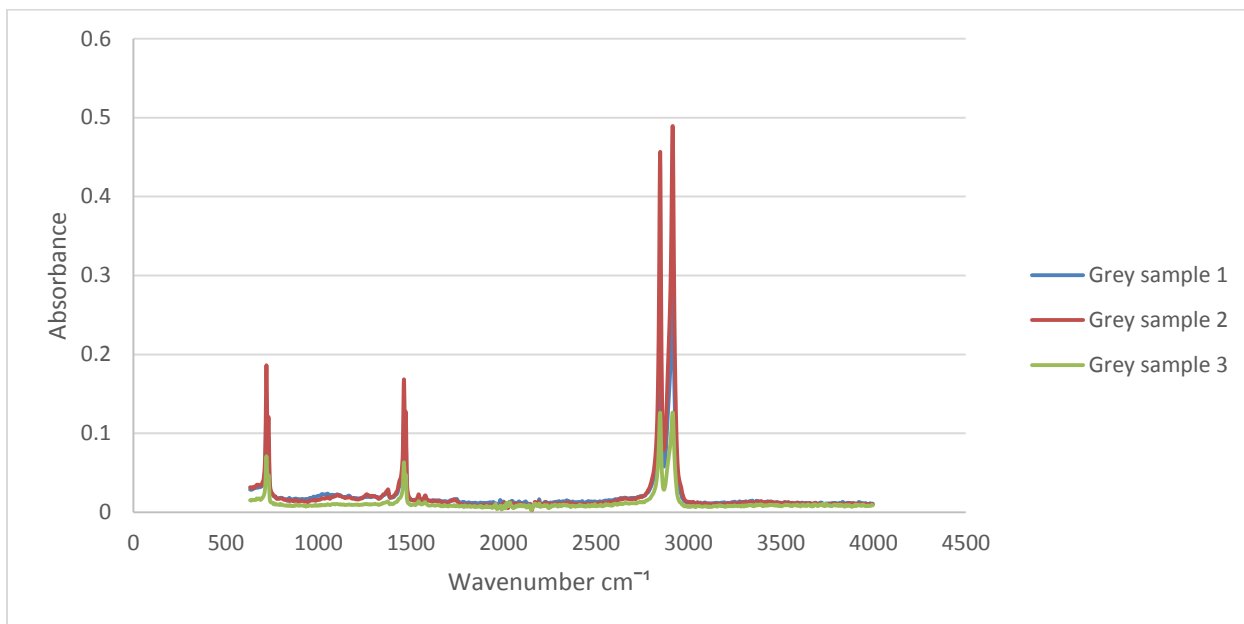
Figure 7.10: Absorptivity of low density of polyethylene – grey sample
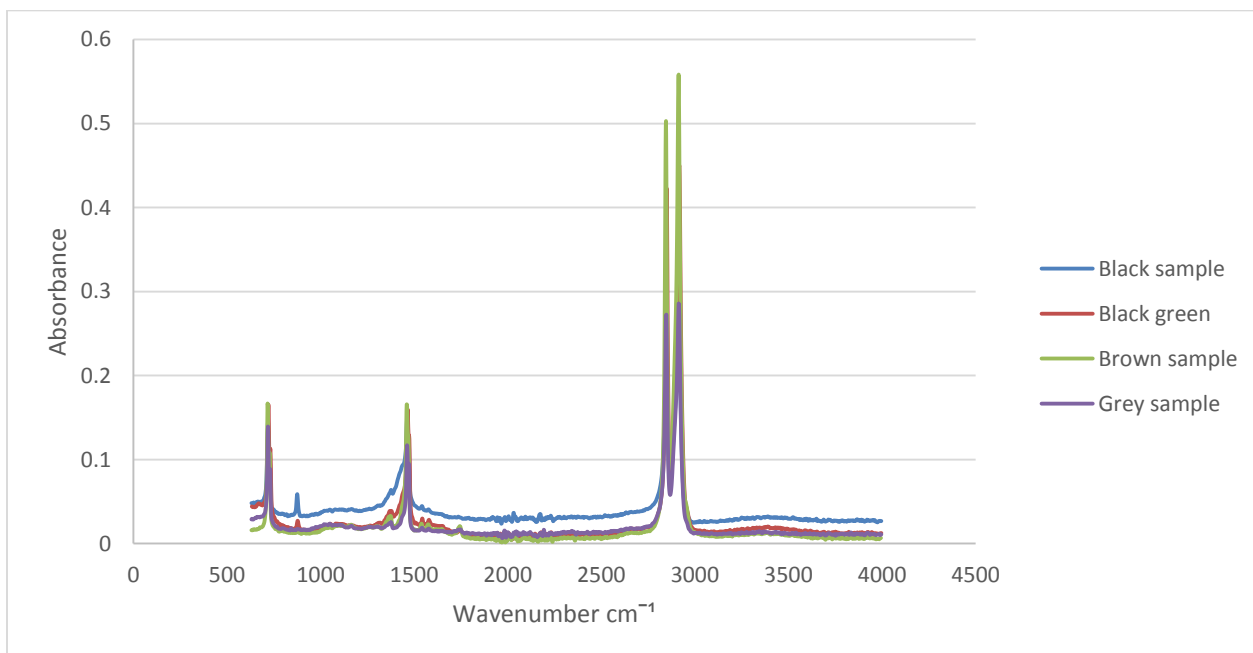
Figure 7.11: Absorptivity of low density polyethylene – all sample combined.

With regard to previous figures, Table 7.2 shows the approximate wavelengths determined from wavenumber of LDPE peak absorption values.

Table 7.2: Measure peak values of LDPE according to colour

LDPE pellet sample	Measured approximate peak value	Measured approximate absorption
Black sample	3.42 µm	45 %
Black-green sample	3.42 µm	55 %
Brown sample	3.42 µm	56 %
Grey sample	3.42 µm	49 %

7.4 Experiment procedures

Considering the gasification of plastic, the plastic feedstock fed into the reactor during each experiment is measured and temperatures are recorded with thermocouples. It was noted however, that in order to observe a clear gasification, to wait for completion of the experiment rather than feeding the reactor at a certain rate because of no clear indication of the completion time of the gasification inside the gasifier.

The operating performance of the IR reactor considered are the start-up time, the time to generate the gas, the total operating time, the amount of gas produced after test. After loading, synthetic gas (syngas) is produced in approximately 57 seconds later and gasification lasted for around 20 to 30 minutes. The gas composition was not evaluated nor calculated as the gasifier was the main focus of the experiment for optimization.

In order to evaluate the electric power consumption a current clamp multimeter was used to record the current during the experiment to determine the power of the reactor. The electric current, power and temperatures in the reactor chamber were recorded and shown in Table 7.1.

The temperature profile during gasification of samples was recorded starting from the time plastic LDPE sample was put into the reactor through the feeding tube. The results of the tests carried out are presented in Table 7.3. The highest temperature reading of 1330 °C with LDPE as feedstock was obtained during gasification time. The graphs of the temperature distribution in

the gasifier with LDPE and HDPE as feedstock against time is plotted for all tests conducted. The operational temperature was found to be sufficient to use for gasification.

Table 7.3: Experimental result for reactor temperature

Date 2015 (DD/MM)	Run #	Sample mass	Heating time (HH:MM)	Operating temperature (°C)	Time in feedstock (HH:MM)	Gas starts after	Gas ends at (HH:MM)	Gasification time (min)	Char (g)	Current (A)	Power rating (W)	Wall temperature (°C)	Comment
19/08	0	5g LDPE	14:25 – 14:55 (30:43 min)	450 - 650	14:56 pm	30 sec	15:31 pm	33:45 min	< 1g	3.2 A	720	45	Few drops on plate as char
24/08	1	Void	15:20 – 15:45 (20 min)	650	Void	N/A	N/A	N/A	N/A	3.2 A	720	45	Test run
25/08	2	5g LDPE	14:49 – 15:14 (24:52 min)	500 – 700	15:14 pm	1 min	15:35 pm	20:11 min	< 0.5g	3.2 A	720	45	Reactor off at 15:25 pm as Temp > 950°C
25/08	3	5g LDPE	15:50 – 16:05 (15:09 min)	500 - 800	16:05 pm	2:20 min	16:17 pm	25:59 min	Very low < 0.5g	3.0 A	684	45	Software simulation stopped
26/08	4	5g LDPE	14:39 – 15:06 (26:42 min)	650 - 1000	15:06 pm	2:39 min	15:29 pm	22:34 min	Very low < 0.5g	3.0 A	690	46	Reactor off at 15:28 pm
28/08	5	5g LDPE	14:22 – 14:52 (30 min)	500 - 600	14:52	2:44 min	15:32 pm	36 min	very low < 0.5g	3.0 A	690	46	Reactor off at 15:20 as Temp > 1000°C
31/08	6	3g LDPE	14:36 – 15:13 (38 min)	600 - 950	15:13	9:41 min	15:37 pm	23:43 min	< 0.5g	3.1 A	713	53	Reactor off at 16:00 pm
02/09	7	N/A	15:03	700 - 800	15:03	46 sec	15:07 pm	4:28 min	N/A	3.1 A	713	63	Full run to clean reactor from slug
02/09	8	3g LDPE	15:09	800 - 1100	15:09	1:37 min	15:47 pm	37:51 min	Plastic stuck	3.1 A	713	63	Reactor off at 15:51

Date 2015 (DD/MM)	Run #	Sample mass	Heating time (HH:MM)	Operating temperature (°C)	Time in feedstock (HH:MM)	Gas starts after	Gas ends at (HH:MM)	Gasification time (min)	Char (g)	Current (A)	Power rating (W)	Wall temperature (°C)	Comment
03/09	9	N/A	12:49	500 – 700 Just letting reactor heat up	N/A	37:15 min	15:52	Not recorded	N/A	3.1 A	713	70	Plastic stuck in feed tube, cleaning reactor
15/09	10	3g LDPE	13:38 – 14:12 (34:04 min)	700 - 1100	14:12	01:34 min	14:47	32:58 min	Ash	3.2A	729.6	70	Low volume of smoke, few drops on plate
15/09	11	3g LDPE	14:54 – 15:05 (11:23 min)	800 - 1200	15:05	56 sec	15:40	34:29 min	Ash	3.2A	729.6	86	High volume of white smoke
15/09	12	3g LDPE	15:46	800 - 1000	15:46	01: 06 min	16:05	17:30 min	Ash	3.1A	713	98	"poof" sound and black smoke for 5 sec, drops on plate
17/09	13	3g LDPE	12:28 – 12:58 (30:05 min)	500 - 800	12:58	56 sec	13:50	48 min	Ash	3.1A	713	70	Light smoke, ash on sieve and drops on plate
17/09	14	3g LDPE	13:56 – 14:02 (07:55 min)	800 - 1000	14:02	57 sec	14:21	18:03 min	Ash	3.0A	690	81	No char on sieve. Light white smoke drops on plate
17/09	15	3g HDPE	14:28 – 14:35 (07:55 min)	800 - 1000	14:35	50 sec	14:55	20:00 min	Ash	3.0A	690	87	High volume of smoke at high speed, drops on plate
17/09	16	3g HDPE	15:00 – 15:07 (7min)	800 - 850	15:09	57 sec	15:31	21:39 min	Ash	3.0A	690	94	High volume of smoke at high speed

Due to high temperature profiles in the gasifier and considering the temperature in literature (800 °C; Wu & Williams, 2010; Brems et al., 2013) for proper gasification of LDPE, it was decided to keep the temperature in the reactor bed in the range of 650 °C – 900 °C.

Gasification of pelletized LDPE was performed by using different scenarios. Three case studies were done to determine the configuration of the heaters in order to maintain the temperature in the reactor bed in the range of 650 °C – 900 °C:

- Four heaters on (fully in operation)
- Two heaters on - two heaters off
- Three heaters on - one heater off

7.5 First case study with four heaters on

The first scenario has been to use the gasifier with its four heaters on. From the recorded temperatures it was observed that the maximum temperature the gasifier reaches was around 1400 °C. The following observations were made during experiments and after the gasifier inspection was complete once the experiments were finished.

7.5.1 Observations:

1. Expected temperature (800 °C) was reached very quickly within 10 minutes, however as starting to run the experiment, it was noticed that temperatures in the reactor were far above the operating temperature of the heaters 900 °C and were damaging the heaters as they face each other and heat propagates directly in the opposite direction of the heater facing it.
2. Smoke was produced. Only temperatures were recorded to evaluate the heaters operating temperature.
3. Plastic got stuck in the feeding tube as soon as it was put in because the tube was very hot.
4. The temperature at the bottom of gasifier increased significantly as no insulation was installed at the bottom of the gasifier
5. Plastic mixture was not totally gasified. From 100 g fed into the reactor, the mass residue was 77.25 g which indicates that only about 23 wt% of the LDPE sample gasified and that is due to heat not penetrating enough through the meshing bed made of stainless steel causing a low-melting mixture as well as blockage inside the gasifier. Figure 7.12 shows clinker that was removed after gasification test run.

This operation prompted several changes in the reactor in order to improve the operation of gasifier such as reducing the sample mass down to 3 to 5 g, as well as changing the meshing bed for the heat to pass through easily. The runs with the present configuration were done three times on the 30th June 2015 and temperature profile is recorded via thermocouples on Figures 7.13, Figure 7.14 and Figure 7.15. After changes were made, less clogging was observed and the gas could exit without restrictions.

Figure 7.12: Plastic residue after first test run. Mass of residue is 77.25 g
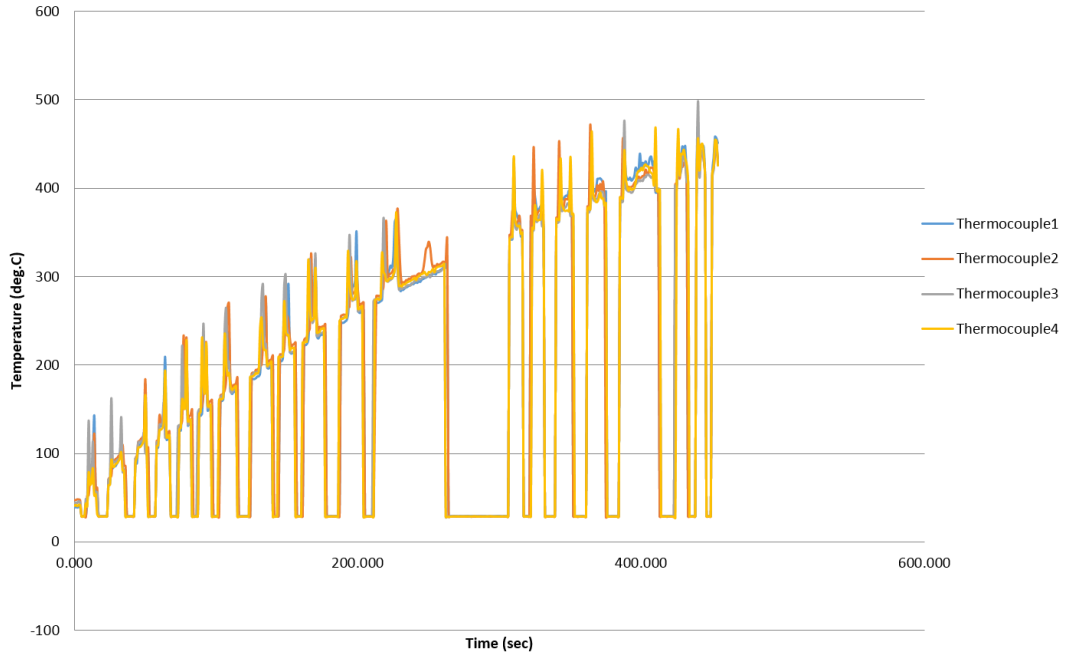
Figure 7.13: Temperature distribution run 1 without plastic pellets – 4 heaters on
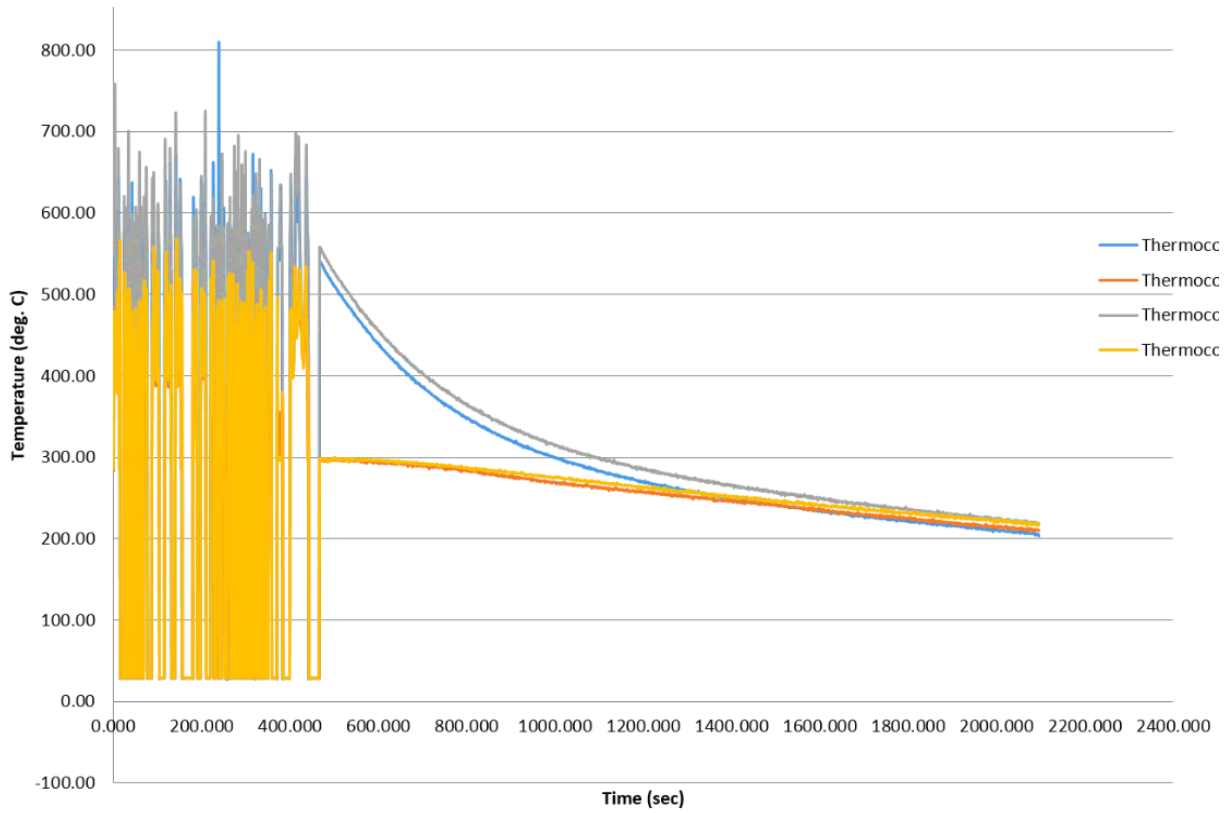
Figure 7.14: Temperature distribution run 2 without plastic pellets – 4 heaters on
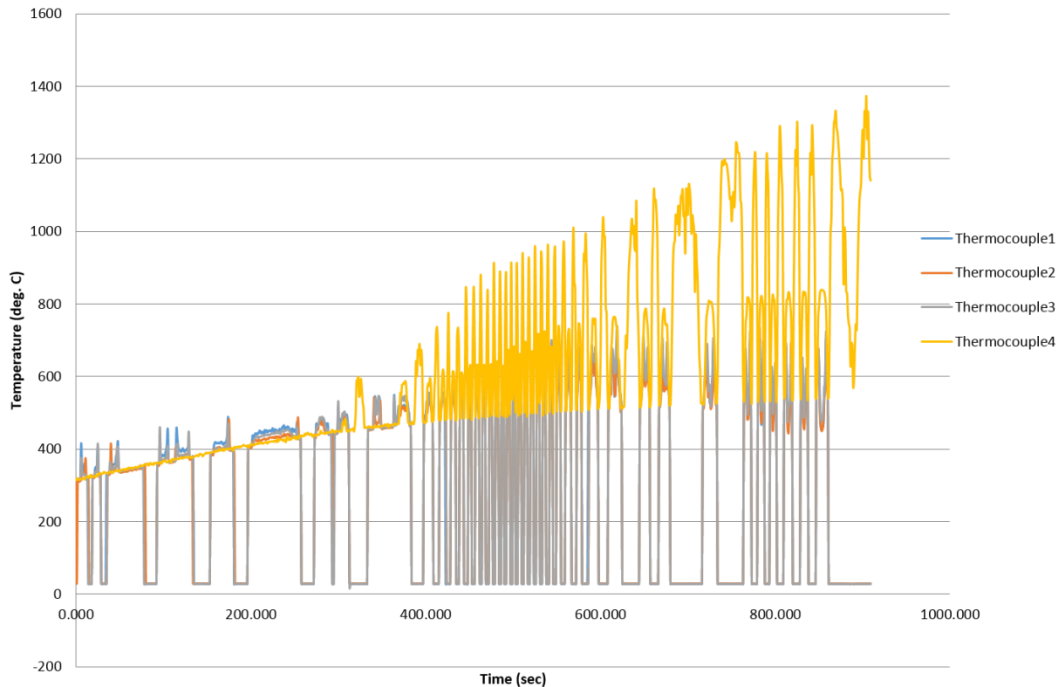
Figure 7.15: Temperature distribution run 3 with plastic sample in – 4 heaters on

7.6   Second case study: 2 heaters on – 2 heaters off

The second scenario was to use the gasifier with its two heaters on and two off although their thermocouples still connected to the DaQ for temperature readings. From the recorded temperatures it was observed that the average temperature the gasifier reached was around 650 °C which was not sufficient enough to gasify the sample in a less amount of time. The gasification time was about 45 minutes for 5 g of LDPE sample.

7.6.1   Observations:

1. Temperature (500 °C) was reached after 10 minutes and 600 °C was reached after 30 minutes
2. A slow rise in temperature was observed from the heaters that were off. The average temperature recorded from those two heaters was around 260 °C due to temperature diffusion uniformly in the reactor. Although the overall temperature was high enough to cause the degradation of plastic, the gasification time was about 40 minutes.
3. Small amount of gas produced therefore, the experiment was stopped and residue weighed. Only 1 g of sample gasified.

114

4. Plastic mixture was not totally gasified due to heat not penetrating enough the meshing bed causing a low-melting mixture.

The second case study led to the conclusion that the use of three heaters rather than two or four heaters as well as changing the meshing bed may help improve heat penetration in the reactor. Runs were done three times for two days 1st and 2nd July 2015 and temperature profiles are recorded via thermocouples as represented in Figure 7.16, Figure 7.17 and Figure 7.18.
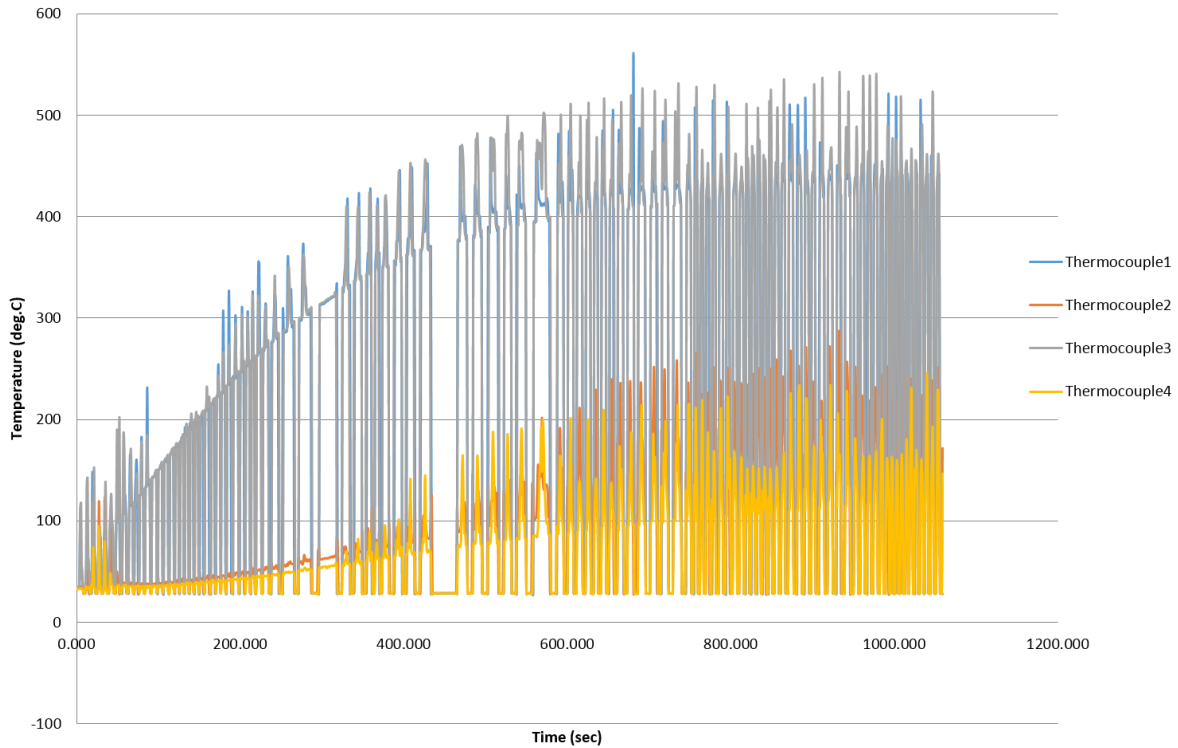
Figure 7.16: 1st July: Temperature distributions run – 2 heaters on 2 heaters off
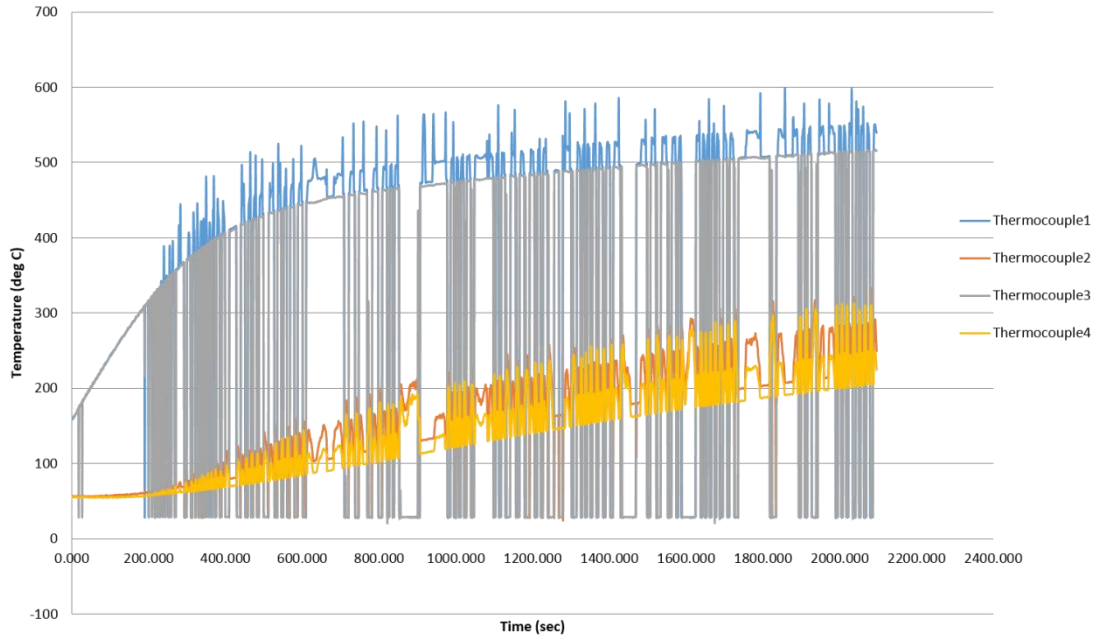
Figure 7.17: 2 July: Temperature distributions run1 – 2 heaters on 2 heaters off
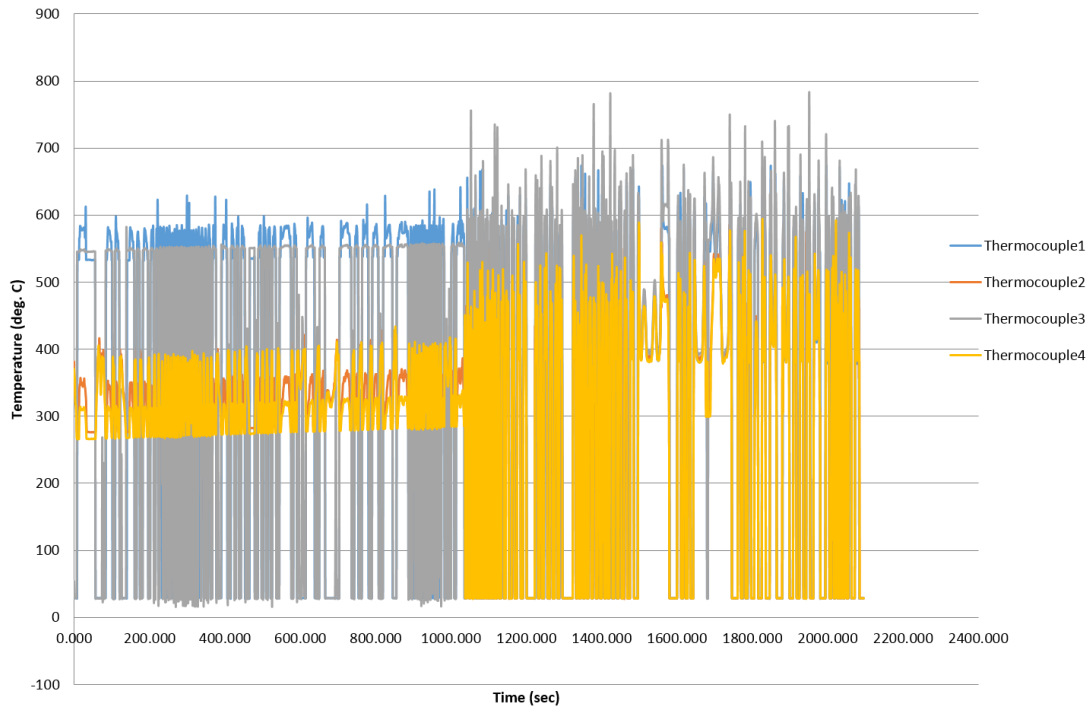
Figure 7.18: 2 July run: Temperature distributions run 2 with plastic pellets added in the reactor during gasification – 2 heaters on 2 heaters off

116

7.7 Third case study: three heaters on – one heater off

The third scenario was to use the gasifier with three heaters on and one off. Temperatures recorded were in the average of 800 °C distributed inside the reactor. The third case scenario was found to be the most suitable as the heater temperature profile was within their operating temperature. Plastic starts to gasifiy within 1 minute and lasted for around 22 minutes in average for the gasification of 5 g of LDPE sample and 15 minutes in average for the gasification 3 g of LDPE sample.

7.7.1 Observations:

1. Temperature (800 °C) was reached after 20 minutes.
2. A slow rise in temperature was observed from the heater that was off the first 200 seconds then temperature rises quickly after 400 seconds. The average temperature recorded from the heater was around 500 °C for a time of 23 minutes. The overall temperature was around 850 °C – 900 °C and the average gasification time was about 20 – 22 minutes.
3. Plastic mixture was totally gasified with ash as residue.
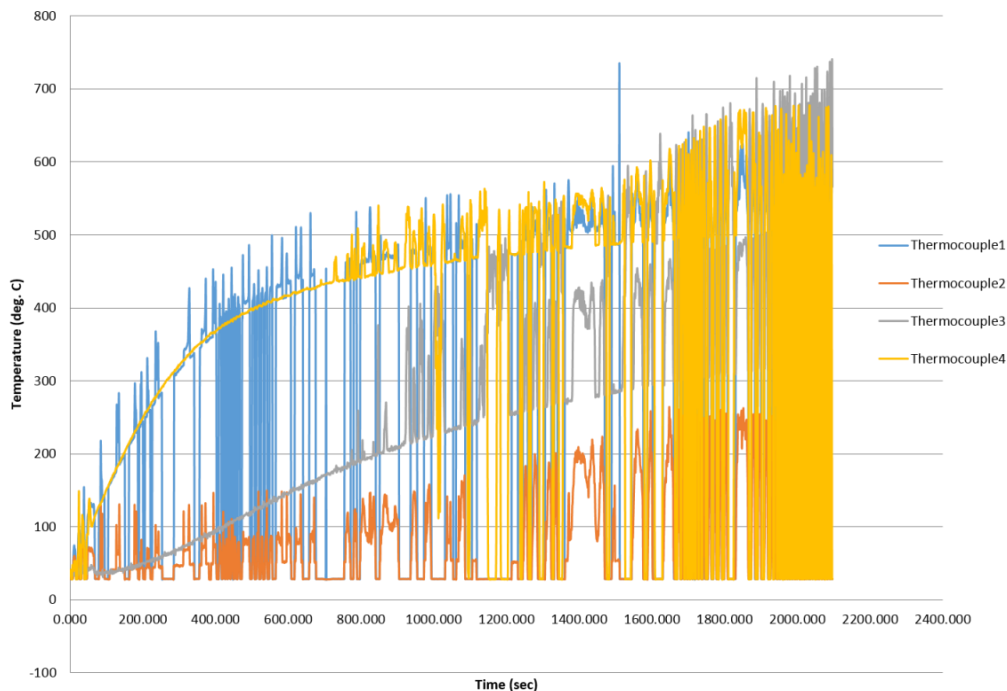
Figure 7.19: 19 August: Temperature distribution run 1 during gasification of 5 g of LDPE sample – 3 heaters on 1 heater off

117
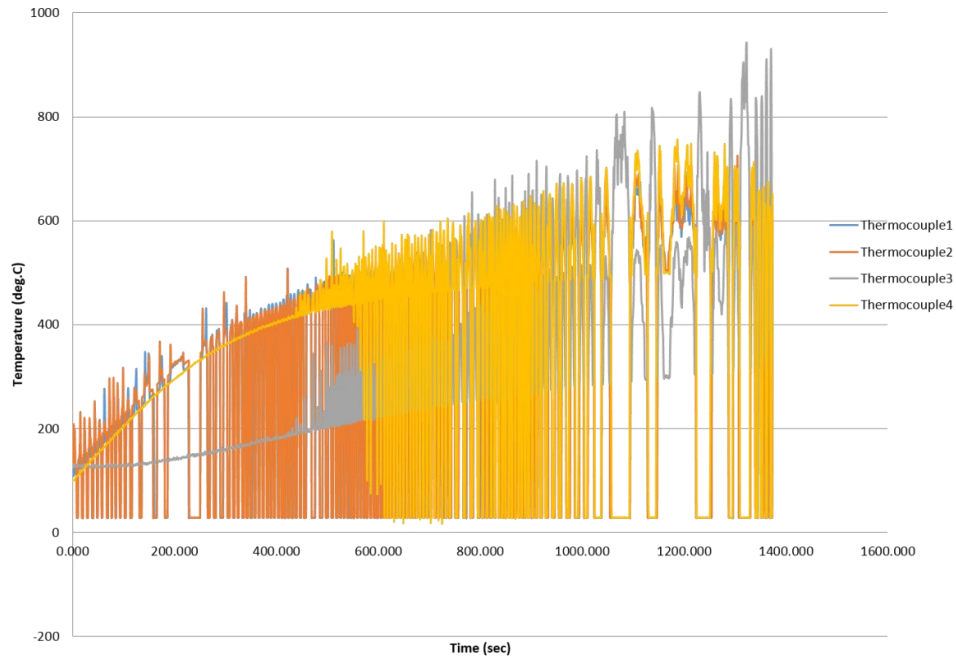
Figure 7.20: 19 August: Temperature distribution run 2 during gasification of 5 g of LDPE sample – 3 heaters on 1 heater off
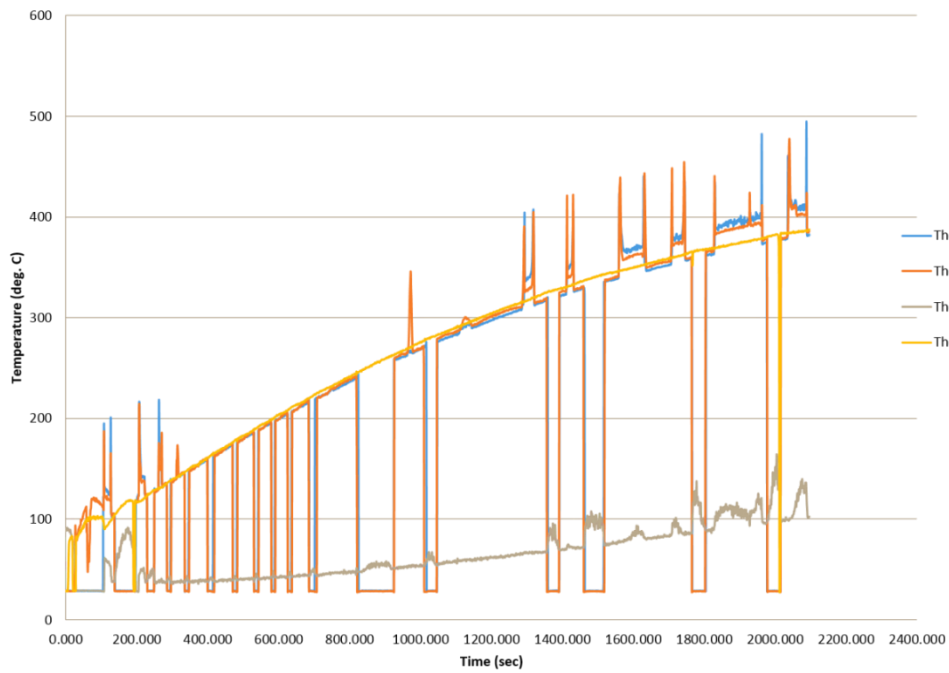
Figure 7.21: 24 August: Temperature distribution run1 during gasification of 5 g of LDPE sample – 3 heaters on 1 heater off
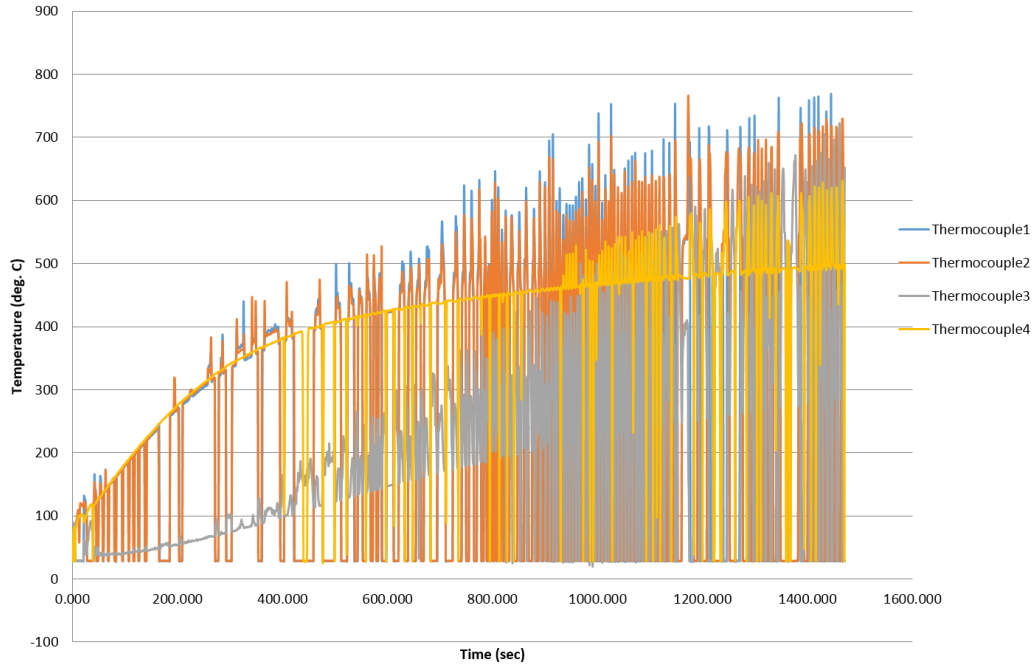
Figure 7.22: 24 August: Temperature distribution run 2 with no plastic in the reactor – 3 heaters on 1 heater off
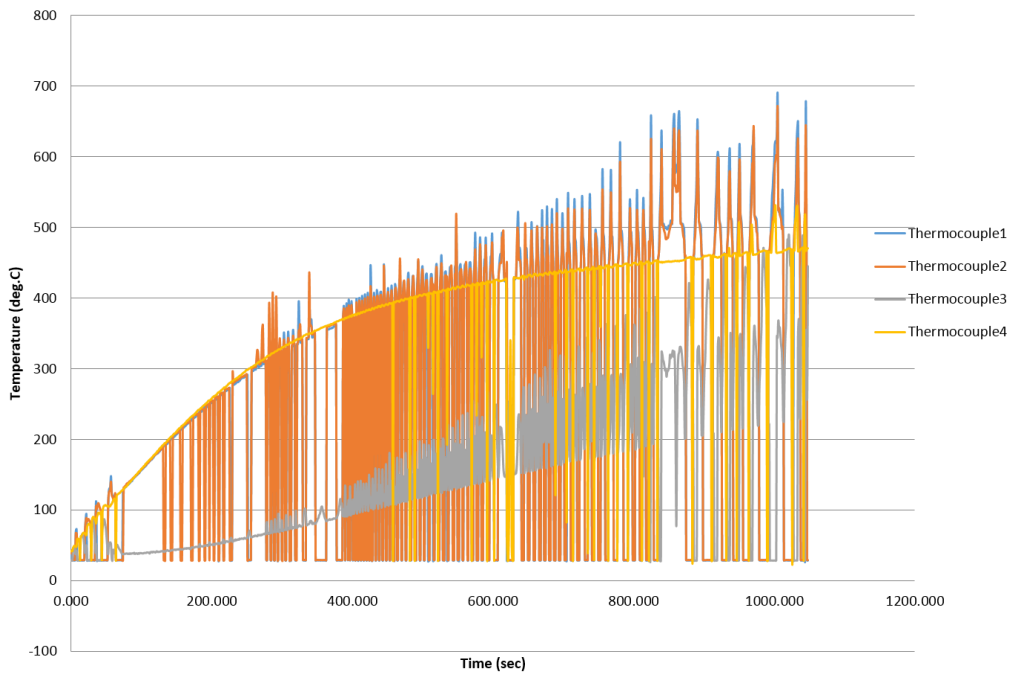
Figure 7.23: 25 August run 1: Temperature distribution during gasification of 5 g of LDPE sample – 3 heaters on 1 heater off
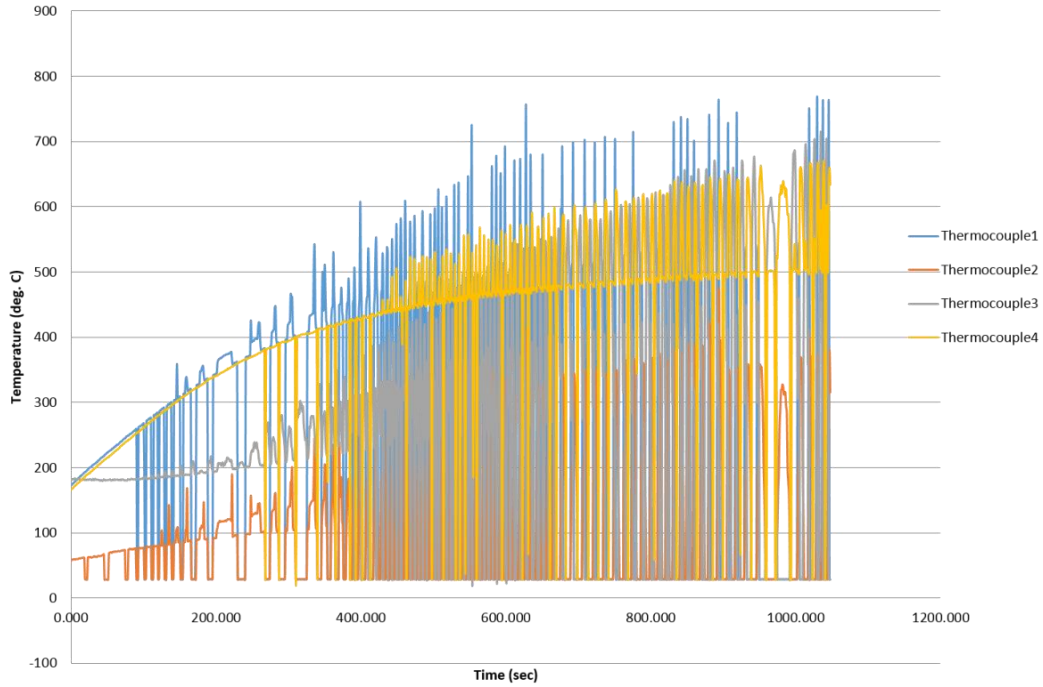
Figure 7.24: 25 August run 2: Temperature distribution during gasification of 5 g of LDPE sample – 3 heaters on 1 heater off
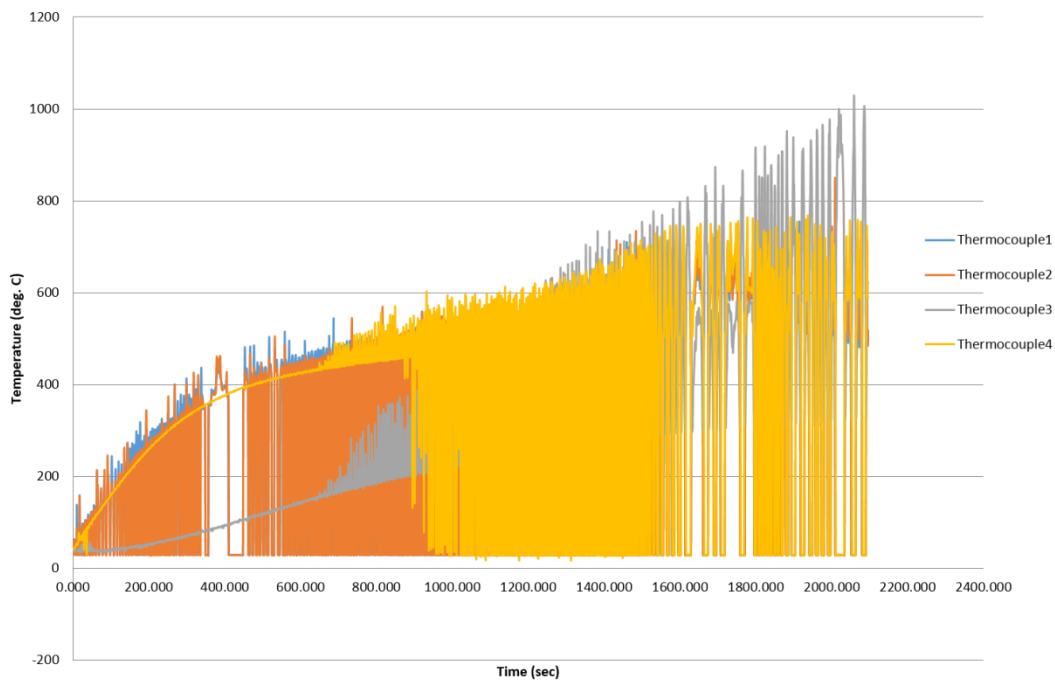
Figure 7.25: 26 August run: Temperature distribution during gasification of 5 g of LDPE sample – 3 heaters on 1 heater off
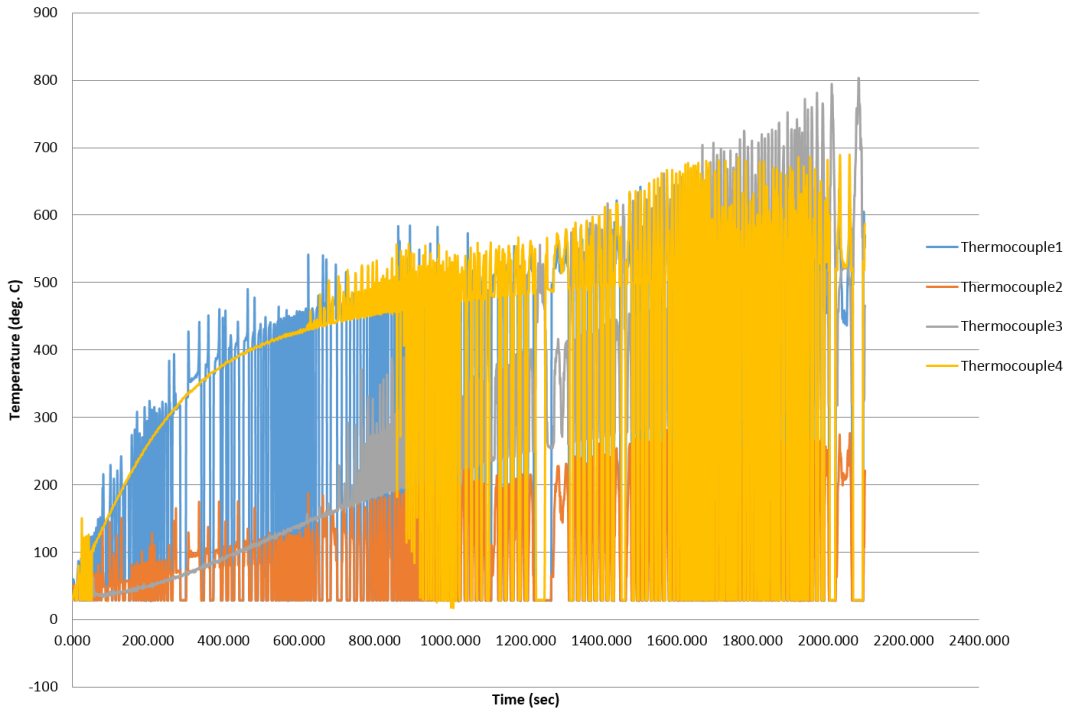
Figure 7.26: 27 August void test run: Temperature distribution – 3 heaters on 1 heater off
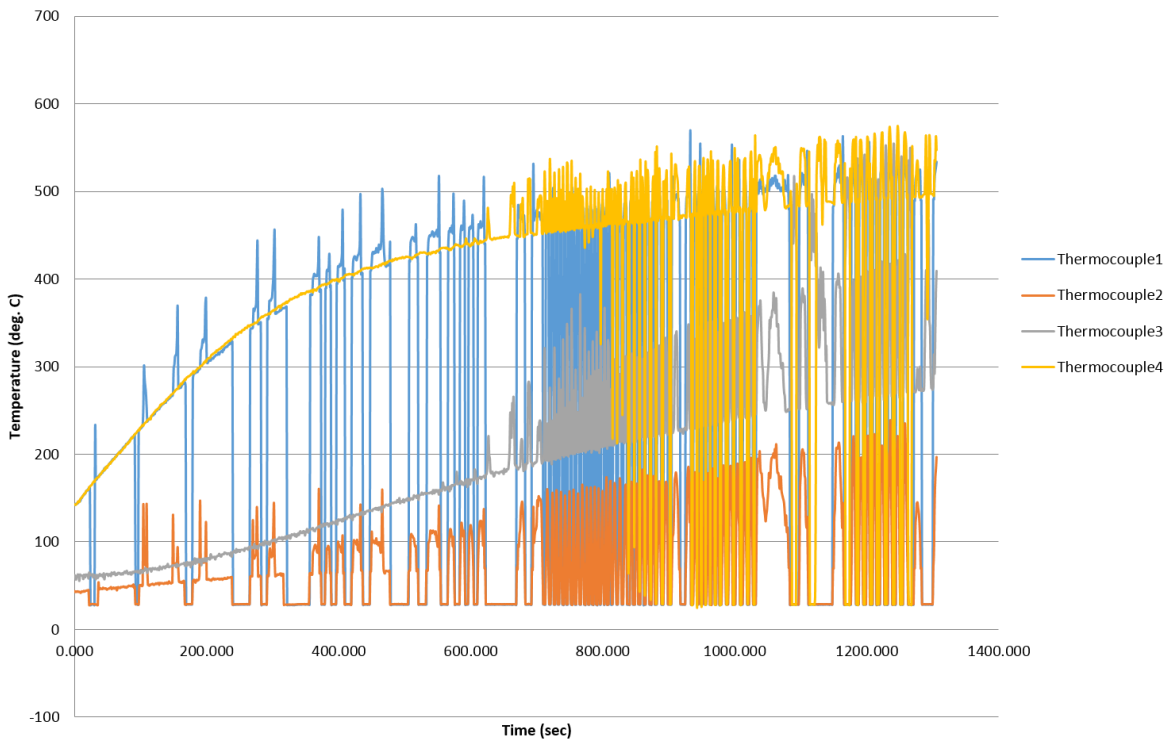
Figure 7.27: 28 August run: Temperature distribution during gasification of 5 g of LDPE sample – 3 heaters on 1 heater off

121
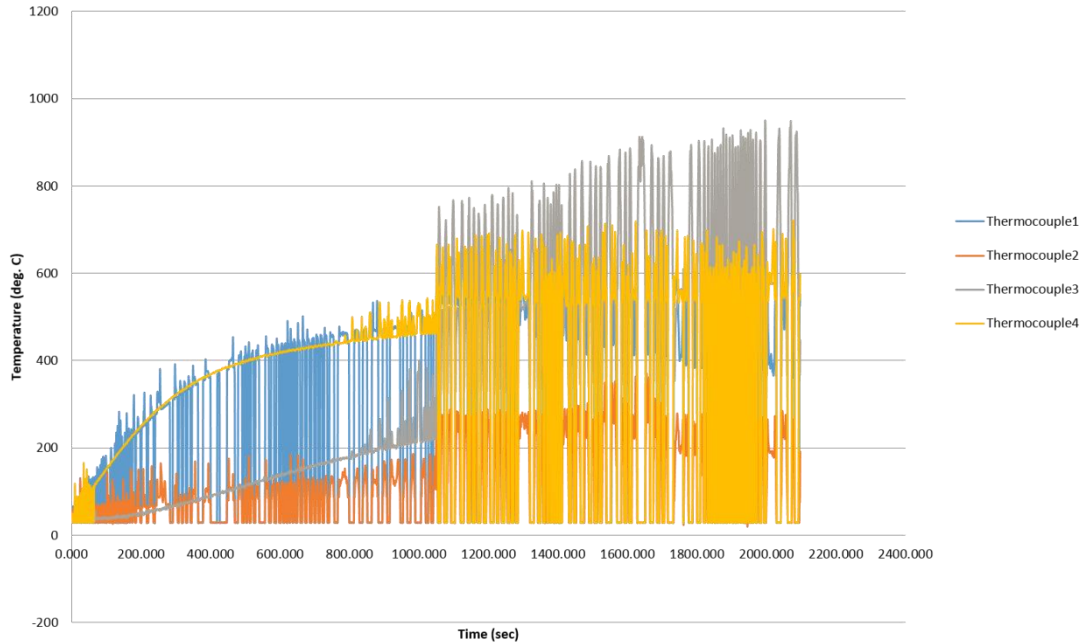
Figure 7.28: 31 August run: Temperature distribution during gasification of 3 g of LDPE sample – 3 heaters on 1 heater off
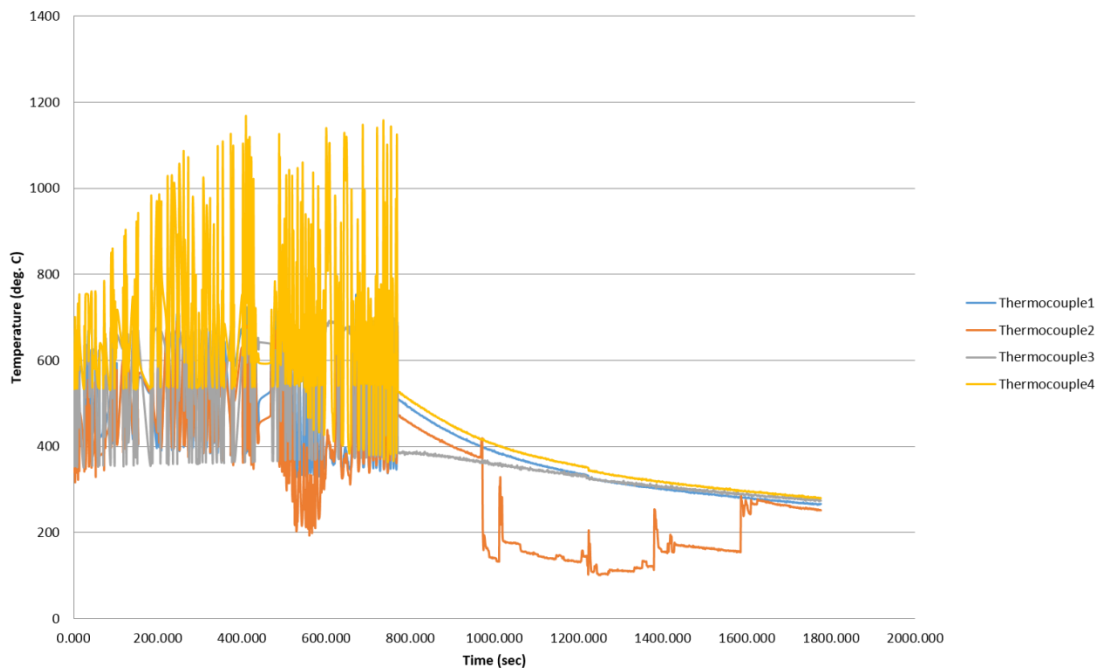
Figure 7.29: 02 September run: Temperature distribution during gasification of 3 g of LDPE sample – 3 heaters on 1 heater off
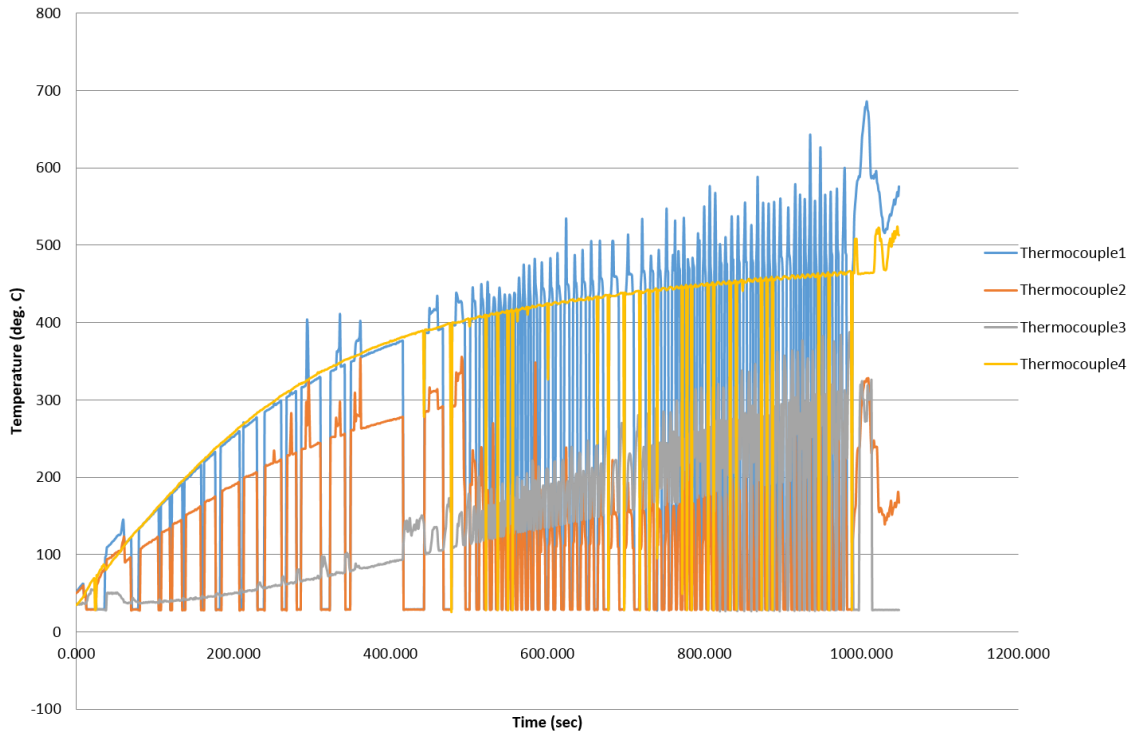
Figure 7.30: 03 September: Temperature distribution during cleaning of feeding tube – 3 heaters on 1 heater off
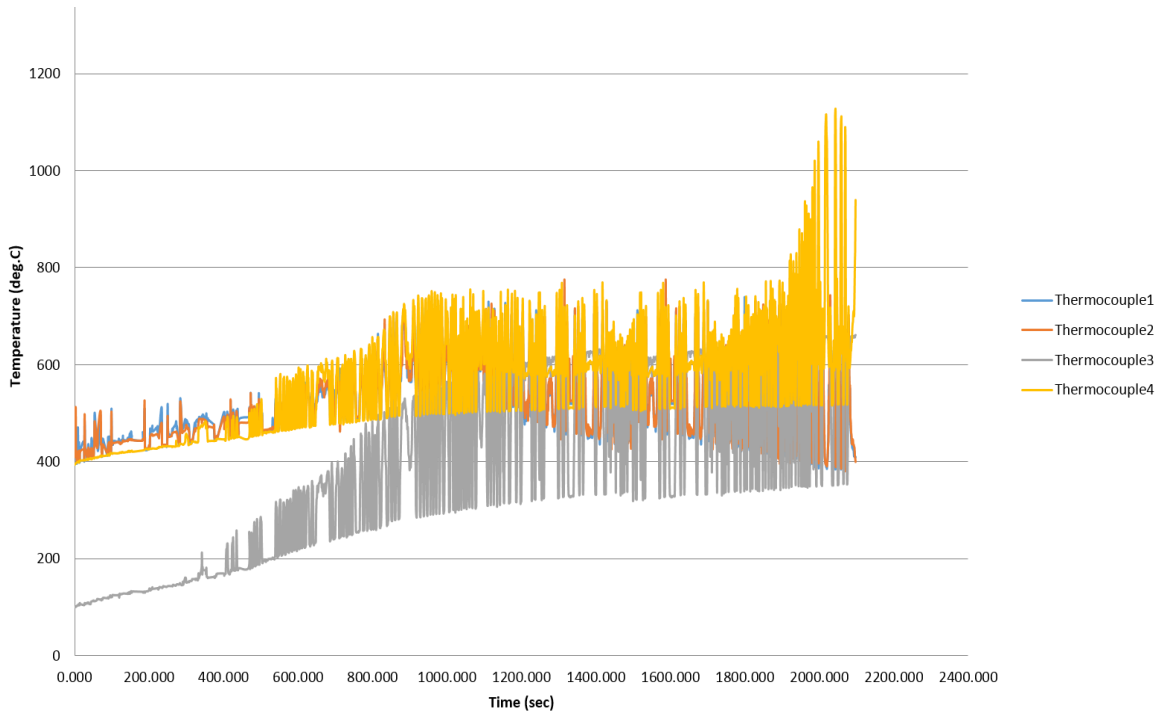
Figure 7.31: 15 September run 1: Temperature distribution during gasification of 3 g of LDPE sample – 3 heaters on 1 heater off

123
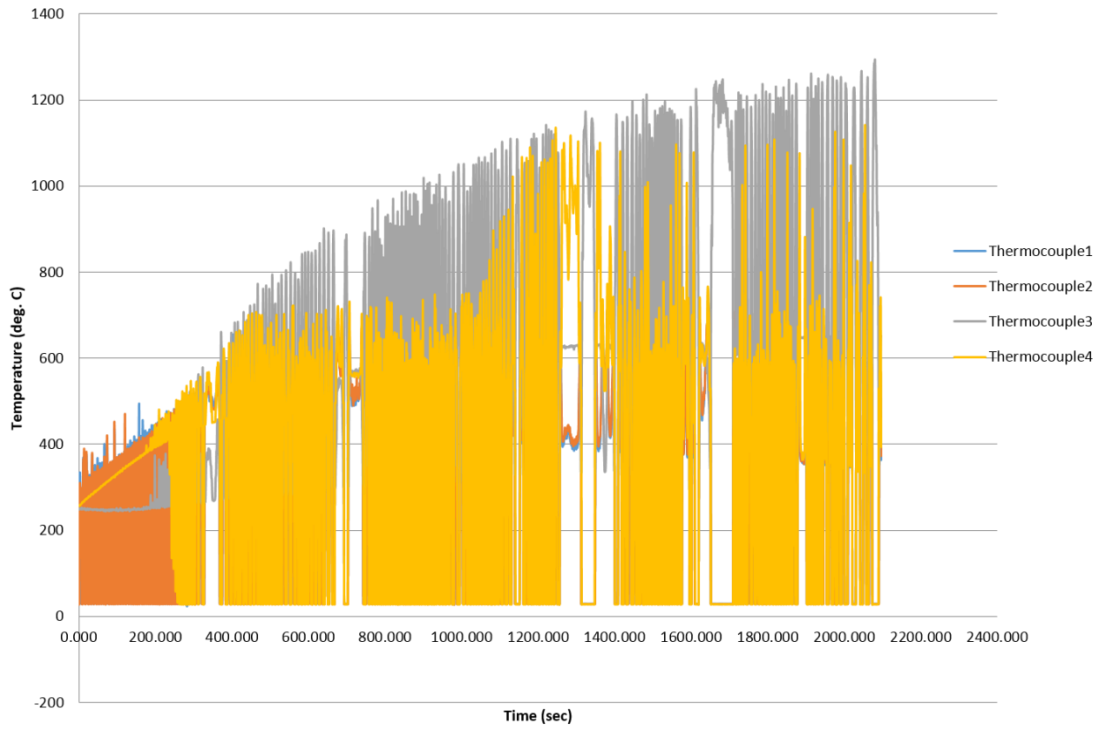
Figure 7.32: 15 September run 2: Temperature distribution during gasification of 3 g of LDPE sample – 3 heaters on 1 heater off
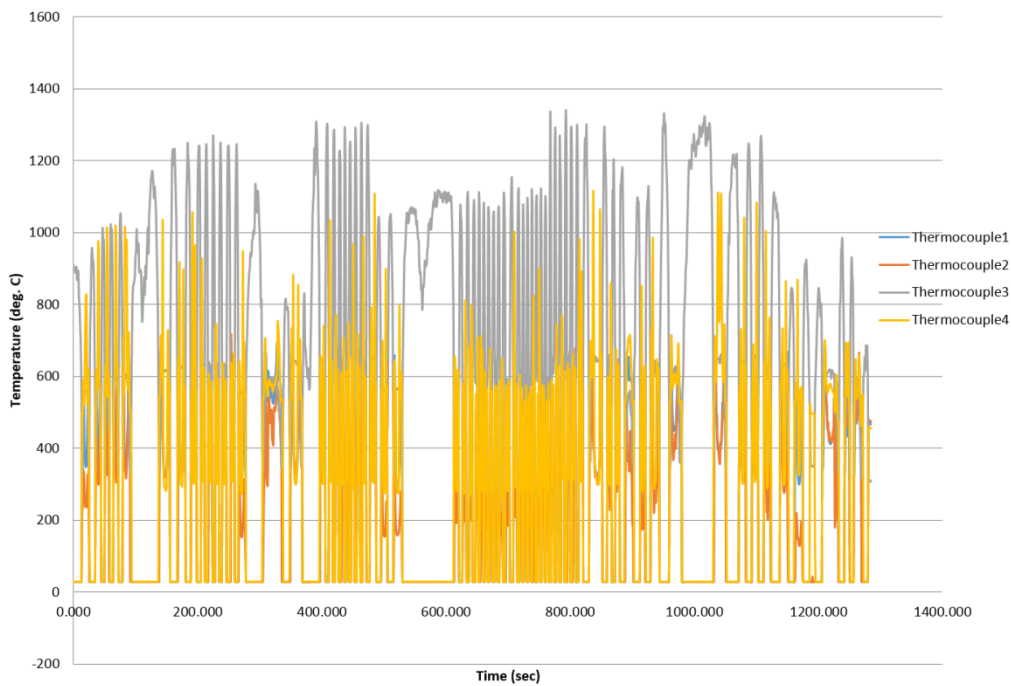
Figure 7.33: 15 September run 3: Temperature distribution during gasification of 3 g of LDPE sample – 3 heaters on 1 heater off
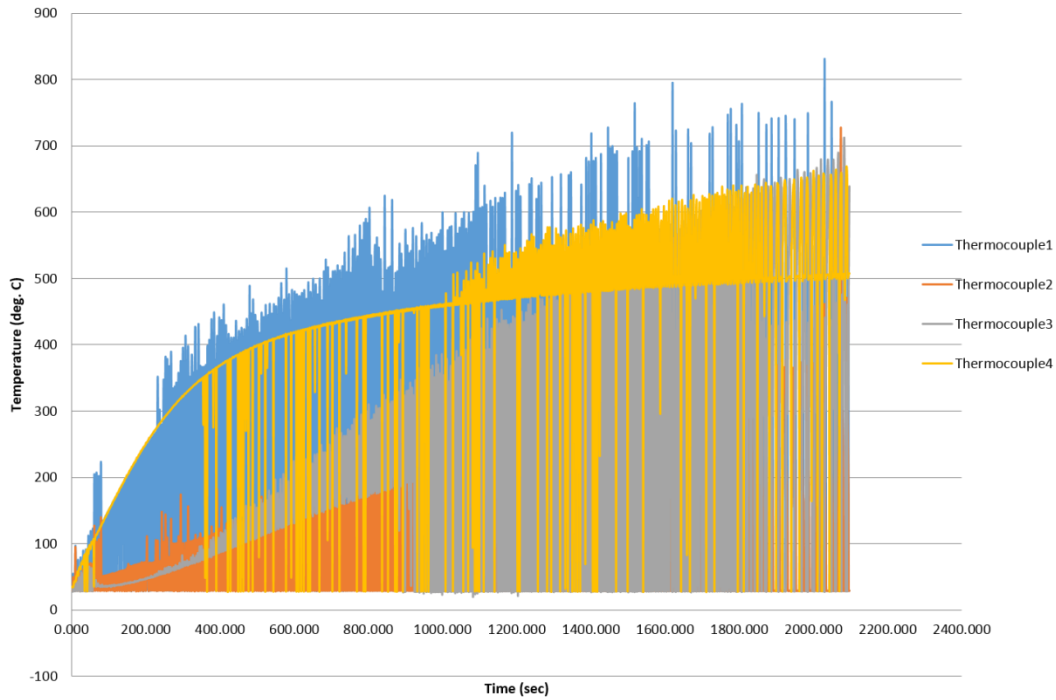
Figure 7.34: 17 September run 1: Temperature distribution during gasification of 3 g of LDPE sample – 3 heaters on 1 heater off
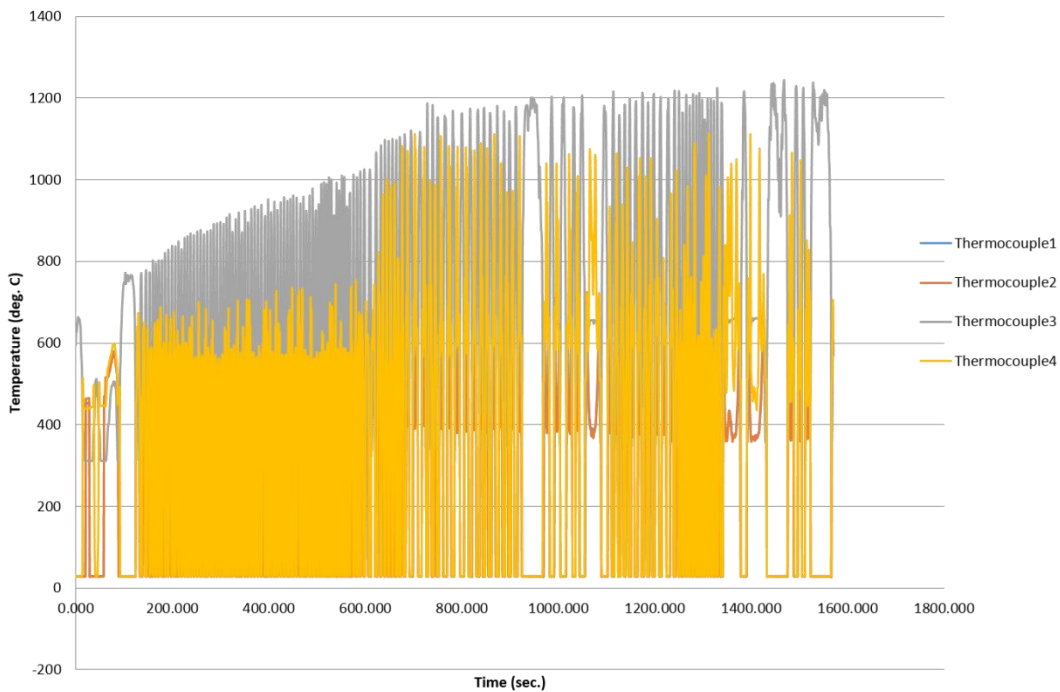
Figure 7.35: 17 September run 2: Temperature distribution during gasification of 3 g of LDPE sample – 3 heaters on 1 heater off

Figure 7.36: 17 September run 3: Temperature distribution during gasification of 3 g of LDPE sample – 3 heaters on 1 heater off
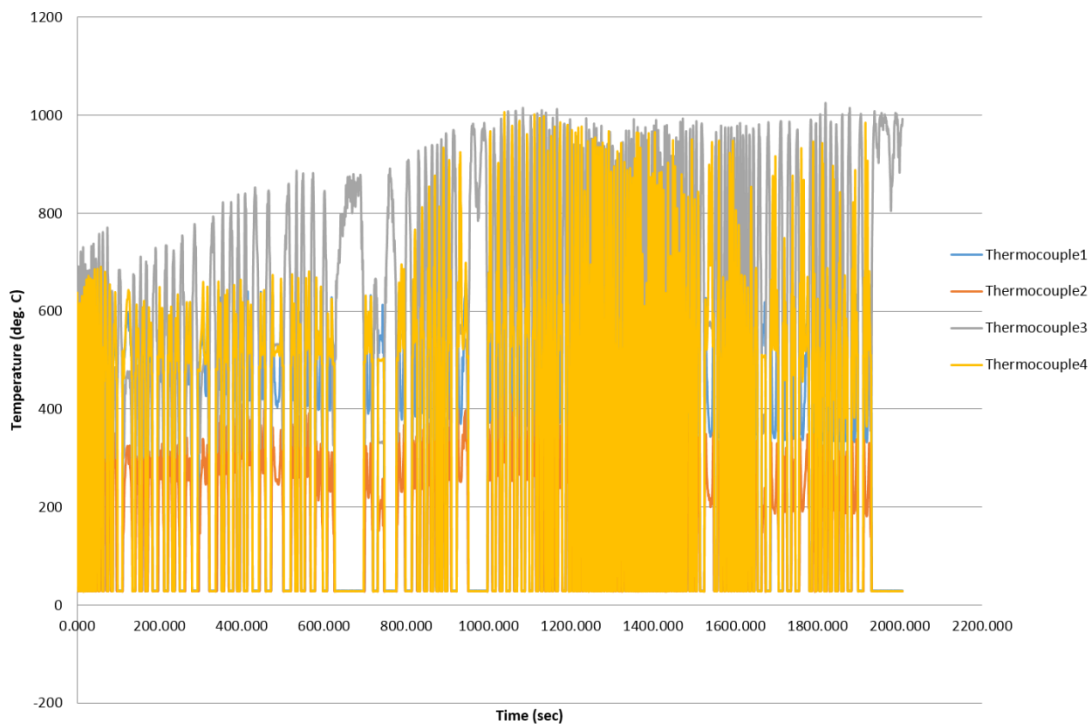
Figure 7.37: 17 September run 4: Temperature distribution during gasification of 3 g of LDPE sample – 3 heaters on 1 heater off

The amount of ash residue from gasification of LDPE shows that using ceramic infrared heaters is efficient as the residue weight is less than 1 %. Gas is released in 57 seconds average after plastic was put in. It was observed that the plastic got stuck inside the feed tube when temperature was below 600 °C inside the reactor and the feeder tube temperature was around 100 °C. The difference in gasification time is explained by the fact that all experiment times were measured by recording the length of time while the amount of gas was being released in the air became visible. It was also noticed that amount of syngas released during the gasification period increased when temperature inside the reactor increased as well as the gasification time will decrease and is less than 20 minutes for temperature above 700 °C.

The figures above (Figure 7.19 – Figure 7.37) illustrate the temperature distribution during the reactor performance test experiments. The temperature readings that were obtained from the experiments conducted show that low density polyethylene is suitable for gasification and that the highest temperatures obtained during the experiments were found to be in accordance with literature (Begum et al., 2014; Baggio et al., 2009; Lopez et al., 2013; Wu & Williams, 2010)

7.8   New system configuration

In order to solve the problem of plastic feeding and feeding rate to turn the reactor into a continuous gasifier, a new configuration was developed by modifying the reactor shape into a conical one with gas exit at the top of the reactor and reducing the feeding tube length to avoid clogging inside it. A lid on the feeding exhaust was found necessary to avoid gas exiting from it, hence increasing gas pressure to exit from the gas exhaust tube as shown in Figure 7.38. Only heating stage experiment was conducted to obtain temperature behaviour in the gasifier. A thermal image outside the reactor was taken using a thermal imager Fluk Ti20 and is shown in Figure 7.39. The new design with regards to the gasification process permitted to eliminate clogging problems and gas leakage from the feeding exhaust. The temperature measurements during gasification are shown in Figure 7.40 and Figure 7.41.

Figure 7.38: Gasifier new configuration
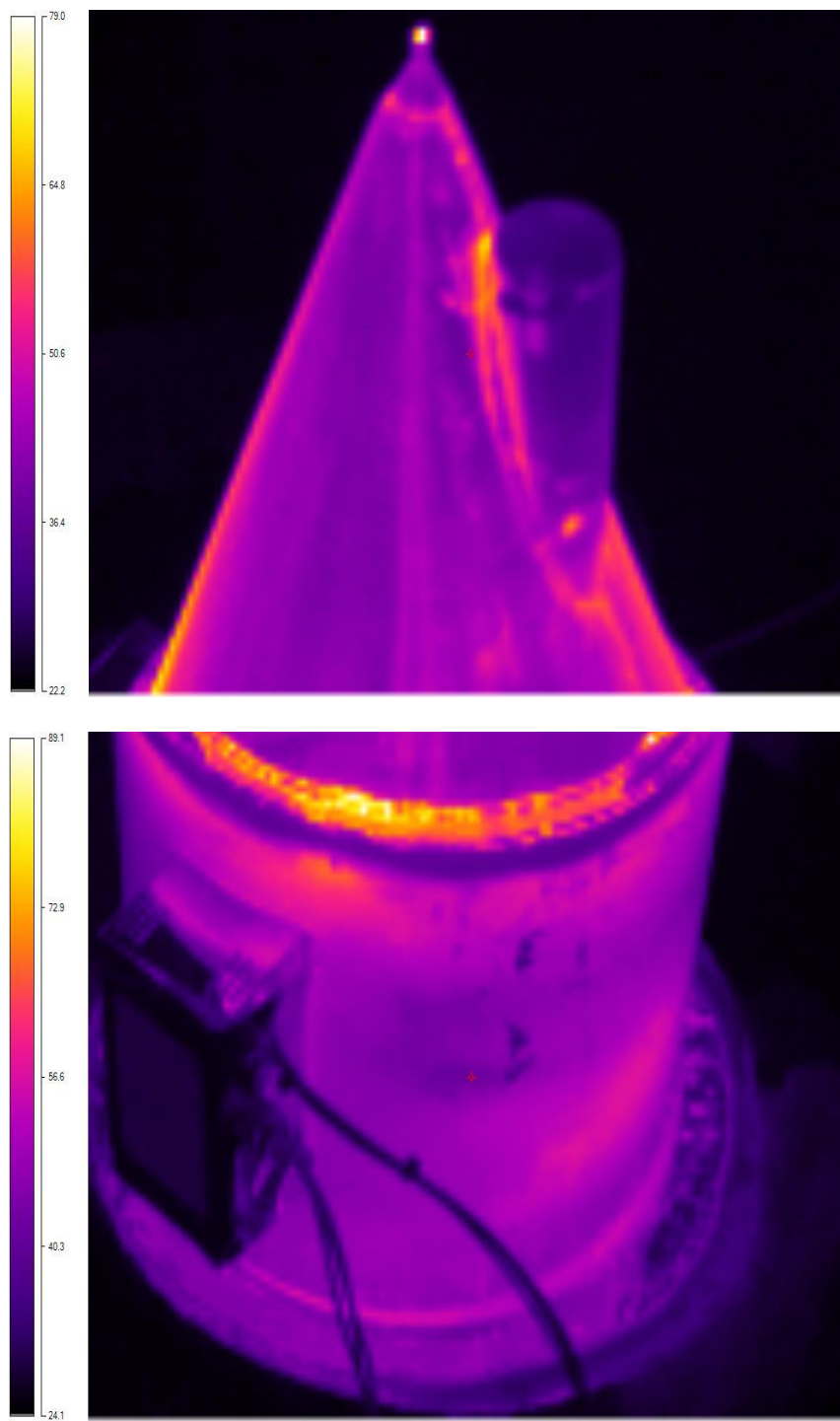
Figure 7.39: IR reactor temperature (thermal imaging) during heating stage
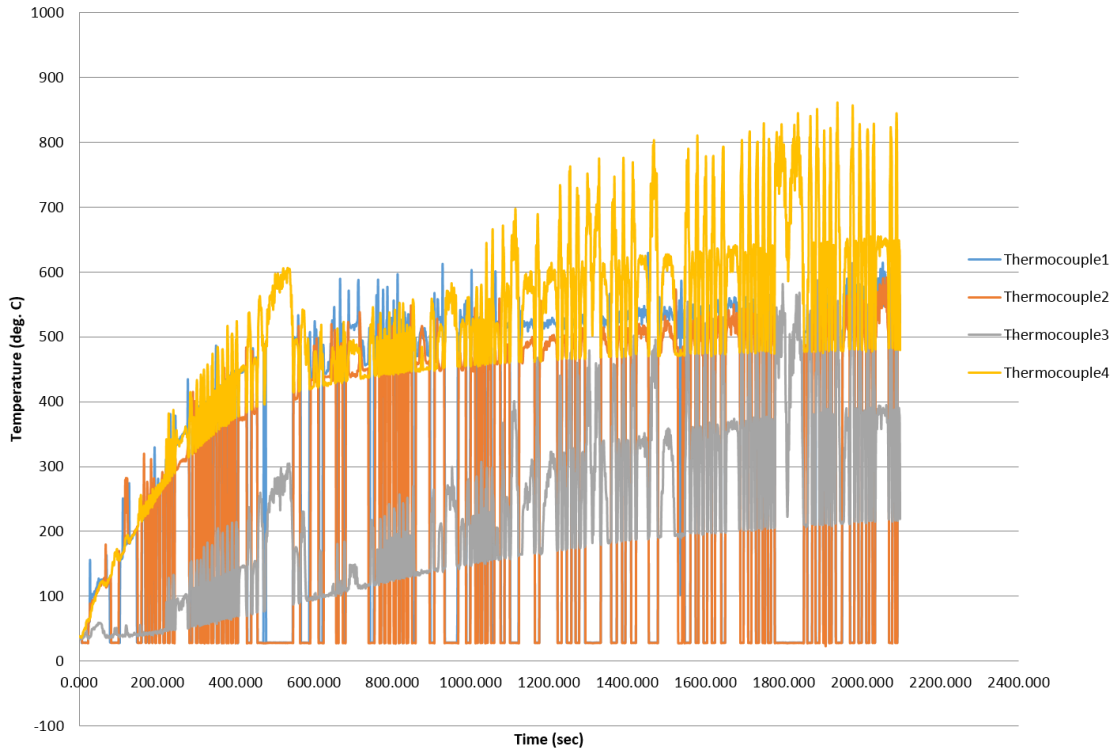
Figure 7.40: 18 December run: Temperature distribution during void test – 3 heaters on 1 heater off
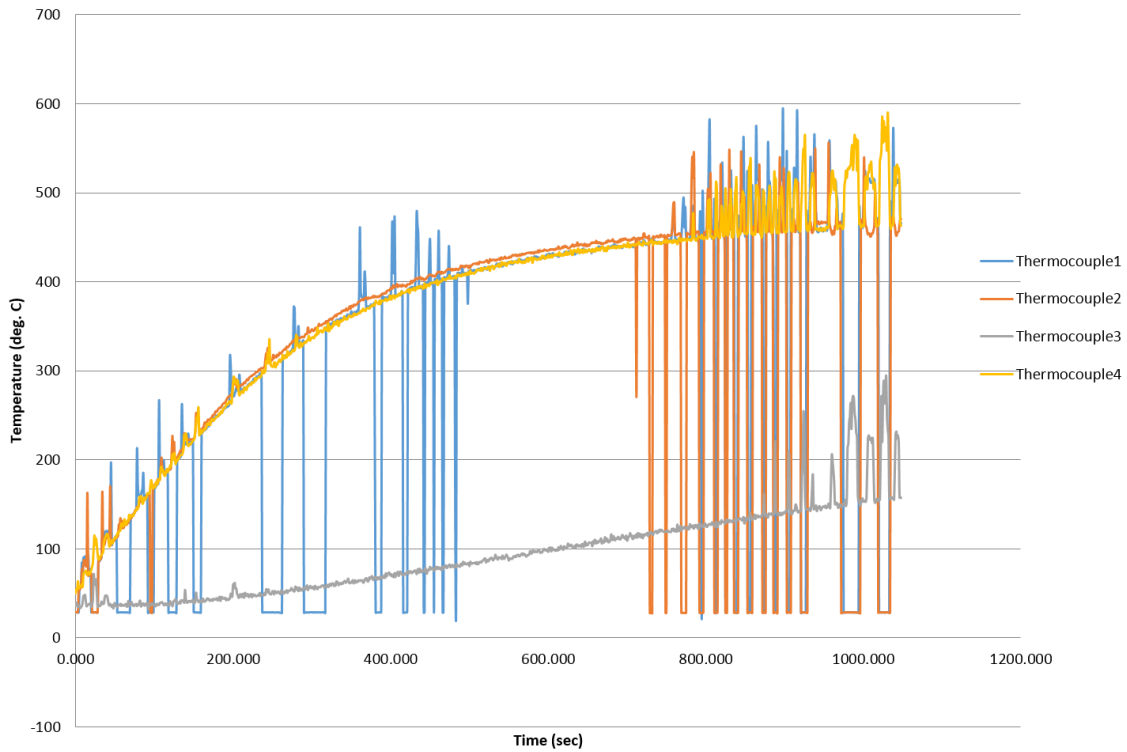
Figure 7.41: 22 December run: Temperature distribution during void test – 3 heaters on 1 heater off

130

CHAPTER 8 : CONCLUSION

The primary purpose of this research was to establish the functionality of a lab-scale gasifier based on infrared heating. To complete the research, a literature study of gasification of plastic waste as well as infrared heating was conducted. A 750 W capacity laboratory scale gasifier was designed and tested after further investigation on a 1000 W capacity in this study with readily available materials such as pelletized low density polyethylene. The infrared reactor was designed to deliver an optimum temperature of 1000 °C. The synthetic gases were noticed soon after introducing sample in the reactor at a nominal temperature of 650 °C. A white smoke was observed during gas production and ash was also produced during gasification process.

This assignment has explained the importance of infrared radiation and that plastic waste may be a suitable candidate for energy production by proving that gas is produced using infrared heating technology. Moreover, a gasifier simulation model was done using COMSOL Multiphysics to establish the temperature distribution inside the gasifier as well as to evaluate possible heat loss during actual experiments. The temperature results obtained in the model are higher than the ones obtained during experiments due to simulation based on a heat source of 1000 W which represent four heaters used. However, the temperature profiles obtained remain in an acceptable range since high temperatures are expected for the gasification experiments (maximum temperature of 1200 °C for model simulated and maximum temperature of 1000 °C for temperatures obtained during experiments). Many reasons can explain this discrepancy: the number on heaters used, model simplified with no heat loss at the reactor wall. A variation in the temperature profile was also expected, with different case scenarios conducted in chapter 7.

The experimental results validate the simulation done through software in terms of temperature. The gasifier was redesigned due to clogging that happened several times during experiments by reducing the feeding tube and increasing the gasifier height which helped to eliminate the problem of plastic sample causing an obstruction and helped increase the amount of gas produced during the gasification process.

8.1 Problems solved in this research

The questions that this research project aimed to solve were the thermal analysis and simulation of a small scale reactor using infrared heater that will be suitable for the gasification

of plastic waste. The problems investigated were therefore divided into sub-problems, including the following:

- To model an infrared gasifier using infrared heaters that could then be used in furnaces for the gasification of plastic waste.
- Simulation and data acquisition of the infrared reactor using software such as COMSOL Multiphysics and LabVIEW for the modelling and data acquisition
- The use of plastic waste as feedstock to study the influence of infrared radiation on polyethylene plastics into syngas
- Tests performed for the production of syngas using a small scale infrared gasifier

8.1.1 To model an infrared gasifier using infrared heaters that could then be used in furnaces for the gasification of plastic waste

A review on infrared heating was conducted in order to obtain the mathematical model expression of the infrared gasifier used for this research based on the model of ceramic infrared heater. The model developed described a proof of concept of the gasifier for plastic waste gasification. The model was represented numerically and graphically.

8.1.2 Simulation and data acquisition of the infrared reactor using software such as COMSOL Multiphysics and LabVIEW for the modelling and data acquisition

The simulation was based on theoretical method and the software package used for the simulation is COMSOL Multiphysics for numerical calculations and simulations. The model is validated by experiments in terms of temperature distribution inside the reactor and therefore contributed to evaluate the error margin between implementation. The results are in good agreement with the experiments conducted.

8.1.3 The use of plastic waste as feedstock to study the influence of infrared radiation on polyethylene plastics into syngas

To evaluate the influence on plastic waste with infrared heating, the gasification process was done using ceramic infrared heaters. Experiments show that three heaters were suitable for the small scale reactor to avoid clogging and overheat; the overall temperature average is 850 °C for a gasification time being less than 20 minutes, which confirm the literature study for

gasification to take place at 800 °C. The residues were mainly ash and with tar being less than 1 % after gasification.

8.1.4 Tests performed for the production of syngas using a small scale infrared gasifier

The small scale reactor has shown to be suitable for the production of syngas. Although gases produced were not analysed due to the infrared reactor being the main focus of study, the temperature were high enough to produce gas within one minute with an average residing time of 20 minutes.

8.2 Application of the results

The results that were obtained in this research provide the following applications:

- Insight into technical information pertaining to the gasification process
- The gasifier using infrared ceramic heaters can be used in the gasification of recycled plastic waste such as plastic pellets
- The COMSOL model can be used into the evaluation of heat diffusion in the plastic waste to study its phase change

- The theoretical and mathematical models represented here can be used to analyse the heat transfer of enclosures.
- The measured wavelength values of the plastic pellet samples can be used as references on designing IR heaters.

8.3 Further study

Following on from this research, there are several aspects that could be further pursued. Among these are the following:

- Research to be done on gasifier temperature control and as well controller to be designed to maintain temperature at 800 °C which was observed to be the suitable temperature for gasification and hence, to avoid heater destruction through overheating.
- Further discussion is recommended as in Case 3 (with three heaters) the heaters were not positioned with equal distance from each other and as a result, the heat transfer maybe non-uniform from different directions and this may affect the gasification process.

- Operation of the whole gasification plant, that is the gasifier connected to the chemical plant for hydrogen production
- A particle (pellet) model should be developed and simulation done for gasification of plastic pellets by studying the heat transfer from solid to liquid then from liquid to gas phase.
- Gas chromatography can be conducted to determine gas composition and hence increase the production of hydrogen to be used with the gas turbine and test for electricity production
- Analysis of the quality of the syngas and the applicability of the developed system.

8.4 Publications emanating from this research

Guyemat Mbourou, SM., & Adonis, M., 2012, *Thermal modelling of an infrared heater for plastic waste gasification,* Stellenbosch, Industrial Commercial Use of Energy (ICUE), pp.259-265

Guyemat Mbourou, SM., & Adonis, M., 2013, *Applying modelling and simulation techniques to characterize an infrared heater,* Cape Town, Joint International Conference on Engineering Education and Research and International Conference on Information Technology (ICEE/ICIT), pp.569-577

Guyemat Mbourou, SM., & Adonis, M., 2015, *Numerical analysis and experimental development of a small scale reactor using Comsol software,* Bellville, SAImechE Postgraduate Conference, pp.1-3

REFERENCES

AB, K., 2003. [Online] Available at: www.kanthal.com [Accessed 19 May 2011].

Adonis, M. & Khan, M., 2008. Software-based Energy Management System For an Infrared Dryer. In Beute, N., ed. *5th Industrial and Comercial Use of Energy, 28-30 May 2008*. Cape Town, 2008.

Adrian Bejan, A.D.K., 2003. *Heat Transfer Handbook*. John Wiley and sons Inc.

Africa, S.S., 2010. *Millenium Development goals 2010*. Country Report. Republic of South Africa.

Afzal, T.M. & Abe, T., 1997. Modelling Far-infrared drying of rough rice. *Journal of Microwave Power of Electromagnetic Energy*, 32.

Akhator, P.E., 2014. *Design and construction of a small scale fixed-bed reactor*. Master Thesis. University of Borad, School of Engineering.

Anaraki, S.T., 2012. *Waste to Energy Conversion by Stepwise Liquefaction, Gasification and "Clean" Combustion of Pelletized Waste Polyethylene for Electric Power Generation – in a Miniature Steam Engine*. MSc Thesis. Boston, Massachusetts: Northeastern University.

Anon., n.d. *Global Application Technologies*. [Online] Gapptec Available at: http://www.gapptec.com/newSite/assets/INFRARED_CURING1.pdf [Accessed 23 June 2015].

Anon., n.d. *IR-spectroscopic polymer analysis*. [Online] Available at: www.bruker.com/optics [Accessed 1 February 2016].

Anonymous, 2006. Gasification of waste 101. *BioCycle*, 47(4), p.1.

Arena, U., 2012. Process and technological aspects of municipal solid waste gasification. A review. *Waste Management*, 32, pp.625–39.

Arena, U. & Mastellone, M.L., 2006. *FluGas Fluidized Bed Gasifier For alternative Fuels*. Technical Manual. Naples: Second University of Naples.

Aznar, M.P., Caballero, M.A., Sancho, J.A. & Frances, E., 2006. Plastic waste elimination by co-gasification with coal and biomass in fluidized bed with air in pilot plant. *Journal of Fuel Processing Technology*, 87, pp.409-20.

Baggio, P. et al., 2009. Experimental and modeling analysis of a batch gasification/pyrolysis reactor. *Energy Conversion and Management*, 50, pp.1426-35.

Bain, R.L., 2008. *National Renewable Energy Laboratory*. [Online] Office of energy and Renewable Energy [Accessed 13 July 2012].

Bajus, M., 2011. Thermal cracking of mixture of plastics and woody material. *Petroleum & Coal*, 53(1), pp.1-7.

Begum, S., Rasul, M.G., Akbar, D. & Cork, D., 2014. An Experimental and Numerical Investigation of Fluidized Bed Gasification of Solid Waste. *Energies*, 7, pp.43-61.

Bejan, A. & Kraus, A.D., 2003. *Heat transfer handbook*. 1st ed. New Jersey: John Wiley and Sons, Inc.

Belgiorno, V., De Feo, G., Della Rocca, C. & Napoli, R.M.A., 2003. Energy from gasification of solid wastes. *Waste Management*, (23), pp.1-15.

Brems, A., Dewil, R., Baeyens, J. & Zhang, R., 2013. Gasification of plastic waste as waste-to-energy or waste-to-syngas recovery route. *Natural Science*, 5(6), pp.695-704.

Bridgwater, A.V., J, T.A. & Brammer, J.G., 2002. A techno-economic comparison of power production by biomass fast pyrolysis with Gasification and Combustion. *Renewable and Sustainable Energy Reviews*, (6), pp.181-248.

Bruker, 2010. *Teaching FT-IR Spectroscopy with the ALPHA*. [Online] Bruker Available at: www.bruker.com/optics [Accessed 11 February 2016].

Bruker, 2012. *Innovation with Integrity Specifications*. [Online] Bruker Optics Available at: www.bionet.nsc.ru/files/2013/news/ALPHA_Specifications.pdf [Accessed 11 February 2016].

Bruker, n.d. [Online] Bruker Available at: https://www.bruker.com/fileadmin/user_upload/8-PDF-Docs/OpticalSpectrospcopy/FT-IR/ALPHA/Brochures/ALPHA_brochure_EN.pdf [Accessed 11 February 2016].

Cheng, H. & Hu, Y., 2010. Municipal solid waste (MSW) as a renewable source of energy: Current and future practices in China (Review). *Bioresource Technology* , (101), pp.3816-24.

Consonni, S. & Viganò, F., 2012. Waste gasification vs. conventional Waste-To-Energy: A comparative evaluation of two commercial technologies. *Waste Management* , (32), pp.653-66.

Council, G.T., n.d. *Gasification*. [Online] Gasification Technologies Council Available at: www.gasification.org [Accessed 6 May 2012].

Das, I. & Das, S.K., 2010. Emitters and Infrared Heating System Design. *Infrared for Food and Agricultural Processing*, pp.57-88.

DEA, D.o.E.A., 2012. *National Waste Information Baseline Report*. Report. Pretoria, South Africa: Department of Environmental Affairs.

Deltat, n.d. *Process Infrared Heating*. [Online] Deltat T Available at: www.deltat.com [Accessed 2 July 2012].

Di Gregorio, F., 2013. *Fuel Gas Technology for Biomass and Waste - Environmental and Techno-Economic Assessments*. PhD Thesis. Caserta, Italy: Doppiavoce AMRA.

DMSE, D.o.M.S.a.E., 2015. *Introduction to Materials Science, Chapter 15, Polymer structure*. [Online] University Tenessee Available at: http://web.utk.edu/~prack/mse201/Chapter%2015%20Polymers.pdf [Accessed 10 June 2015].

DST, D.o.S.a.T., 2012. *An analysis of the formal private and public waste sectors in South Africa. A National Waste RDI Roadmap for South Africa: Phase 1 Status Quo Assessment*. Report. Pretoria, South Africa: Department of Science and Technology.

Dupleix, A. et al., 2013. *Rational production of veneer by IR-heating of green wood during peeling: Modeling experiments*. [Document] Available at: https://hal.archives-ouvertes.fr/hal-00844587 [Accessed 15 January 2015].

Heraeus, 2011. *Understanding infrared heating*. [Booklet] Haraeus Available at: http://www.noblelight.net/ [Accessed 22 August 2012].

Heraeus, n.d. [Online] Available at: www.noblelight.net/resources/pdf_downloads/technical_notes/ir_properties_of_selected_materials.pdf [Accessed 08 June 2012].

Heraeus, n.d. *Infrared basics and Technology*. [Online] Available at: www.heraeus-noblelight.com/media/webmedia_local/media/pdf/ip/downloads/IR_basics_and_technology.pdf [Accessed 22 August 2012].

He, M. et al., 2009. Syngas production from catalytic gasification of waste polyethylene: Influence of temperature on gas yield and composition. *International Journal of Hydrogen Energy* , 1348(34), p.1342.

Hudson, R.D., 2006. *Infrared System Engineering*. Wiley.

IEA, W.e.O.2., 2011. *Electricity access in Africa - 2009*. [Online] International Energy Agency Available at: http://www.iea.org/weo/electricity.asp [Accessed 6 March 2012].

Kanoglu, M., 2011. *Chapter 13: Radiation Heat Transfer*. [Online] The McGraw-Hill Companies Available at: http://www.kostic.niu.edu/352/_352-posted/Heat_4e_Chap13-Radiation_HT_lecture-PDF.pdf [Accessed 16 November 2015].

Kayes, I. & Tehzeeb, A.H., 2009. Waste to energy: A lucrative alternative. In *nternational Conference in Developments in Renewable Energy Technology (ICDRET), 2009*., 2009.

Krelus Infrared, 2011. *Krelus Infrared*. [Online] Available at: http?//www.krelus.ch/www/images/pdf/Prospekt_en.pdf [Accessed 08 June 2012].

Krishnamurthy, K. et al., 2008. Infrared Heating In Food Processing. *Comprehensive Reviews in Food Science and Food Safety*, 7, pp.1-13.

Kurkela, E., 2010. *Thermal Gasification for Power and Fuels*. [Online] VTT - Gasification Team Available at: www.vtt.fi [Accessed 11 April 2016].

Lin, Y.-P., Tsen, J.-H. & King, V.A.-E., 2004. Effects of far-infrared radiation on the freeze-drying of sweet potato. *Journal of Food Engineering*, 68, pp.249-55.

Long, C. & Sayma, N., 2009. *Heat transfer*. Ventus Publishing Aps.

Lopez, G. et al., 2013. Steam Gasification of Waste Plastics in a Conical Spouted Bed Reactor. In Archives, E.D., ed. *14th International Conference on Fluidization - From Fundamentals to Products*., 2013. ECI Digital Archives.

Lorcet, H., 2009. *Contribution a l'etude et a la modelisation de la pyro-gazeification de la biomasse par plasma technique*. PhD Thesis. Limoges: Universite de Limoges.

Lowry, S. & Bradley, M., 2011. *Advaned Materials and Processes*. [Online] Thermo Fisher Scientific Available at: www.thermofisher.com [Accessed 19 May 2015].

Luo, S., Yangmin, Z. & Chuijie, Y., 2012. Syngas production by catalytic steam gasification of municipal solid waste in fixed-bed reactor. *Energy*, (44), pp.391-95.

Magubane, M., 2011. 978-0-621-40414-2 *Annual Report 2010/2011*. Annual Report. Pretoria: Formeset Print (Pty) Ltd Republic of South Africa.

Management, D.o.P.a.W., 2005. *A guide to reporting and estimating emission for the integrated polluant and waste information system (IPWIS)*. Report.

Mastellone, M. & Zaccariello, L., 2013. Metals flow analysis applied to the hydrogen production. *International Journal of Hydrogen Energy*, 38, pp.3621-29.

Mastellone, M.L. & Zaccariello, L., 2015. Gasification of Wood and Plastics in a Bubbling Fluidised Bed: The Crucial Role of the Process Modelling. In Kim, H.K., Amouzegar, M.A. & Ao, S.-l., eds. *World Congress on Engineering and Computer Science 2014*. San Fransisco, 2015. Springer Science+Business Media Dordrecht.

Mbourou, S. & Adonis, M., 2012. Thermal modeling of infrared heater for plastic waste gasification. In *International Conference of Use of Energy ICUE*. Stellenbosch, 2012. IEEE.

McKendry, P., 2002. Energy production from biomass (part 3): gasification technologies. *Bioresource Technology*, (83), pp.55-63.

Meng, X., 2012. *Biomass gasification: the understanding of sulfur, tar and char reaction in fluidized bed gasifiers*. PhD Thesis. Ipskamp Drukkers, the Netherlands.

Modest, M.F., 2003. *Radiative Heat Transfer*. 2nd ed. California: Academic Press.

Moran, M.J., Shapiro, H.N., Munson, B.R. & DeWitt, D.P., 2003. *Introduction to Thermal Systems Engineering: Thermodynamics, Fluid Mechanics, and Heat Transfer*. 1st ed. New York: John Wiley & Sons, Inc.

Morgan Advanced Materials, 2011. *Superwool ht blanket*. [Online] Morgan Thermal Ceramics Available at:
http://www.morganthermalceramics.com/sites/default/files/datasheets/1_superwool_ht_blanket.pdf
[Accessed 17 November 2015].

Ngabonziza, Y. & Delcham, H., 2014. The Enhancement of Students Learning Through COMSOL Simulation Projects. In *Zone 1 Conference of the American Society for Engineering Education (ASEE Zone 1).*, 2014. 2014 IEEE.

Nordgreen, T., 2011. *Iron-based materials as tar cracking catalyst in waste gasification*. Doctoral Thesis. Stockholm, Sweden: KTH – Royal Institute of Technology.

Okajima, I., Shimoyama, D. & Sako, T., n.d. Waste Plastic Gasification and Hydrogen production in Supercritical Waster.

Olliver, R.A., 2012. *Gasification Technology Council*. [Online] Available at:
www.gasification.org/uploads/downloads/Workshops/2012/Olliver, GTC Kingsport.pdf [Accessed 17 May 2012].

Omega, 1998. *Transactions in Measurements and Control*. 2nd ed. Putman Publishing Company and OMEGA Press LLC.

Panda, A.K., Singh, R.K. & Mishra, D.K., 2010. Thermolysis of waste to liquid fuel. A suitable method for plastic waste management and manufacture of value added products - A World prospective. *Renewable and Sustainable Energy Reviews*, 14, pp.233-48.

Patz, C.D., Blieke, A., Ristow, R. & Dietrich, 2004. Application of FT-MIR spectrometry in wine analysis. *Analytica Chimica Acta*, (513), pp.81-89.

Pettersson, M. & Stenstrom, S., 2000. Modelling of an electric IR heater at transient and steady state conditions Part 1: model and validation. *International Journal of Heat and Mass Transfer*, 43, pp.1209-22.

PlasticsEurop, 2012. *Plastics – the Facts 2012 - An analysis of European plastics production, demand and waste data for 2011*. [Online] PlasticsEurope Available at: www.plasticseurop.org [Accessed 6 October 2015].

Pletka, R., Brown, R. & Smeenk, J., 1998. Indirectly heated fluidized biomass gasification using a latent heat ballast. *Bio Energy*, pp.396-403.

Portal, S.A.D., 2015. *South Africa Total Petroleum Consumption 1980-2013*. [Online] Available at: http://southafrica.opendataforafrica.org/hyzwyjc/south-africa-total-petroleum-consumption-1980-2013 [Accessed 27 May 2016].

Rao, N.S. & Schott, N.R., 2012. *Plastics Engineering Calculations - Hands on Examples and Case Studies*. Hanser Publishers.

Roongprasert, K., Phasukkit, P., Pintavirooj, C. & Sangworasil, M., 2013. Heat and Mass transfer of infant radiant warmer by Computer Simulation. In *The 2013 Biomedical Engineering International Conference (BMEiCON-2013).*, 2013. IEEE.

Roth, K. & Brodrick, J., 2007. Infrared radiant heaters. *ASHRAE Journal*, pp.72-73.

Ryu, C., 2010. Potential of Municipal Solid Waste for Renewable Energy Production and Reduction of Greenhouse Gas Emissions in South Korea. *Journal of the Air and Waste Management Association*, 60, pp.176–83.

SA, P., 2014. *Pastics_part2*. [Online] Plastics SA Available at: www.plasticsinfo.co.za [Accessed 6 October 2015].

SA, P., 2014. *Sustainable Catalyst an Annual Review*. [Online] Plastics SA Available at: http://www.plasticsinfo.co.za/wp-content/uploads/2014/10/55841.pdf [Accessed 05 May 2016].

SA, P., 2015. *2015 Annual Report*. [Online] Plastics SA Available at: http://www.plasticsinfo.co.za/wp-content/uploads/2015/10/2015_Annual_Report.pdf [Accessed 27 May 2016].

Salga, Ameu & Eskom, 2011. *Position paper on inclining block rate tariffs*. [Online] Elexpert (PTY) Ltd Available at: www.elexpert.co.za [Accessed 28 November 2016].

Sarker, M. & Rashid, M.M., 2013. Mixture of LDPE, PP and PS Waste Plastics into Fuel by Thermolysis Process. *International Journal of Engineering and Technology Research*, 1(1), pp.01-16.

Shakya, B.D., 2007. *Pyrolysis of waste plastic to generate useful fuel containing Hydrogen using a solar thermochemical process*. MSc thesis. the University of Sidney.

Sharp, L.L. & Jr, R.O.N., 1992. Gasification of Plastic Waste for the production of Fuel-grade Gas. In R. Khan, ed. *Clean energy from waste and Coal*. 1993 American Chemical Society. Ch. 11. pp.129-42.

Shi, B., Wang, Y. & Chuai, C., 2011. Pyrolysis of Plastic wastes to fuel oil with and without catalyst. In *Bioinformatics and Biomedical Engineering (iCBBE) 2011 5th International conference.*, 2011.

Shnawa, H.A., Abdulah, N.A. & Mohamad, F.J., 2011. Thermal Properties of Low Density Polyethylene with Oyster Shell Composite: DSC Study. *World Applied Sciences Journal*, 14(11), pp.1730-33.

Siegel, R. & Howell, J.R., 1992. *Thermal radiation Heat Transfer*. 3rd ed. Washington: Hemisphere Publishing Corporation.

Solar Products Inc., The Infrared Heater Company, 2007. *A simplified approach*. [Online] Solar Products Inc. Available at:
http://www.solarproducts.com/images/stories/resource_pdf/a_simplified_approach.pdf [Accessed 14 December 2012].

Stephen, D., 2009. Briefing: Energy from municipal solid waste. *Proceeding of the ICE - Energy* , 163(2), pp.53-59.

Steyn, C., 2015. *Progress Plastics Sector*. [Online] Department of Trade and Industry Available at:
www.thedti.gov.za/parliament/2015/Progress_Plastics_Sector.pdf [Accessed 10 June 2015].

Stiegel, G.J. & Rusell, C.M., 2001. Gasification technologies: the path to clean, affordable energy in the 21st century. *Fuel Processing Technology*, 71(1-3), pp.79-97.

Stuart, B., 2004. *Infrared Spectroscopy: Fundamentals and Applications*. Chichester: John Wiley & Sons, Ltd.

Tiefenbacher, A.M., 2013. *WASTE GASIFICATION IN THE UK – Waste Gasification in the UK - Potentials and Limitations*. Master Thesis. Cranfield: Cranfield University, School of Applied Sciences.

Toledo, M., 2013. *Thermal Analysis of Polymer*. [Online] Mettler Toledo Available at:
http://br.mt.com/dam/LabDiv/guides-glen/ta-polymer/TA_Polymers_Selected_Apps_EN.pdf [Accessed 20 May 2015].

Toledo, J.M., Aznar, M.P. & Sancho, J.A., 2011. Catalytic air Gasification of plastic Waste (Polypropylene) in a Fluidized bed. Part II: effects of some operating variables on the quality of the raw gas produced using olivine as the in-bed material. *Industrial and Engineering Chemistry Research (ACS Publications)*, 50(21), pp.11815-21.

Toskov, S., Glatz, R., Miskovic, G. & Radosavljevic, G., 2013. Modeling and Fabrication of Pt Micro– Heaters Built on Alumina Substrate. In IEEE, ed. *36th International Spring Seminar on Electronics Technology*., 2013. IEEE.

UNEP, 2009. *Converting Waste Plastics into a Resource*. Compendium of Technologies. Osaka/Shiga, Japan: United Nations Environmental Programme.

Varadi, A.S., Strand, L. & Takacs, J., 2007. Clean electrical Power Generation from Municipal solid Waste. In *Clean Electrical Power, 2007. ICCEP '07 International Conference*., 2007.

Vechot, L., Bombard, I., Laurent, P. & Lieto, J., 2006. Experimental and modelling study of the radiative curing of a polyester-based coating. *International Journal of Thermal Sciences*, 45, pp.86-93.

Wang, J. & Sheng, K.C., 2004. Modeling of Multy-Layer far-Infrared Dryer. *Drying Technology*, 22(4), pp.809-20.

Watlow, 1997. *Watlow*. [Online] Watlow Electric Manufacturing Company Available at: www.watlow.com/downloads/en/training/STL-RADM-89.pf [Accessed 22 August 2012].

Wu, C. & Williams, P.T., 2010. Pyrolysis–gasification of plastics, mixed plastics and real-world plastic waste with and without Ni–Mg–Al catalyst. *Fuel*, (89), pp.3022-32.

Xiao, R. et al., 2007. Air gasification of polypropylene plastic waste in fluidized bed gasifier. *Energy Conversion and Management*, 48(3), pp.778-86.

Xion, W., 2010. *Application of Comsol Multiphysics software to heat transfer processes*. Thesis. Helsinki: Arcada University of Applied Sciences.

Yanga, Y. et al., 2012. Recycling of composite materials. *Chemical Engineering and Processing* , (51), pp.53-68.

APPENDIX A: STA 6000 TEMPERATURE CALIBRATION (DSC)

STA 6000 TEMPERATURE CALIBRATION:

Calibration Type: Use Standards One and Two
Date: 3/13/2013 1:49:37 PM

Rate 1: 10.0 °C/min

Reference	Expected (°C)	Measured at Rate 1
Indium	156.6	156.97
Silver	960.85	956.326

NEWPAGE

DSC HEAT FLOW CALIBRATION INPUTS:

Range: Low (320 mW)
Reference Material: Indium

	28.450	Measured	45.970
Expected Enthalpy:	J/g	Enthalpy:	J/g
	9.485		
Weight:	mg	Method:	IndCal

DSC HEAT FLOW CALIBRATION COMPUTED RESULTS:

Range: Low (320 mW)
Low Range Factor   0.619   Date: 3/13/2013 1:49:37 PM

PROFILE VALUES FOR THIS DATA:

Software Version	9.1.0.0203
Firmware Version	STA 6000 V1.00 Sep 04 2008
Instrument Serial Number	521A0032606
Load Temperature	30.0 °C
Go To Temp Rate	50.0 °C/min

APPENDIX B: DATA LOGGED FROM SIGNAL EXPRESS

Root Name	Title	Author	Date/Time	Groups	Description
Thermocouple	09/15/2015 01:38:34 PM	210021934	09/15/2015 01:38:34.000 PM	2	Gasification run10

Group	Channels	Description	*DateTime*	*DecimationLevel*	*IntervalIndex*
09/15/2015 01:38:34 PM - Thermocouple - All Data	4		09/15/2015 01:38:34.000 PM	0	
09/15/2015 01:38:34 PM - Thermocouple - All Data_1	4		09/15/2015 01:38:34.000 PM	0	

09/15/2015 01:38:34 PM - Thermocouple - All Data

Channel	Datatype	Unit	Length		Minimum	Maximum
Dev1_ai1	DT_DOUBLE	Deg C		230500	18.44406471	804.63455
Dev1_ai2	DT_DOUBLE	Deg C		230500	16.80345843	810.10385
Dev1_ai3	DT_DOUBLE	Deg C		230500	23.51582921	1020.1840
Dev1_ai4	DT_DOUBLE	Deg C		230500	24.98403534	766.54056

Implicit	Start	Interval	Length
Time	0	0.01	230500

09/15/2015 01:38:34 PM - Thermocouple - All Data_1

Channel	Datatype	Unit	Length	Minimum	Maximum
Dev1_ai1	DT_DOUBLE	Deg C	5100		
Dev1_ai2	DT_DOUBLE	Deg C	5100		
Dev1_ai3	DT_DOUBLE	Deg C	5100		

144

Dev1_ai4		DT_DOUBLE	Deg C	5100
Implicit		**Start**	**Interval** **Length**	
Time			0 0.01	5100

Time*	Dev1_ai1	Dev1_ai2	Dev1_ai3	Dev1_ai4
0	30.99898152	33.58948971	34.55930472	31.48518514
0.01	32.13310876	33.42776816	33.26602204	33.91285921
0.02	32.45692182	34.07450722	34.55930472	34.23613079
0.03	33.26602204	32.29502767	33.91285921	34.39772994
0.04	32.78063594	32.94245595	33.10425131	33.26602204
0.05	32.94245595	32.78063594	33.91285921	34.55930472
0.06	32.29502767	34.07450722	31.64720329	33.91285921
0.07	32.45692182	34.07450722	33.75118671	33.58948971
0.08	32.13310876	32.29502767	37.46352935	34.72085517
0.09	32.45692182	33.91285921	31.97116508	35.68964891
0.1	29.86363444	32.78063594	33.42776816	34.39772994
0.11	33.10425131	34.07450722	28.40210565	33.75118671
0.12	31.48518514	33.75118671	34.07450722	34.23613079
0.13	32.94245595	34.07450722	31.80919659	34.23613079
0.14	31.16107428	33.58948971	33.91285921	34.88238131
0.15	32.29502767	33.58948971	32.94245595	33.75118671
0.16	32.61879123	33.10425131	33.42776816	33.10425131
0.17	32.29502767	33.75118671	32.29502767	35.8510301
0.18	31.97116508	33.91285921	32.61879123	33.26602204
0.19	33.10425131	32.78063594	34.39772994	33.42776816
0.2	32.94245595	32.29502767	31.16107428	33.58948971
0.21	32.78063594	32.94245595	32.45692182	33.91285921

0.22	32.78063594	33.58948971	31.64720329	34.72085517
0.23	31.97116508	32.29502767	33.42776816	35.68964891
0.24	31.80919659	33.91285921	33.26602204	33.26602204
0.25	31.80919659	32.78063594	32.45692182	33.42776816
0.26	30.6747213	33.75118671	35.52824367	34.55930472
0.27	32.13310876	32.94245595	35.04388319	33.75118671
0.28	31.16107428	34.07450722	30.6747213	34.39772994
0.29	30.83686387	34.07450722	33.26602204	34.39772994
0.3	31.97116508	33.42776816	33.26602204	33.91285921
0.31	31.97116508	34.07450722	31.48518514	34.39772994
0.32	31.64720329	32.45692182	36.01238728	34.23613079
0.33	31.32314214	33.26602204	30.18814402	33.26602204
0.34	31.32314214	32.61879123	33.75118671	34.88238131
0.35	31.97116508	33.75118671	32.61879123	34.39772994
0.36	32.29502767	33.91285921	33.10425131	33.58948971
0.37	31.16107428	33.58948971	32.94245595	34.23613079
0.38	32.29502767	31.16107428	35.20536085	33.75118671
0.39	31.97116508	33.75118671	33.75118671	33.58948971
0.4	31.97116508	33.75118671	32.61879123	33.58948971
0.41	31.97116508	33.91285921	33.91285921	34.23613079
0.42	31.64720329	33.10425131	34.23613079	34.72085517
0.43	32.61879123	33.75118671	33.42776816	34.23613079
0.44	31.80919659	33.10425131	33.26602204	32.78063594
0.45	33.26602204	33.26602204	33.58948971	34.07450722
0.46	31.97116508	33.91285921	37.14121925	34.72085517
0.47	31.64720329	34.07450722	33.91285921	34.23613079
0.48	30.83686387	34.88238131	31.80919659	35.68964891
0.49	32.45692182	34.23613079	33.75118671	34.72085517
0.5	32.29502767	33.26602204	34.72085517	34.07450722
0.51	31.16107428	34.88238131	33.91285921	33.42776816
0.52	32.13310876	34.39772994	35.52824367	33.91285921

0.53	31.97116508	32.94245595	33.42776816	34.07450722
0.54	32.61879123	33.75118671	32.78063594	34.23613079
0.55	31.97116508	31.80919659	31.48518514	34.72085517
0.56	32.29502767	33.91285921	32.61879123	34.72085517
0.57	32.29502767	33.58948971	32.29502767	34.55930472
0.58	32.29502767	33.75118671	33.91285921	33.91285921
0.59	33.26602204	34.23613079	33.91285921	34.39772994
0.6	33.10425131	33.91285921	33.10425131	33.58948971
0.61	31.97116508	33.75118671	33.75118671	34.55930472
0.62	31.97116508	32.94245595	33.58948971	34.72085517
0.63	32.29502767	34.23613079	33.42776816	32.94245595
0.64	31.80919659	33.58948971	33.91285921	33.91285921
0.65	32.29502767	33.26602204	33.91285921	33.75118671
0.66	33.75118671	33.10425131	33.26602204	34.07450722
0.67	31.64720329	32.29502767	33.10425131	35.68964891
0.68	32.29502767	33.10425131	33.91285921	33.10425131
0.69	33.10425131	33.58948971	33.10425131	33.91285921
0.7	32.61879123	33.10425131	34.72085517	34.23613079
0.71	32.45692182	34.55930472	32.29502767	34.72085517
0.72	31.32314214	32.61879123	33.91285921	33.91285921
0.73	32.94245595	30.83686387	33.42776816	34.88238131
0.74	31.64720329	33.10425131	31.64720329	34.23613079
0.75	31.97116508	33.58948971	33.58948971	34.39772994
0.76	31.97116508	33.58948971	32.45692182	33.91285921
0.77	32.13310876	32.78063594	30.83686387	35.68964891
0.78	30.6747213	33.10425131	34.23613079	34.39772994
0.79	30.99898152	34.07450722	36.1737205	34.23613079
0.8	31.97116508	34.23613079	30.99898152	33.42776816
0.81	32.61879123	30.83686387	32.29502767	35.04388319
0.82	32.29502767	32.13310876	33.75118671	34.55930472
0.83	30.99898152	34.55930472	31.80919659	34.07450722

0.84	31.64720329	33.42776816	33.91285921	34.88238131
0.85	33.10425131	33.10425131	34.07450722	34.07450722
0.86	32.78063594	32.29502767	35.36681433	34.07450722
0.87	31.32314214	34.39772994	33.75118671	34.55930472
0.88	31.97116508	32.78063594	33.58948971	32.78063594
0.89	32.45692182	32.78063594	34.23613079	34.07450722
0.9	31.97116508	33.75118671	32.29502767	33.58948971
0.91	32.78063594	33.75118671	34.55930472	34.55930472
0.92	31.97116508	34.72085517	34.72085517	33.26602204
0.93	31.80919659	32.78063594	37.14121925	34.07450722
0.94	32.29502767	32.78063594	31.32314214	34.23613079
0.95	33.42776816	33.42776816	29.70134222	32.45692182
0.96	29.86363444	33.91285921	30.6747213	35.20536085
0.97	31.16107428	33.91285921	34.07450722	34.07450722
0.98	32.29502767	32.78063594	32.78063594	34.23613079
0.99	32.61879123	32.61879123	35.20536085	33.26602204
1	32.45692182	33.58948971	34.72085517	31.97116508
1.01	31.32314214	31.64720329	32.45692182	34.55930472
1.02	31.97116508	34.23613079	30.83686387	34.72085517
1.03	31.16107428	32.13310876	37.30238608	33.58948971
1.04	31.32314214	32.61879123	34.39772994	32.13310876
1.05	31.32314214	33.91285921	33.91285921	34.23613079
1.06	32.13310876	34.72085517	33.26602204	32.45692182
1.07	32.13310876	32.78063594	31.16107428	34.23613079
1.08	32.45692182	34.23613079	33.42776816	34.07450722
1.09	32.29502767	33.91285921	33.42776816	34.72085517
1.1	30.6747213	34.39772994	34.07450722	34.39772994
1.11	32.13310876	33.75118671	34.07450722	34.39772994
1.12	31.97116508	34.23613079	33.10425131	34.23613079
1.13	32.13310876	32.45692182	33.75118671	34.23613079
1.14	31.97116508	33.58948971	34.39772994	34.72085517

1.15	30.83686387	33.42776816	33.10425131	34.39772994
1.16	32.94245595	32.29502767	36.01238728	33.26602204
1.17	31.97116508	33.91285921	33.26602204	33.91285921
1.18	31.16107428	33.75118671	34.55930472	32.29502767
1.19	30.6747213	33.10425131	35.68964891	33.91285921
1.2	30.35036139	32.45692182	32.61879123	34.23613079
1.21	33.10425131	33.75118671	28.07704696	33.10425131
1.22	32.78063594	34.07450722	34.88238131	34.23613079
1.23	32.45692182	34.39772994	33.75118671	33.26602204
1.24	32.78063594	33.75118671	31.16107428	34.55930472
1.25	32.13310876	34.07450722	34.23613079	34.23613079
1.26	31.80919659	34.23613079	34.07450722	34.39772994
1.27	30.99898152	32.78063594	32.29502767	34.39772994
1.28	33.58948971	33.58948971	34.23613079	34.88238131
1.29	31.97116508	35.04388319	30.35036139	34.39772994
1.3	32.29502767	33.91285921	32.78063594	35.68964891
1.31	31.16107428	32.13310876	34.07450722	34.07450722
1.32	31.32314214	34.23613079	33.42776816	34.39772994
1.33	31.97116508	34.39772994	36.3350298	34.39772994
1.34	31.80919659	34.88238131	34.07450722	31.48518514
1.35	32.29502767	32.94245595	29.05192365	34.39772994
1.36	31.64720329	34.39772994	30.6747213	32.45692182
1.37	32.45692182	33.58948971	30.6747213	34.23613079
1.38	31.97116508	32.78063594	36.1737205	32.94245595
1.39	30.99898152	32.29502767	35.8510301	33.91285921
1.4	32.45692182	33.58948971	33.75118671	34.39772994
1.41	29.70134222	34.23613079	30.99898152	35.52824367
1.42	31.48518514	33.75118671	34.23613079	34.88238131
1.43	31.97116508	32.61879123	33.75118671	34.23613079
1.44	32.13310876	31.64720329	33.42776816	34.72085517
1.45	31.80919659	32.29502767	35.52824367	34.39772994

1.46	31.64720329	33.91285921	34.72085517	34.23613079
1.47	31.32314214	34.23613079	32.45692182	33.10425131
1.48	32.45692182	33.10425131	28.07704696	35.20536085
1.49	31.64720329	32.94245595	34.07450722	34.23613079
1.5	32.61879123	31.48518514	30.35036139	34.07450722
1.51	31.48518514	33.42776816	32.94245595	34.55930472
1.52	31.80919659	34.07450722	33.42776816	33.91285921
1.53	32.45692182	31.97116508	33.75118671	34.55930472
1.54	32.94245595	32.45692182	33.58948971	34.07450722
1.55	32.13310876	33.58948971	32.29502767	34.88238131
1.56	30.18814402	32.61879123	31.97116508	34.07450722
1.57	32.29502767	34.07450722	31.80919659	34.88238131
1.58	31.48518514	32.29502767	36.65757684	34.23613079
1.59	31.97116508	32.13310876	34.55930472	35.04388319
1.6	31.32314214	33.58948971	33.91285921	34.23613079
1.61	32.61879123	31.97116508	34.55930472	33.42776816
1.62	31.80919659	32.94245595	31.32314214	34.72085517
1.63	32.45692182	33.26602204	33.10425131	33.42776816
1.64	32.61879123	34.23613079	33.91285921	34.39772994
1.65	30.99898152	33.75118671	34.88238131	34.07450722
1.66	33.26602204	33.58948971	34.07450722	34.72085517
1.67	32.29502767	33.42776816	33.10425131	34.07450722
1.68	31.48518514	34.23613079	34.07450722	34.39772994
1.69	30.83686387	33.91285921	30.51255381	33.26602204
1.7	32.13310876	33.75118671	32.94245595	34.72085517
1.71	30.35036139	34.55930472	31.64720329	34.23613079
1.72	32.61879123	33.75118671	33.91285921	33.42776816
1.73	32.29502767	34.23613079	28.07704696	32.78063594
1.74	32.29502767	33.75118671	33.91285921	34.55930472
1.75	32.94245595	33.58948971	33.91285921	34.72085517
1.76	32.45692182	34.55930472	33.91285921	34.07450722

1.77	31.16107428	34.72085517	33.42776816	34.39772994
1.78	32.45692182	33.75118671	33.10425131	34.07450722
1.79	32.29502767	34.72085517	35.8510301	34.39772994
1.8	31.64720329	34.23613079	32.94245595	35.04388319
1.81	32.13310876	34.39772994	27.58927198	33.75118671
1.82	32.29502767	32.45692182	34.07450722	33.10425131
1.83	32.13310876	34.88238131	30.83686387	33.42776816
1.84	32.13310876	32.94245595	31.32314214	34.23613079
1.85	31.32314214	32.94245595	33.26602204	33.42776816
1.86	32.61879123	33.75118671	32.29502767	32.94245595
1.87	31.32314214	32.94245595	37.14121925	33.91285921
1.88	30.35036139	33.26602204	35.52824367	34.55930472
1.89	33.75118671	33.75118671	27.58927198	32.61879123
1.9	30.99898152	34.72085517	34.39772994	34.07450722
1.91	32.45692182	34.88238131	32.94245595	34.23613079
1.92	28.88950659	28.88950659	36.65757684	28.72706457
1.93	57.60463408	50.60363024	27.75188855	34.23613079
1.94	28.88950659	28.72706457	34.07450722	28.88950659
1.95	57.76343917	55.22103711	32.13310876	37.46352935
1.96	28.72706457	29.05192365	35.36681433	29.05192365
1.97	58.55728613	52.19731207	27.91448021	36.01238728
1.98	28.72706457	28.88950659	35.20536085	29.05192365
1.99	59.82684931	52.67510345	27.75188855	37.30238608
2	28.88950659	28.72706457	32.78063594	28.88950659
2.01	58.08101332	55.53902141	27.75188855	38.590877
2.02	29.05192365	29.05192365	35.20536085	28.72706457
2.03	57.28698731	51.71937831	27.91448021	38.590877
2.04	28.72706457	28.88950659	33.26602204	28.72706457
2.05	55.85695138	53.1527553	28.72706457	36.3350298
2.06	28.88950659	28.72706457	34.88238131	28.88950659
2.07	59.35084572	53.31194206	28.23958877	38.75183375

2.08	28.88950659	28.88950659	35.04388319	28.88950659
2.09	57.92223222	54.10765174	28.40210565	38.42989714
2.1	29.05192365	28.88950659	34.07450722	28.88950659
2.11	60.14413182	53.31194206	29.05192365	38.10786785
2.12	28.88950659	29.05192365	37.7857454	28.56459759
2.13	55.22103711	54.10765174	30.83686387	39.39543083
2.14	28.72706457	28.72706457	36.49631523	28.88950659
2.15	59.03345548	52.19731207	29.53902502	42.9288101
2.16	28.72706457	28.88950659	36.3350298	28.72706457
2.17	56.65154433	52.03801677	29.05192365	40.68153471
2.18	29.05192365	28.88950659	35.8510301	28.72706457
2.19	58.55728613	53.94853933	28.88950659	48.6889801
2.2	28.88950659	28.88950659	35.52824367	28.72706457
2.21	58.55728613	53.47111374	27.75188855	42.60803036
2.22	28.88950659	28.88950659	32.61879123	28.72706457
2.23	58.71602059	54.26674959	29.05192365	48.6889801
2.24	28.88950659	28.88950659	36.3350298	28.72706457
2.25	59.50952437	54.10765174	27.58927198	50.60363024
2.26	29.05192365	28.72706457	35.8510301	28.88950659
2.27	58.55728613	54.10765174	28.23958877	48.52931104
2.28	28.88950659	28.88950659	34.72085517	28.56459759
2.29	59.19215612	53.1527553	29.21431574	50.76307254
2.3	28.88950659	28.88950659	35.8510301	28.56459759
2.31	61.25429944	54.7439569	31.97116508	51.40067534
2.32	28.88950659	29.05192365	34.72085517	28.72706457
2.33	58.39854017	53.47111374	29.21431574	50.60363024
2.34	28.72706457	28.88950659	31.48518514	28.56459759
2.35	59.35084572	54.7439569	26.12460484	54.10765174
2.36	28.72706457	28.88950659	34.55930472	28.40210565
2.37	60.61997801	54.26674959	28.72706457	57.44581683
2.38	28.72706457	28.72706457	35.52824367	28.72706457

2.39	58.08101332	55.06202432	32.13310876	56.81042403
2.4	28.72706457	28.72706457	35.68964891	28.88950659
2.41	59.19215612	53.63027044	27.58927198	57.44581683
2.42	28.88950659	29.05192365	37.6246491	28.56459759
2.43	59.50952437	52.67510345	29.37668287	65.53230956
2.44	28.72706457	28.88950659	32.29502767	28.88950659
2.45	61.88846727	54.7439569	32.29502767	66.16562735
2.46	28.88950659	28.72706457	34.39772994	28.72706457
2.47	58.39854017	56.17482789	23.51582921	64.42374544
2.48	28.56459759	28.88950659	36.49631523	28.56459759
2.49	58.87474367	56.49265182	30.18814402	70.12191374
2.5	28.72706457	28.72706457	35.20536085	28.72706457
2.51	59.03345548	54.26674959	28.56459759	69.6473056
2.52	28.88950659	28.72706457	28.72706457	28.88950659
2.53	57.92223222	54.26674959	25.96174021	69.01444184
2.54	28.88950659	28.72706457	36.01238728	28.72706457
2.55	60.30275745	53.47111374	29.70134222	73.75976545
2.56	28.88950659	28.88950659	34.88238131	29.05192365
2.57	59.35084572	56.49265182	31.97116508	72.81086299
2.58	28.88950659	28.72706457	36.1737205	28.72706457
2.59	59.98549581	54.425833	29.37668287	79.92772721
2.6	28.72706457	28.88950659	37.7857454	28.72706457
2.61	57.60463408	56.33374637	26.28744477	79.61136502
2.62	28.72706457	28.88950659	35.52824367	28.72706457
2.63	61.09573377	55.69799313	27.91448021	81.82616433
2.64	28.88950659	28.88950659	37.7857454	28.72706457
2.65	58.87474367	55.85695138	25.7988509	90.85397236
2.66	28.56459759	28.88950659	37.6246491	28.88950659
2.67	59.03345548	58.2397826	27.26396418	85.62488698
2.68	28.88950659	28.88950659	36.3350298	28.88950659
2.69	61.09573377	53.78941227	29.37668287	94.02744766

2.7	28.88950659	28.88950659	34.72085517	28.72706457
2.71	61.09573377	57.12814541	28.40210565	95.29791039
2.72	28.72706457	28.88950659	38.91276744	28.88950659
2.73	59.19215612	53.47111374	29.05192365	96.09228334
2.74	28.72706457	28.88950659	33.91285921	28.72706457
2.75	64.26535055	57.60463408	29.05192365	99.90909412
2.76	29.05192365	28.88950659	36.1737205	28.72706457
2.77	61.57140211	57.44581683	28.56459759	100.0682719
2.78	28.88950659	28.56459759	35.36681433	28.72706457
2.79	64.10694818	55.85695138	30.6747213	103.8922331
2.8	28.88950659	29.05192365	36.65757684	28.72706457
2.81	65.84898119	59.03345548	29.21431574	108.6827746
2.82	28.88950659	28.88950659	33.26602204	28.72706457
2.83	64.74051322	57.12814541	29.70134222	111.5631044
2.84	28.88950659	28.88950659	36.49631523	28.88950659
2.85	60.77857316	59.19215612	29.70134222	109.8023541
2.86	28.72706457	28.88950659	39.71709231	28.88950659
2.87	62.04698606	61.25429944	29.37668287	117.337939
2.88	28.88950659	28.72706457	33.10425131	28.72706457
2.89	61.88846727	60.46137281	28.56459759	117.8200467
2.9	28.88950659	28.72706457	35.68964891	28.72706457
2.91	62.83944662	63.94853823	29.70134222	117.1772665
2.92	28.72706457	28.88950659	32.94245595	28.72706457
2.93	62.83944662	59.03345548	31.48518514	120.0716768
2.94	28.88950659	28.72706457	35.8510301	29.05192365
2.95	63.94853823	60.61997801	29.21431574	117.337939
2.96	28.40210565	29.05192365	34.88238131	28.72706457
2.97	62.52248863	59.03345548	28.56459759	119.2671834
2.98	28.56459759	28.88950659	29.05192365	28.72706457
2.99	64.26535055	57.28698731	26.61305041	119.9107479
3	28.88950659	28.72706457	31.97116508	28.72706457

3.01	63.94853823	60.14413182	33.10425131	120.5545544
3.02	28.72706457	28.72706457	35.8510301	29.05192365
3.03	62.83944662	59.03345548	29.70134222	117.6593291
3.04	28.88950659	28.88950659	30.99898152	28.72706457
3.05	60.77857316	57.92223222	26.45025997	118.7846687
3.06	28.88950659	28.88950659	33.58948971	28.72706457
3.07	62.36399663	61.41285552	29.21431574	119.4280518
3.08	28.72706457	28.56459759	35.20536085	28.56459759
3.09	61.72993932	57.92223222	30.83686387	119.2671834
3.1	28.88950659	28.88950659	37.6246491	28.72706457
3.11	65.21561157	61.25429944	25.7988509	119.4280518
3.12	28.88950659	28.88950659	35.8510301	28.72706457
3.13	63.15637068	61.25429944	30.02590171	118.4630677
3.14	28.56459759	28.72706457	36.1737205	28.72706457
3.15	63.79012057	62.04698606	31.32314214	121.0375682
3.16	28.88950659	28.88950659	33.75118671	28.88950659
3.17	59.6681922	58.08101332	29.21431574	114.1273306
3.18	28.56459759	28.72706457	37.46352935	28.88950659
3.19	62.52248863	58.55728613	26.77581608	118.9454918
3.2	28.72706457	28.88950659	38.10786785	28.88950659
3.21	57.60463408	55.85695138	26.12460484	115.2503652
3.22	28.88950659	28.88950659	31.97116508	28.56459759
3.23	60.14413182	52.03801677	29.86363444	111.7232591
3.24	28.88950659	28.88950659	36.01238728	28.88950659
3.25	57.44581683	50.60363024	28.56459759	117.337939
3.26	28.88950659	28.72706457	35.8510301	28.72706457
3.27	58.39854017	50.9224981	29.70134222	113.1653062
3.28	28.88950659	28.88950659	34.72085517	28.72706457
3.29	56.81042403	53.1527553	28.07704696	113.1653062
3.3	28.72706457	28.72706457	32.94245595	28.72706457
3.31	59.50952437	52.5158553	29.21431574	115.0898872

3.32	28.72706457	28.72706457	35.52824367	28.72706457
3.33	57.76343917	53.94853933	29.21431574	107.5638828
3.34	29.05192365	28.88950659	37.6246491	28.72706457
3.35	57.92223222	55.85695138	29.70134222	107.4040966
3.36	28.72706457	28.88950659	38.590877	28.72706457
3.37	52.19731207	52.8343361	28.07704696	113.3256068
3.38	29.05192365	28.72706457	36.81881468	28.56459759
3.39	57.76343917	52.19731207	28.07704696	107.0845657
3.4	28.72706457	28.72706457	31.48518514	28.88950659
3.41	57.92223222	51.87870555	30.02590171	109.4824035
3.42	28.72706457	28.88950659	36.01238728	28.72706457
3.43	54.425833	53.78941227	27.75188855	115.8924265
3.44	28.72706457	28.72706457	36.01238728	29.05192365
3.45	53.47111374	56.96929102	30.83686387	108.522891
3.46	28.88950659	28.88950659	36.01238728	28.72706457
3.47	56.81042403	56.49265182	28.56459759	102.9355624
3.48	28.88950659	28.56459759	35.36681433	28.88950659
3.49	58.2397826	56.01589627	29.70134222	103.8922331
3.5	28.72706457	28.88950659	33.75118671	28.88950659
3.51	74.55048909	58.87474367	30.51255381	112.2038102
3.52	28.72706457	28.88950659	34.23613079	28.88950659
3.53	74.23420181	75.65748458	29.53902502	108.3630215
3.54	28.88950659	28.56459759	35.52824367	28.72706457
3.55	66.48224891	75.02491661	30.35036139	108.2031659
3.56	28.72706457	28.88950659	35.52824367	28.88950659
3.57	71.70373476	70.75467721	30.02590171	110.7625479
3.58	28.88950659	28.72706457	35.8510301	28.72706457
3.59	73.91791177	68.38151126	29.05192365	113.0050202
3.6	28.88950659	29.05192365	32.61879123	28.72706457
3.61	70.5964911	68.53975055	29.70134222	116.5347266
3.62	28.88950659	28.88950659	37.7857454	28.88950659

3.63	69.48909554	71.38739279	29.21431574	105.3281205
3.64	28.88950659	29.05192365	35.8510301	28.72706457
3.65	71.86190216	71.38739279	27.26396418	110.6024798
3.66	28.88950659	28.88950659	36.49631523	28.88950659
3.67	69.48909554	71.86190216	31.64720329	108.3630215
3.68	28.88950659	28.88950659	32.61879123	28.72706457
3.69	72.02006731	68.06501874	32.61879123	105.9666383
3.7	28.88950659	28.72706457	37.9468183	29.05192365
3.71	74.07605718	69.6473056	28.72706457	118.4630677
3.72	28.88950659	28.88950659	33.42776816	28.88950659
3.73	68.06501874	68.22326736	30.02590171	111.8834282
3.74	28.72706457	28.88950659	35.68964891	28.88950659
3.75	59.35084572	59.03345548	30.35036139	102.298038
3.76	28.56459759	28.72706457	34.72085517	28.72706457
3.77	61.41285552	55.06202432	30.35036139	109.1625096
3.78	28.72706457	28.72706457	33.91285921	28.56459759
3.79	58.71602059	53.31194206	33.10425131	98.95427595
3.8	28.72706457	28.56459759	35.68964891	28.56459759
3.81	60.93715838	53.31194206	30.35036139	107.5638828
3.82	28.72706457	28.88950659	36.3350298	28.72706457
3.83	57.60463408	55.85695138	27.91448021	117.8200467
3.84	28.88950659	28.72706457	35.8510301	28.56459759
3.85	63.4732617	52.8343361	30.18814402	98.95427595
3.86	28.72706457	28.88950659	35.52824367	28.72706457
3.87	60.46137281	56.96929102	29.37668287	106.4456684
3.88	28.72706457	28.72706457	37.7857454	28.72706457
3.89	61.09573377	55.06202432	27.91448021	109.8023541
3.9	28.88950659	28.88950659	36.1737205	28.72706457
3.91	60.61997801	55.85695138	30.02590171	101.6607152
3.92	28.88950659	28.88950659	37.46352935	28.72706457
3.93	60.61997801	55.38003611	28.56459759	106.4456684

3.94	28.88950659	28.88950659	34.39772994	28.72706457
3.95	60.77857316	53.47111374	29.53902502	106.2859781
3.96	28.88950659	28.72706457	32.45692182	28.72706457
3.97	58.87474367	54.90299762	29.37668287	110.2823867
3.98	28.72706457	28.88950659	33.58948971	28.88950659
3.99	60.30275745	52.35659154	30.02590171	107.8834965

APPENDIX C: Heating up Simulink sub-systems

- Power rating:
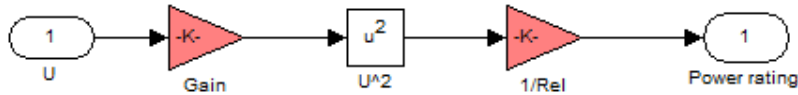
- Radiation heat transfer:
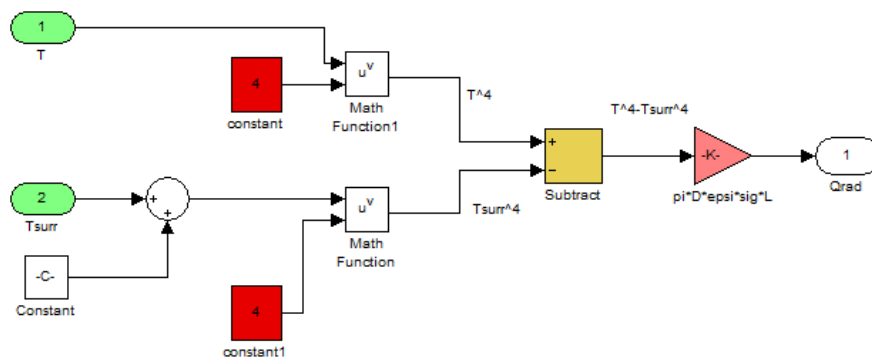
- Convection heat transfer:
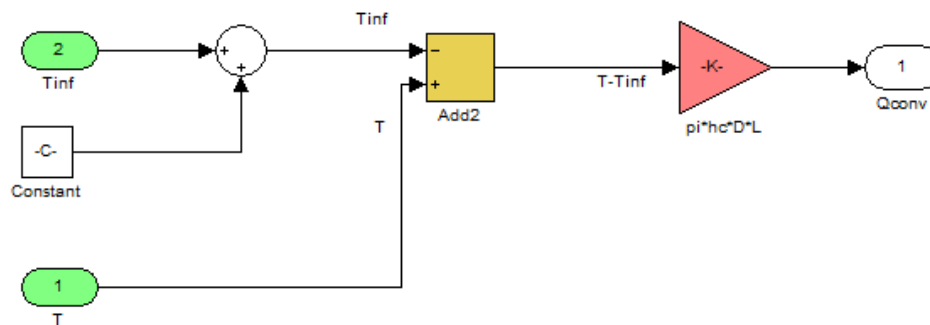
- Energy balance:
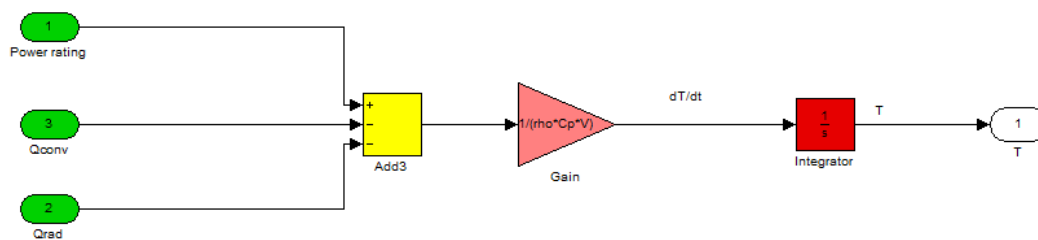
APPENDIX D : Matlab codes

```matlab
%***********************************************************
% S.M. Guyemat Mbourou                                     *
% Student number 210021934                                 *
% Department of Electrical Engineering                     *
%                                                          *
% MTech Project:                                           *
% Plastic waste gasification of a small scale reactor      *
% Experimental and modelling analysis                      *
%                                                          *
%***********************************************************
% Implementation of Runge Kutta 4th order algorithm        *
% where func4 is an .m file                                *
%***********************************************************




clear;
clf;
clc;

Re= 61.67;                          % Resistance [Ω]
U = sqrt(12019.8);                  % Voltage [V]
L = 4;                              % Length of filament wire [m]
Tinf = 295.25;                      % ambient Temperature [°K]
Tsurr = 295.15;                     % Temperature surrounding [°K]
hc = 17;                            % Heat transfer coefficient by Convection
for air [W/m².K]
D = 3*1e-4;                         % Filament diameter [m]
epsi = 0.88;                        % Emissivity of filament
Cp = 460;                           % Specific heat of filament @20°C
[kJ/(Kg*K)]
rho = 8300;                         % Density of filament [kg/m³]
sig = 5.670*1e-8;                   % Stephan-Boltzmann constant [W/m².K?]

i = 1;
h = 1;
T(1) = 295.15;
t(1) = 0;
Rel = Re/L;
V = pi*(D^2/4)*L;
A = pi*D*L;
Eps = epsi*sig*A;
B = 1/(rho*Cp*V);

while t(i)<100
    k1=h*func4(T(i),B,U,Rel,Eps,Tsurr,hc,A,Tinf);
    k2=h*func4(T(i)+k1,B,U,Rel,Eps,Tsurr,hc,A,Tinf);
    k3=h*func4(T(i)+k2/2,B,U,Rel,Eps,Tsurr,hc,A,Tinf);
    k4=h*func4(T(i)+k3,B,U,Rel,Eps,Tsurr,hc,A,Tinf);
    T(i+1)=T(i)+(1/6)*(k1+2*k2+2*k3+k4);
    t(i+1)=i*h;
```

160

```matlab
    i=i+1;
end

plot(t,T);
grid on
xlabel('Time (s)');
ylabel('Filament Temperature (°K)');
title('Heating rate')
```

```matlab
%*********************************************************
% S.M. Guyemat Mbourou                                  *
% Student number 210021934                              *
% Department of Electrical Engineering                  *
%                                                       *
% MTech Project:                                        *
% Modeling of an electrical far-infrared ceramic heater *
% Heating rate simulation                               *
%                                                       *
%*********************************************************
% Implementation of Runge Kutta 4th order algorithm     *
% Sub-program : func4.m                                 *
%*********************************************************


function f=func4(T,B,U,Rel,Eps,Tsurr,hc,A,Tinf)
f=B*((U^2/Rel)- Eps*(T^4-(Tsurr)^4)- hc*A*(T-Tinf));
```